University of California
Santa Cruz

Precise protein-protein interactions contribute to 24-hour timekeeping in mammals

A dissertation submitted in partial satisfaction
of the requirements for the degree of

DOCTOR OF PHILOSOPHY

in

CHEMISTRY

by

Alicia Kathleen Michael

June 2017

The Dissertation of Alicia Kathleen Michael
is approved:

Professor Carrie L. Partch, Advisor

Professor Seth M. Rubin, Chair

Professor Susan Strome

Tyrus Miller
Vice Provost and Dean of Graduate Studies

TABLE OF CONTENTS

1 CHAPTER 1 — Animal cryptochromes: divergent roles in light perception, circadian timekeeping and beyond 1

1.1 Abstract 1

1.2 Introduction 2

1.2.1 Biological timekeeping by circadian rhythms 3

1.2.2 Circadian rhythms in *Drosophila* 5

1.3 Cryptochromes as circadian photoreceptors 6

1.3.1 The search for a circadian photoreceptor 6

1.3.2 Photochemistry and phototransduction of Drosophila CRY 10

1.3.3 *Drosophila* CRY as a magnetoreceptor 11

1.3.4 Circadian photoreception in vertebrates 12

1.3.5 Melanopsin as a circadian photoreceptor 14

1.4 Commonalities and differences in animal cryptochromes 16

1.4.1 Evolutionary diversity of animal cryptochromes 16

1.5 Cryptochromes as transcriptional repressors 19

1.5.1 Circadian rhythms in vertebrates 19

1.5.2 Control of cryptochrome expression 21

1.5.3 Mechanism of transcriptional repression by cryptochrome 22

1.5.4 Transcriptional regulation by CRYs 23

1.6 New roles for cryptochromes 24

1.6.1 Communication of temporal information by cryptochromes 24

1.6.2 Cryptochromes in metabolism 26

1.6.3 DNA damage response 28
1.6.4 Cryptochromes in cancer 29
1.7 Summary and Perspectives 31
1.8 References 32
2 CHAPTER 2 — Formation of a repressive complex in the mammalian circadian clock is mediated by the secondary pocket of CRY1 49
2.1 Abstract 49
2.2 Introduction 49
2.3 Results 52
2.3.1 CRY1 interacts directly with the CLOCK:BMAL1 PAS domain core 52
2.3.2 The CLOCK PAS-B domain docks into the CRY1 secondary pocket 56
2.3.3 Solution scattering studies highlight flexibility of clock protein complexes 63
2.3.4 Low resolution model of the CRY1:CLOCK:BMAL1 ternary complex 67
2.4 Discussion 73
2.5 Materials and Methods 76
2.5.1 Recombinant protein expression and purification. 76
2.5.2 Analytical size-exclusion chromatography. 79
2.5.3 Transcriptional reporter assays and western blotting. 79
2.5.4 HADDOCK modeling. 80
2.5.5 GST pulldown assays. 80
2.5.6 Small angle x-ray scattering (SAXS). 81

2.5.7 X-ray crystallography. 82
2.5.8 Nuclear magnetic resonance (NMR). 82
2.6 References 83
3 CHAPTER 3 — bHLH-PAS proteins: Functional specification through modular domain architecture 89
3.1 Abstract 89
3.2 Introduction 89
3.3 Discussion 90
3.3.1 The PAS domain 90
3.3.2 Modularity within the bHLH-PAS family 92
3.3.3 Evolutionarily related repressors of bHLH-PAS transcription factors 95
3.3.4 Tissue-specific regulation of gene expression 99
3.4 Conclusion 102
3.5 References 103
4 CHAPTER 4 — Cancer/testis antigen PASD1 silences the circadian clock 108
4.1 Abstract 108
4.2 Introduction 108
4.3 Results 111
4.3.1 Identification of a CLOCK paralog in humans 111
4.3.2 PASD1 is a nuclear protein that represses transcriptional activation by CLOCK:BMAL1 117
4.3.3 Regulation of CLOCK:BMAL1 by PASD1 CC1 and CLOCK Exon 19 are functionally linked 126

4.3.4 PASD1 suppresses circadian cycling 128
4.3.5 Identification of PASD1-positive cancer cell lines 129
4.3.6 Downregulation of PASD1 improves amplitude of cycling in human cancer cells 132
4.4 Discussion 136
4.5 Materials and Methods 139
4.5.1 Immunofluorescence 139
4.5.2 Antibodies 140
4.5.3 Co-immunoprecipitations 140
4.5.4 Transient transfection and reporter assays 143
4.5.5 Lentiviral constructs and production 143
4.5.6 Lentiviral transduction 144
4.5.7 siRNA-mediated PASD1 knockdown 145
4.5.8 Bioluminescence recording and data analysis 146
4.5.9 Reverse transcription and qPCR 146
4.5.10 Immunohistochemistry 148
4.5.11 Western blotting 149
4.6 References 149
5 CHAPTER 5 — Biochemical properties of CRY1 and CRY2 contribute to their distinct and shared roles in the mammalian clock 158
5.1 Introduction 158
5.2 Results 162
5.2.1 CRY1 and CRY2 bind the BMAL1 TAD with similar affinity 162

5.2.2 CRY2 does not form a stable complex with CLOCK:BMAL1 PAS-AB core 163
5.2.3 PER2 CRY-binding domain shows independent nodes of interaction with CRY 166
5.2.4 CRY2:PER2 complexes bind the BMAL1 TAD synergistically ... 172
5.3 Discussion 174
5.4 Materials and Methods 178
5.4.1 Recombinant protein expression and purification. 178
5.4.2 Analytical size-exclusion chromatography. 179
5.4.3 Fluorescence anisotropy. 180
5.5 References 180
6 CHAPTER 6 — Molecular assembly of circadian repressive complexes 184
6.1 Introduction 184
6.1.1 An oscillator requires a periodic fluctuation between two states 184
6.1.2 Investigating the assembly of circadian repressive complexes .. 186
6.2 Results 187
6.2.1 CRY1 associates slowly with CLOCK PAS-B 187
6.2.2 The PER2 CBD impedes the fast CLOCK PAS-B association with CRY1 PHR 192
6.2.3 PER2:CRY1:CLOCK:BMAL1 complexes are compatible with DNA binding 197
6.3 Conclusion 201
6.4 Materials and Methods 203
6.4.1 Recombinant protein expression and purification. 203

6.4.2 Analytical size-exclusion chromatography. 203
6.4.3 X-ray crystallography. 204
6.4.4 Electromobility gel shift assay. 204
6.5 References 205
7 CHAPTER 7 — Future directions 209
7.1.1 Structural studies of a PER2:CRY1:CLOCK:BMAL1 complex ...209
7.1.2 Cryo-electron microscopy (EM) of PER2:CRY1:CLOCK:BMAL1 complexes 210
7.2 References 211

LIST OF FIGURES

Figure 1-1. Schematic model for the light-responsive degradation of dCRY and TIM. 8
Figure 1-2. Comparison of C-terminal tail extensions in representative photolyase and cryptochrome proteins. 18
Figure 1-3. Roles of CRY outside of CLOCK:BMAL1 regulation. 26
Figure 2-1 CRY interacts directly with CLOCK:BMAL1 PAS domain core. 53
Figure 2-2. A single point mutation disrupts CRY1:CLOCK:BMAL1 complex formation. 55
Figure 2-3 CLOCK PAS-B docks into secondary pocket of CRY1. 59
Figure 2-4 CRY1 PHR is compact and CLOCK:BMAL1 bHLH-PAS-AB dimer is highly flexible in solution. 65
Figure 2-5. A model for the CRY1:CLOCK:BMAL1 repressive complex. 70
Figure 3-1 bHLH-PAS transcription factors are evolutionarily related and have homologous repressors with internal deletions. 94
Figure 3-2. Tissue-specific expression of bHLH-PAS transcriptional repressors provides cell-type specific responses to external stimuli and cell fate control. 97
Figure 4-1. Identification of a novel circadian repressor that is homologous to CLOCK. 113
Figure 4-2. The C-terminus of PASD1 is sufficient to repress CLOCK:BMAL1 121
Figure 4-3. PASD1 requires its CC1 domain and Exon 19 of CLOCK to repress CLOCK:BMAL1 123
Figure 4-4 Overexpression of PASD1 lengthens period and increases damping of circadian cycling in cell culture. 127
Figure 4-5. PASD1 mRNA and protein is expressed in a diverse array of human cancers. 131

Figure 4-6. Reducing expression of PASD1 in cancer cells increases robustness of circadian rhythms.....134
Figure 5-1. CRY1 and CRY2 bind the minimal BMAL1 TAD.....163
Figure 5-2. CRY2 does not interact stably with CLOCK PAS-B or the CLOCK:BMAL1 PAS-AB dimer. 165
Figure 5-3. Domain schematic and alignment of PER2 Cry-binding domain across vertebrates. 167
Figure 5-4. PER2 CRY-binding domain makes multiple stable contacts with the CRY PHR. 169
Figure 5-5. PER2 CBD does not induce a CRY2-CLOCK PAS-B interaction. 171
Figure 5-6. PER2 CBD and BMAL1 TAD can both bind to the CRY CC simultaneously.....173
Figure 5-7. Functionally differentiating region of CRY1 and CRY2. 177
Figure 6-1. Schematic of nuclear circadian repressive complexes. 184
Figure 6-2. CLOCK PAS-B requires long incubation to form stoichiometric complex with CRY1 PHR. 188
Figure 6-3. CRY1 contains a disordered loop near the CLOCK PAS-B binding pocket. 190
Figure 6-4. The N-terminus of the PER2 CBD impedes initial association of CLOCK PAS-B with CRY1 PHR.....195
Figure 6-5. PER2 CBD:CRY1 PHR complex does not interfere with CLOCK:BMAL1 DNA binding. 199
Figure 7-6. Structural studies of a PER2:CRY1:CLOCK:BMAL1 complex...209

LIST OF SUPPLEMENTARY FIGURES

Supplementary Figure 2-1. CRY1:CLOCK PAS-B HADDOCK modeling 61
Supplementary Figure 2-2. Point mutations in CLOCK PAS-B and CRY1 secondary pocket reduce repression of Clock:Bmal1 by Cry1 62
Supplementary Figure 2-3. Small angle x-ray scattering profile of CRY1 and CLOCK:BMAL1 bHLH PAS-AB. 64
Supplementary Figure 2-4. Small angle x-ray scattering profile of the CRY1:CLOCK:BMAL1 repressive complex. 68
Supplementary Figure 2-5. CLOCK PAS-B and BMAL1 PAS-B form a native dimer in solution. 72
Supplementary Figure 4-1. Human PASD1 has significant sequence homology with CLOCK and lacks a murine homolog. 116
Supplementary Figure 4-2. Co-transfection of PASD1 with CLOCK or BMAL1 does not transactivate the Per1:luc gene. 118
Supplementary Figure 4-3. Characterization of PASD1 and CLOCK:BMAL1 mutants. 125
Supplementary Figure 4-4. Validation of reagents used in PASD1 overexpression studies. 129
Supplementary Figure 4-5. Knockdown of PASD1 in cancer cell lines shows a trend towards lengthened period. 135

LIST OF TABLES

Table 2-1 Statistics of data collection and refinement.....57
Table 2-2 HADDOCK cluster statistics.....58
Table 4-1 siRNA sequences.....145
Table 4-2. Oligonucleotides for qPCR.....147
Table 6-1 Data collection and refinement statistics for CRY1-PER2 at 3.1Å
.....191

Abstract

Precise protein-protein interactions contribute to 24-hour timekeeping in mammals

Alicia K. Michael

Nearly all walks of life, from single cell cyanobacteria to humans, have evolved an intimate connection to the light dark cycle and coordinate physiology and behavior to the solar day. This phenomenon is known as circadian rhythms and is an adaptation that organisms use to anticipate daily environmental changes. In mammals, disruption of circadian rhythms through environmental stimulus or genetic means leads to the onset of many diseases such as: diabetes, cardiovascular disease, premature aging and cancer. Nearly every cell in the human body has an endogenous molecular clock that controls integrated biochemical processes on a ~24-hour period. At the core of this molecular clock is the heterodimeric basic helix-loop-helix Per:Arnt:Sim (bHLH-PAS) transcription factor CLOCK:BMAL1 that together with its repressors, *Period* (PER) and *Cryptochrome* (CRY), forms an autoregulatory feedback loop that results in the rhythmic transcription of nearly 40% of the genome including essential genes in metabolism, hormone secretion and the cell cycle. While this model for transcription-translation feedback loop has been accepted for over two decades, it is still not well understood how CLOCK:BMAL1 activity is directly regulated to generate intrinsic 24-hour timing in mammals. Using a

combination of biochemistry, structural and cell biology we have elucidated a mechanism by which CRY1 directly interacts with CLOCK:BMAL1 to form a critical repressive circadian complex in circadian rhythms. We have also discovered an uncharacterized PAS domain containing protein in humans, PAS Domain containing protein 1 (PASD1), that inhibits CLOCK:BMAL1 activity and suppresses circadian cycling in cancer cells, providing a molecular link from oncogenesis to circadian disruption.

Chapter 2 describes our work to elucidate how CRY1 directly inhibits CLOCK:BMAL1 activity. CRYs close the tightly regulated transcriptional feedback loop to control circadian rhythms, however, the mechanistic underpinnings of how CRYs interact with and repress CLOCK:BMAL1 have remained elusive. Previous studies in our lab showed that tuning affinity of CRY1 for the transactivation domain (TAD) of BMAL1 controls circadian period by competing with the coactivator CBP/p300. CRY1 also binds to CLOCK, although it was not yet understood how multivalent interactions with CLOCK:BMAL1 contribute to CRY1 function. I have shown that CRY1 directly binds the CLOCK:BMAL1 PAS-AB core and this interaction is driven by a single domain in this multi-domain protein complex, CLOCK PAS-B. Furthermore, I have worked with experts in small angle x-ray scattering analysis to generate a model of the CRY1:CLOCK:BMAL1 complex that situates CRY1 atop the CLOCK:BMAL bHLH PAS-AB domains in the solution envelope providing the first low resolution description of the CRY1:CLOCK:BMAL1 complex. These

studies have paved the way for circadian-directed therapeutics and have provided a basis for comparative analysis between the CRY1 and CRY2 proteins as described in Chapter 5. Further studies on the assembly of circadian repressive complexes, including CRY and PERIOD proteins, is described in Chapter 6.

In Chapter 4 we report the discovery of a previously uncharacterized repressor of circadian rhythms, PAS domain containing protein 1 (PASD1). Upon joining Dr. Partch's lab I chose to work on the "long-shot project" – an interesting but undeveloped project that was based entirely off Dr. Partch's initial discovery of an uncharacterized gene that bears significant similarity to a clock protein, potentially possessing the ability to modulate the circadian clock. This CLOCK-like protein, PASD1, is not expressed in healthy somatic tissues, but is instead limited to gametogenic tissues where there are no functional clocks. Using transcriptional reporter assays I confirmed initial results that PASD1 inhibits transactivation of genes by the core circadian transcription factor, CLOCK:BMAL1. Through series of truncation experiments I found that the C-terminus of PASD1 is sufficient to repress CLOCK:BMAL1 in the nucleus. Furthermore, deletion of one region that is highly conserved with CLOCK alleviates repression by PASD1 to suggest it utilizes molecular mimicry to interfere with CLOCK:BMAL1 function. Furthermore, knockdown of PASD1 in both colon and lung cancer cell lines improves the amplitude of cycling, indicative of a more robust oscillator. These data together provide a tool to

rescue the clock in PASD1+ tumors.

In summary, I have used biochemistry and biophysics to describe how the essential circadian protein, CRY1, serves as a potent repressor of CLOCK:BMAL1 activity to establish circadian rhythms. This work provides molecular details of the CRY1-CLOCK:BMAL1 interaction that are being actively used to create circadian-based therapeutics and study the structure of circadian repressive complexes. I have also used cell biology to identify a novel repressor of CLOCK:BMAL1 that is highly up-regulated in many forms of cancer and suppresses circadian cycling.

ACKNOWLEDGEMENTS

The text of this dissertation includes whole or partial reprints of the following previously published material:

Michael AK*, Fribourgh JL*, Van Gelder RN, Partch CL. “Animal Cryptochromes: Divergent Roles in Light Perception, Circadian Timekeeping and Beyond.” Photochem Photobiol. (2017) Jan;93(1):128-140

The following co-authors are acknowledged for their contributions to the published work: A.K.M, J.L.F, C.L.P and R.V.G wrote the manuscript. A.K.M. and J.L.F. contributed equally to this work.

Michael AK, Fribourgh JL, Chelliah Y, Sandate C, Tripathi S, Hura G, Takahashi JS, Partch CL “Formation of a repressive complex in the mammalian circadian clock is mediated by the secondary pocket of CRY1” Proc Natl Acad Sci U S A. (2017) 114 (7) 1560-1565

The following co-authors are acknowledged for their contributions to the published work: A.K.M. and C.L.P. designed research; A.K.M., J.L.F., and G.L.H. performed research; A.K.M., Y.C., and J.S.T. contributed new reagents/analytic tools; A.K.M., J.L.F., C.R.S., G.L.H., D.S.-D., S.M.T., and C.L.P. analyzed data; and A.K.M. and C.L.P. wrote the paper.

Michael A.K., Harvey SL, Sammons PJ, Anderson AP, Kopalle HM, Banham AH, Partch CL. “Cancer/testis antigen PASD1 silences the circadian clock” *Molecular Cell* (2015) Jun 4;58(5):743-54

The following co-authors are acknowledged for their contributions to the published work: A.K.M. and C.L.P. designed the study. A.K.M. and P.J.S. cloned constructs and performed luciferase reporter assays. S.L.H. and P.J.S. performed co-immunoprecipitations. A.K.M generated stable cell lines and performed knockdown experiments. RT-qPCR was conducted by A.K.M. and A.P.A. Immunohistochemistry was performed by A.P.A. and H.M.K generated reagents. A.K.M, S.L.H., A.P.A., A.H.B. and C.L.P. interpreted the data. A.K.M and C.L.P and wrote the paper.

Michael AK, Partch CL. Tissue-specific regulation of evolutionarily conserved bHLH-PAS proteins. (2013) OA Biochemistry. 1:16-21

For my grandmother R. Kathleen Roberts:

Your strong-willed character will always be with me.

For Juan:

Thank you for helping me keep some of my sanity through this. I couldn't ask for a better partner. Off to the next adventure!

And for my parents, Linda and Jason:

Thank you for giving me continuous love and support.

1 CHAPTER 1 — ANIMAL CRYPTOCHROMES: DIVERGENT ROLES IN LIGHT PERCEPTION, CIRCADIAN TIMEKEEPING AND BEYOND

1.1 Abstract

Cryptochromes are evolutionarily related to the light-dependent DNA repair enzyme photolyase, serving as major regulators of circadian rhythms in insects and vertebrate animals. There are two types of cryptochromes in the animal kingdom: *Drosophila*-like CRYs that act as non-visual photopigments linking circadian rhythms to the environmental light/dark cycle, and vertebrate-like CRYs that do not appear to sense light directly, but control the generation of circadian rhythms by acting as transcriptional repressors. Some animals have both types of CRYs, while others possess only one. Cryptochromes have two domains, the photolyase homology region (PHR) and an extended, intrinsically disordered C-terminus. While all animal CRYs share a high degree of sequence and structural homology in their PHR domains, the C-termini are divergent in both length and sequence identity. Recently, cryptochrome function has been shown to extend beyond its pivotal role in circadian clocks, participating in regulation of the DNA damage response, cancer progression, and glucocorticoid signaling, as well as being implicated as possible magnetoreceptors. In this review, we provide a historical perspective on the discovery of animal cryptochromes, examine similarities and differences of the

two types of animal cryptochromes, and explore some of the divergent roles for this class of proteins.

1.2 Introduction

Earth receives almost all of its energy from the Sun's radiation, which provides the driving force for the photosynthetic production of oxygen, patterns of climate and weather, and the coordination of our behavior and physiology with its daily light-dark cycle. Sunlight also contains harmful ultraviolet (UV) radiation that can induce mutations in DNA to interfere with genetic stability. One of the most elegant solutions for the repair of UV-induced DNA damage occurs by a process termed photoreactivation, in which UV-induced pyrimidine dimers are repaired enzymatically with blue light (1). Photolyase enzymes specifically recognize cyclobutane pyrimidine dimers or pyrimidine-pyrimidone (6-4) photoproducts, both of which accumulate when DNA is exposed to sunlight (2, 3). After recognition of damaged DNA, photolyase captures a photon of blue light with one of its two light-harvesting cofactors, a secondary antenna chromophore (either methenyltetrahydrofolate (MTHF) or the deazaflavin, 8-HDF) or the catalytic chromophore flavin adenine dinucleotide (FAD), which undergoes an electron transfer cycle to split the pyrimidine dimer (4).

Not all organisms possess the capability to photoreactivate; those that don't have photolyase use mechanisms such as nucleotide excision repair to replace damaged DNA (5). The discovery of photolyase homologs that lack

DNA repair activity, known as cryptochromes, were first identified over twenty years ago in plants, followed by insects, vertebrates, and are now found across the domains of life (6). By definition, cryptochromes lack DNA repair activity, but they capitalize on their evolutionary relationship to photolyase to regulate other aspects of our intimate biological relationship with the Sun. Although insect and vertebrate-like cryptochromes have different functions, both remain primarily associated with biological clocks that serve as an interface between host physiology, behavior, and the daily light-dark cycle. However, new roles are being revealed for animal cryptochromes outside circadian clocks, including their involvement in cancer biology and the response to DNA damage, metabolic signaling, and possibly even in magnetoreception. Here, we provide a historical perspective on our understanding of cryptochromes and how our knowledge of photolyase structure and function has informed studies on cryptochrome.

1.2.1 Biological timekeeping by circadian rhythms

Circadian rhythms are nearly-24 hour rhythms of physiology and behavior that are a nearly ubiquitous feature of eukaryotic life. These internal rhythms were first noted by Jean-Jacques de Marain (1678-1771), who observed that the daily opening and closing of the flowers of a Mimosa plant persisted in total darkness. The modern field of circadian rhythms was established by Jürgen Aschoff (1913-1998) and Colin Pittendrigh (1918-1996), who delineated the defining properties of these rhythms: Circadian rhythms

are self-sustaining in the absence of external time cues and possess an intrinsic (or free-running) period of approximately 24 hours under constant conditions such as complete darkness. Circadian rhythms are synchronized (or entrained) to the 24-hour solar light-dark cycle and exhibit relatively constant free-running periods with changes in temperature (7).

Under 24-hour light-dark cycles (i.e. 12 hours light and 12 hours dark, or LD 12:12), circadian rhythms demonstrate a period of exactly 24 hours. However, in constant conditions that occur in the absence of environmental cues, these rhythms display their internal free-running periods, which are close to, but usually not exactly, 24 hours. For instance, the human sleep-wake cycle has a free running period of about 24.3 hours, while the mouse has a rest-activity rhythm with a free-running period of about 23.6 hours (8). Light acts as a time cue (or *Zeitgeber*) to entrain internal rhythms to the exact 24-hour solar day. Light accomplishes this by shifting the phase of free-running rhythms to match the environmental light-dark cycle. Most organisms share a common phase response to light, whereby a short pulse of light during the subjective day (i.e. a time that coincides with daytime based on the free-running clock of an organism in complete darkness) does not shift the clock, but a pulse of light in the early subjective night phase delays the clock, while the same pulse of light given in the late subjective night phase advances the clock. By virtue of being able to shift the phase of internal rhythms with brief pulses of light, circadian clocks provide organisms with the ability to align physiology and

behavior to daily environmental cycles for enhanced fitness (9). Remarkably, the spectral character of light that phase shifts the clock is also relatively conserved across a broad range of phylogeny, and is centered in the blue portion of the spectrum.

1.2.2 Circadian rhythms in *Drosophila*

Colin Pittendrigh was the first to study the circadian rhythms of *Drosophila* (7). He noted that flies show two separate free-running rhythms, one of eclosion from pupae to adult, and a second in locomotion. Both are entrainable by light. Using *Drosophila* genetics, Ron Konopka (1947-2015) and Seymour Benzer (1921-2007) performed mutagenesis on flies and identified three mutants with abnormal free-running rhythms (one with a long period, one with a short period, and an arrhythmic mutant) (10). Remarkably, all three mapped to a single gene, dubbed *period* due its profound effects on the timing, or period, of circadian rhythms (11, 12). Equally remarkably, *period* mutants affected both eclosion rhythms and locomotor rhythms in the same way. Work over several decades since has demonstrated that the circadian clock mechanism in *Drosophila* consists of a small number of dedicated clock genes (i.e. *period, timeless, clock, cycle*) that establish a time-delayed transcription-translation feedback loop controlling circadian expression of a number of genes (13).

1.3 Cryptochromes as circadian photoreceptors

1.3.1 The search for a circadian photoreceptor

Drosophila circadian rhythms are entrainable to light-dark cycles. It would be logical to assume that the eyes and visual system mediate this effect. However, studies with eyeless mutants such as *norpA* and *glass* demonstrated that blind flies maintained behavioral entrainment to light-dark cycles (14). Further, severe vitamin A depletion that rendered visual opsins non-functional did not block light-induced phase shifting (15). In addition, explanted tissues from *Drosophila* expressing green fluorescent protein under the control of the *period* promoter/enhancer elements showed direct photoentrainment in culture (16) despite the absence of opsin expression in these tissues. Collectively, these lines of evidence suggested the presence of a cell autonomous circadian photoreceptor.

In 1998, Stanewsky et al. conducted a forward mutagenesis screen in *Drosophila* designed to identify additional clock genes (17). Using a luciferase reporter driven by the *period* gene, this group found a recessive mutation that blunted circadian gene oscillations. The mutation mapped to the *Drosophila cryptochrome (cry)* locus, and was named cry^b (short for 'crybaby'). Previously, light was shown to reduce expression of the TIMELESS (TIM) protein, one of the core clock genes in *Drosophila*; cry^b mutant flies no longer exhibited the light-dependent reduction of TIM protein levels. Based on its similarity to photolyase and plant cryptochromes that act as blue light photoreceptors, *cry*

was suspected of encoding a circadian receptor in flies. In addition, cry^b flies did not phase shift their rhythms to short, bright pulses of light and overexpression of CRY protein resulted in flies that were super-sensitive to phase shifting by light. Of note, cry^b flies still demonstrated free-running behavioral rhythms, and showed some behavioral entrainment to light. However, this entrainment was lost when cry^b mutant flies were compounded with the *glass* mutation (18), which removes all known photoreceptors in the fly eye. Taken together, these results strongly suggested that *Drosophila* CRY functions as the primary blue light photopigment that mediates circadian photoentrainment.

To test this, Emery et al. established an *in vitro* system to study cryptochrome's photoreceptive function (19). In cultured *Drosophila* S2 cells expressing CRY and TIM, exposure to light resulted in the rapid degradation of TIM, followed by the substantially slower degradation of CRY itself. These results suggested that light might induce a structural change in CRY that allows it to interact with TIM, similar to light-dependent changes in conformation observed with *Arabidopsis* cryptochromes (20, 21). The discovery of two novel alleles of *cryptochrome* (cry^m *and cryΔ*) missing the short, C-terminal extension from the photolyase homology region (PHR) supported this model (19, 22). Wild-type CRY bound TIM only after exposure to light (23, 24), while deletion of the CRY C-terminal extension led to constitutive interactions with TIM that triggered its degradation (19, 25). The E3 ubiquitin ligase encoded by *Jetlag*

was subsequently found to be the protein that recognized TIM after interaction with CRY, marking it for degradation to induce phase shifts in the circadian clock (Figure 1-1) (26-28).

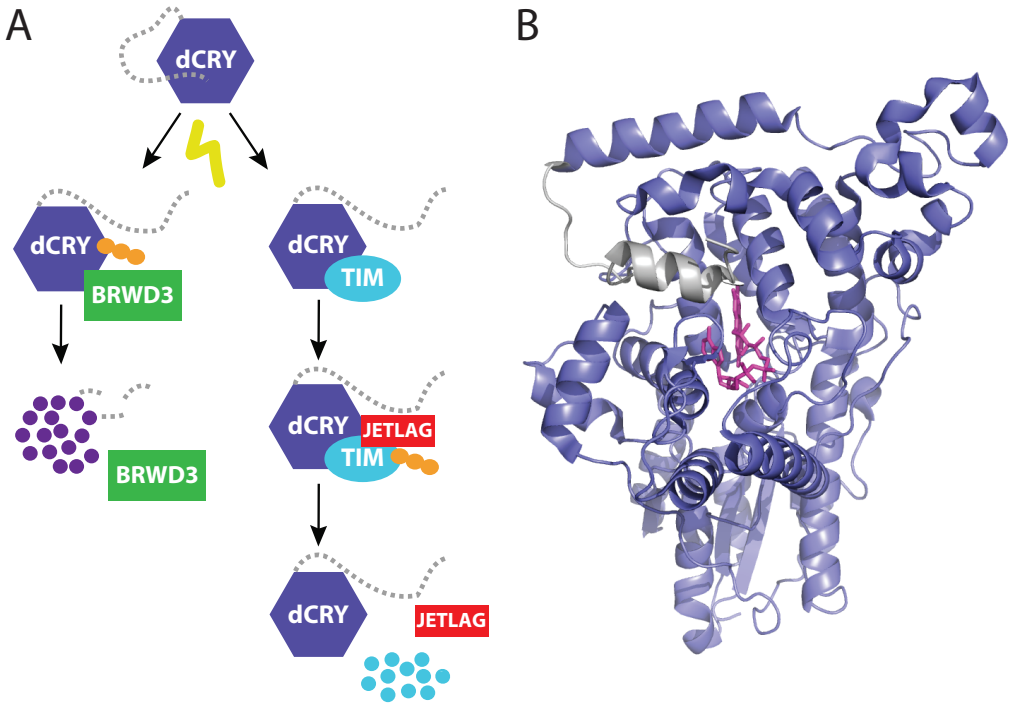

Figure 1-1. Schematic model for the light-responsive degradation of dCRY and TIM.

(A) Light stimulates a structural change in dCRY that exposes the binding interface for TIM and JETLAG. This interaction results in the polyubiquitination (depicted as orange circles) and proteasomal degradation of TIM. The same light-induced conformational change in dCRY also renders it sensitive to polyubiquitination by BRWD3. (B) Structure of full-length dCRY (PDB: 4GU5) in the dark-adapted state. A hydrophobic motif in the C-terminal extension (gray) docks onto the PHR domain (purple) in close proximity to the flavin (pink).

Following on these *in vitro* studies, Chavez et al. developed a cryptochrome-luciferase (CRY-luc) fusion protein to characterize light-mediated CRY degradation in S2 cells (29). They found that a one-hour exposure to light resulted in greater than 80% degradation of the CRY-luc fusion protein. Using this assay, Chavez et al. measured the action spectrum for CRY degradation, demonstrating that maximum degradation of CRY occurred when S2 cells were supplied with near UV light at approximately 380 nm. Light-dependent CRY degradation was blocked by the proteasomal inhibitor MG132, strongly suggesting that CRY, like TIM, is degraded by the proteasome after ubiquitination. However, JETLAG does not regulate CRYs degradation in response to light (30).

In subsequent work, Ozturk et al. (30) knocked down every known F-box E3 ubiquitin ligase present in S2 cells to identify the protein(s) that recognize light-activated cryptochrome in the fly. One E3 ligase, BRWD3 encoded by the *ramshackle* gene, resulted in loss of light-dependent CRY degradation in S2 cells. CRY and BRWD3 were shown to interact in a light-dependent manner by a yeast two-hybrid assay, and purified CRY and BRWD3 proteins formed complex only after exposure to light to result in the ubiquitination of CRY *in vitro*. Therefore, *Drosophila* CRY undergoes a light-dependent change in conformation that regulates its ability to interact with TIM and BRWD3, controlling the stability of both TIM and CRY itself.

1.3.2 Photochemistry and phototransduction of Drosophila CRY

The photocycle of *Drosophila* cryptochrome was initially assumed to be similar to that of *Arabidopsis* cryptochromes (31-33). Like their ancestral photolyase homolog, cryptochromes can bind non-covalently to a flavin adenine dinucleotide (FAD) chromophore to absorb blue light. When *Drosophila* CRY protein was first purified from S2 cells, the catalytic chromophore FAD was found in an oxidized state (FAD_{OX}) that has been generally assumed to represent the ground state of cryptochromes. Following exposure to light *in vitro*, FAD was reduced to the anionic semiquinone form ($FAD^{\bullet -}$) (34, 35). Hoang *et al.* demonstrated by fluorescence and paramagnetic spin techniques that both *Drosophila* and human cryptochromes could be photoreduced by light in Sf21 cell culture (36). Structurally, this electron transfer appears to be dependent on a triad of conserved tryptophan residues (Trp-342, -397, and -420) (37-39). However, mutagenesis of the 'Trp triad' as well as a fourth tryptophan (Trp-536) did not affect light-induced proteolysis of CRY or TIM in S2 cells (40, 34). Crane and colleagues then showed that chemical reduction of the dCRY flavin is sufficient to trigger conformational changes in the protein that are similar to those induced by light (41). Therefore, reduction of the flavin by either light excitation or chemical reduction thus appears to be sufficient to cause conformational changes that are important for CRY activation.

Similar to those observed with *Arabidopsis* CRYs, light-dependent changes in the structure of *Drosophila* CRY are easily assayed by limited trypsin proteolysis *in vitro* (27, 20). It was shown that absorption of light efficiently drove changes in both oxidized and reduced CRY *in vitro*. The structural basis for conformational changes driven by light excitation or chemical reduction of the flavin in *Drosophila* CRY are suggested by crystal structures of its dark-adapted state, which depict how a hydrophobic motif ("FFW") in the C-terminal extension docks onto the PHR domain in close proximity to the flavin (See Figure 1-1) (37, 38). While some of the mechanistic details of CRY signaling still remain to be determined (42), it appears that light-induced changes in *Drosophila* CRY structure are relatively long-lasting—on the order of 30 minutes—after even a millisecond pulse of light (43). Further studies on the photocycle of *Drosophila* CRY and its mechanisms of phototransduction will help inform studies of its biological role in circadian entrainment.

1.3.3 *Drosophila* CRY as a magnetoreceptor

Remarkably, in addition to light sensing, it appears that cryptochromes may also mediate magnetoreception in *Drosophila*. In a binary-choice behavioral assay for magnetosensitivity, wild-type flies showed significant naïve and trained responses to a magnetic field under full-spectrum light, but could not respond to a magnetic field when short wavelengths were blocked (44). Moreover, cry^{b} flies did not exhibit responses to a magnetic field under

full-spectrum light, nor did the *cryΔ* mutant lacking the C-terminal extension (22). Theoretical studies have suggested models explaining how light absorption could induce a paramagnetic triplet excited state in cryptochromes that allows for light-dependent magnetoreception, but it remains to be demonstrated that this is essential for magnetoreception (45). Moreover, CRY was also recently shown to interact with *Drosophila* CG8198 (named MagR for Magnetic Receptor) to yield a protein complex that exhibits light-dependent responses to an induced magnetic field *in vitro* (46). Genetic studies substituting *Drosophila* CRY with cryptochromes from vertebrates suggest that the capability to sense both light and magnetic field may be conserved in animals, while others have provided evidence of light-dependent conformational changes in some vertebrate cryptochromes that are expressed in the retina (47, 43, 48).

1.3.4 Circadian photoreception in vertebrates

In the late 1990s, two cryptochrome homologs (*Cry1* and *Cry2*) were identified in mice (49, 50). Initially, a role for mammalian CRYs in circadian photoreception was suggested by photoentrainment experiments that mirrored early work done in flies. Mice blind from degeneration of the outer retina due to the *rd1* mutation continued to show circadian entrainment to light, even to light as dim as 1-2 lux (51, 52). Unlike the fly, which utilizes a cell autonomous mechanism for circadian entrainment, mice that lacked eyes (through enucleation) or optic nerves did not exhibit circadian photoentrainment,

demonstrating that mammals require retinal phototransduction to entrain to a light/dark cycle (53). Cryptochromes seemed to be viable candidates for non-visual phototransduction based on their expression in retinal ganglion cells (54) and similarity to *Drosophila* and *Arabidopsis* cryptochromes. Upon genetic deletion of both mouse cryptochromes, several lines of evidence suggested that the function of vertebrate cryptochromes might be quite different from *Drosophila* cryptochrome. While flies lacking cryptochrome continued to show behavioral rhythmicity, *Cry1 –/–;Cry2 –/–* mice no longer consolidated behavioral rhythms into circadian patterns (55, 56). Subsequent work demonstrated that mammalian cryptochromes had taken over a role similar to TIM in the fly clock as the major binding partner of PER in the negative transcriptional complex of the core clock mechanism (57, 58).

Although the finding that cryptochromes function as essential transcriptional regulators in the mammalian clock mechanism complicated studies of entrainment, it did not formally eliminate the possibility that they might also function as circadian photopigments. Several lines of evidence initially supported this possibility. First, mice with severe vitamin A depletion (due to dietary vitamin A starvation in a retinol binding protein knockout background) continued to show light-dependent activation of gene expression in the suprachiasmatic nucleus of the hypothalamus, the site of the light-responsive ‘master clock’ in mammals (59, 60). Second, while

Cry1 –/–;Cry2 –/– animals continued to show masking-type effects in a light-dark cycle, the *Cry1 –/–;Cry2 –/–;rd1/rd1* triple mutant resulted in substantially reduced rhythmicity and reduced *c-fos* activation in the suprachiasmatic nucleus in response to light (61).

1.3.5 Melanopsin as a circadian photoreceptor

The discovery of mammalian melanopsin, a rhabdomeric opsin photopigment expressed in a small number of retinal ganglion cells, in 2000 soon led to its rise as the most likely candidate for a dedicated mammalian circadian photoreceptor (62). Although originally discovered in the photosensitive dermal melanocytes of *Xenopus* (63), melanopsin was soon found to form a network of intrinsically photosensitive retinal ganglion cells in mice (64-67). While knockouts of melanopsin (*Opn4*) by itself had little effect on circadian entrainment, combining the *rd1/rd1* mutation with deletion of melanopsin had a stronger phenotype than seen in mice with the *rd1* mutation that also lacked both cryptochromes. Specifically, *rd1/rd1;Opn4 –/–* animals had free-running rhythms that never entrained to external light-dark cycles, and had no pupillary light responses under any light intensities (68), while *rd1/rd1*; *Cry1 –/–;Cry2 –/–* mutants showed pupillary light responses, albeit with markedly decreased sensitivity (69).

It appears that a combination of the unique signaling properties of melanopsin and effects due to the loss of circadian rhythms lead to the misattribution of cryptochrome as a circadian photopigment in mammals.

Vitamin A depletion renders mice visually blind, as the ciliary opsins (rod and cone opsins) release their chromophore with each photocycle and are thus highly dependent on new, vitamin-A-derived photopigment for restoring function. Melanopsin, by contrast, is a rhabdomeric opsin that appears to bind its chromophore irreversibly, using a combination of second photon absorption and thermal relaxation to regenerate its chromophore (70). Subsequent work has shown that melanopsin is remarkably resistant to photic bleaching, and can function in the absence of retinal pigment epithelium and other enzymes of the visual photocycle (62, 71). Thus, earlier studies with vitamin A depletion likely did not result in loss of melanopsin function.

How to explain the reduced pupillary light responses in *rd1/rd1*;*Cry1 –/– ;Cry2 –/–* animals? Several lines of evidence suggest that *Cry*-dependent disruption of the retinal circadian clock reduces melanopsin-dependent pupillary light responses. Identical phenotypes are seen with deletion of other core clock genes that also disrupt circadian rhythms, notably in *Bmal1–/–;Opn4 –/–* and *Per1 –/–; Per –/–;Opn4 –/–* mice (72). Taken together, these results confirm that there is a circadian rhythm of retinal function; in the absence of a circadian clock, reduced retinal sensitivity results in decreased photosignaling to the SCN and pupillary light response centers.

Thus, it appears that the role of cryptochromes is significantly different between insects and vertebrates. Whereas CRY is primarily a blue light photoreceptor that entrains circadian rhythmicity in *Drosophila* and other

insects, cryptochromes in mammals and other vertebrates have evolved to become light-independent transcriptional regulators within the core clock mechanism. Such results, however, must be reconciled with the finding that some vertebrate cryptochromes can bind flavin when purified from eukaryotic expression systems (73, 74, 36) and appear capable of substituting for *Drosophila* CRY in magnetoreception assays *in vivo* (75). However, if vertebrate cryptochromes retain the ability to signal in response to light, the physiology behind these influences remains to be discovered.

1.4 Commonalities and differences in animal cryptochromes

1.4.1 Evolutionary diversity of animal cryptochromes

Phylogenetic analysis of the photolyase/cryptochrome superfamily distributes the group into seven broad subfamilies: cyclobutane pyrimidine dimer (CPD) photolyase classes I-III, (6-4) photolyase, plant cryptochromes, animal cryptochromes and CRY-DASH, which selectively repairs UV-induced damage in single-stranded DNA and RNA (76-78, 6). Animal cryptochromes are more similar to (6-4) photolyase than photolyases that repair cyclobutane pyrimidine dimers. The animal cryptochrome subfamily can be further divided into two groups: Type I cryptochromes, which are light-responsive circadian photoreceptors found only in *Drosophila* and other insects; and Type II cryptochromes in vertebrates (and some insects) that act as transcriptional repressors. Notably, one feature that appears to distinguish the molecular architecture of *Drosophila* and vertebrate clocks is the functional role of

cryptochromes—does CRY act as a non-visual photopigment for entrainment (*Drosophila*) or does it act as a transcriptional repressor (vertebrates)? However, even this distinction may not be clear-cut, as some studies show that *Drosophila* CRY may act as a transcriptional repressor in some tissues (13). Furthermore, some species of insects have both types of animal cryptochromes (monarch butterflies and mosquitos), while others have only a vertebrate-like Type II cryptochrome (honeybees and ants) (79-81). In yet another an interesting twist, some vertebrates (chickens and zebrafish) possess yet another type of cryptochrome (Type IV) that is also sensitive to light, although functional roles for these cryptochromes have yet to be firmly established (6, 43, 48).

Cryptochromes share a high degree of structural homology within their PHR domain both to each other and to all photolyases (82, 37, 39). Despite this overarching similarity, variation in the PHR domains of animal cryptochromes may play a role in their profoundly different functions. Ning Zheng and colleagues first showed that mouse CRY2, a representative vertebrate cryptochrome, appears to have decreased affinity for FAD due to the presence of a much shallower FAD-binding pocket, further supporting their light-insensitive roles as transcriptional repressors (74). Although the pockets in vertebrate CRYs may not be dedicated to chromophore binding, the conservation of these pockets might point to new roles for repressor-type CRYs.

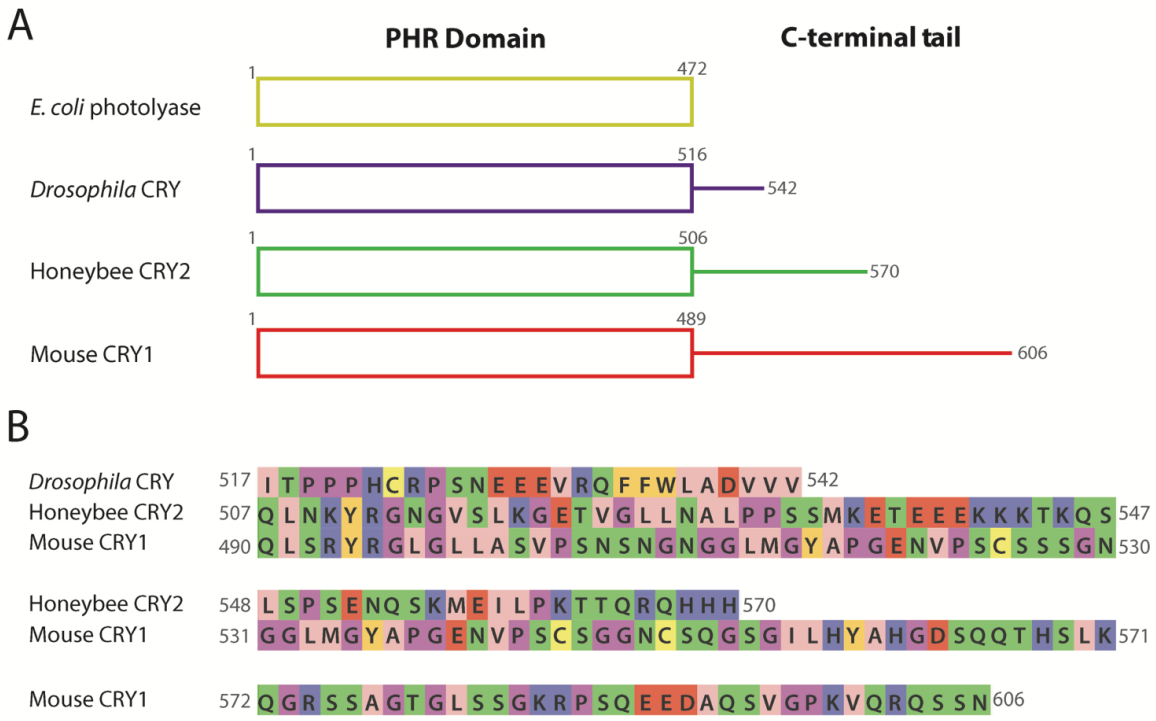

Figure 1-2. Comparison of C-terminal tail extensions in representative photolyase and cryptochrome proteins.

(A) Schematic representation of the domains present in E. coli photolyase, Drosophila CRY, honeybee CRY2, and mouse CRY1. The overall structure and organization of the PHR domain remains relatively unchanged between the different proteins, but the C-terminal tails vary in length. **(**B) Sequences of the unstructured C-terminal extensions of Drosophila CRY, honeybee CRY2, and mouse CRY1. Amino acids are colored according to their physicochemical properties using the Jalview Zappo coloring scheme (138): pink, aliphatic/hydrophobic; gold, aromatic; purple, positive; red, negative; green, hydrophilic; light purple, conformationally special; yellow, cysteine.

There is also some indication that variation in the sequence composition and length of Type I and Type II cryptochromes may help to explain their diverse functions (Figure 1-2). For example, mouse CRY1 and *Drosophila* CRY are only 43% identical, whereas honeybee CRY2 and mouse CRY1, both Type II cryptochromes, are 69% identical. A great deal of the sequence variation in

animal cryptochromes falls outside of the PHR domain in their extended and intrinsically unstructured C-termini (See Figure 1-2). While the role of the *Drosophila* CRY C-terminus in regulating light-dependent interactions with target proteins is well established (19, 25, 24), the role of C-termini in vertebrate-like cryptochrome function is less resolved. Studies of light-dependent Type IV cryptochromes suggest that their C-termini act similarly to *Drosophila* cryptochromes, exhibiting changes in conformation and/or interaction with the PHR domain in response to light (48). The C-termini of Type II CRYs are not essential for circadian transcriptional repression, but their deletion led to changes in circadian period and the amplitude of cycling in genetic reconstitution assays (83-85). Several groups have shown that phosphorylation of the C-termini of CRY1 and CRY2 regulates their stability, suggesting one mechanism by which the C-termini could affect circadian rhythms (86, 87). The C-terminus of human CRY2 was shown to bind the PHR domain and adopt a proteolytically stable structure (20); however, no crystal structures of vertebrate cryptochromes thus far have managed to capture the PHR domain bound to its disordered C-terminus, so a complete reckoning of the vertebrate cryptochrome structure still remains to be determined (37, 74).

1.5 Cryptochromes as transcriptional repressors

1.5.1 Circadian rhythms in vertebrates

Circadian rhythms in vertebrates and most insects are driven by a time-delayed transcription-translation feedback loop that shares similarity with the

Drosophila clock mechanism through moderate conservation of most of the core clock genes. In vertebrates, the basic helix-loop-helix (bHLH) PER-ARNT-SIM (PAS) domain-containing transcription factor complex CLOCK:BMAL1 binds to conserved E-box sequences in the promoters of clock-controlled genes to activate their transcription on a daily basis. Of the approximately 40% of the genome that is rhythmically driven by the circadian clock (88), a small subset of these target genes (*Per1, Per2, Cry1, Cry2*) make up the core negative component of this feedback loop. Additionally, the nuclear receptors ROR and REV-ERB make up an additional feedback loop that interfaces with the primary loop by controlling the expression of a subset of clock genes, including *Bmal1* (89). Large, heteromultimeric PER:CRY complexes slowly enter the nucleus, where they repress CLOCK:BMAL1 activity (90, 91). Recent data demonstrate the presence of at least two distinct phases of repression: an early repressive PER:CRY complex and a late complex where CRY1 directly inhibits CLOCK:BMAL1-driven transcription independently of PER (92-94). Ultimately, the regulated degradation of PER and CRY proteins alleviates repression of CLOCK:BMAL1 activity to allow this cyclical process to begin again. Precise control of protein levels, cellular location and specific complex formation all play an important role in allowing this cycle to occur with ~24 hour periodicity.

1.5.2 Control of cryptochrome expression

As mentioned above, proper regulation of CRY abundance and subcellular localization is critical for accurate clock timing. At the transcriptional level, specific regulatory mechanisms result in the postponement of *Cry1* transcription in relation to *Cry2*; this phase delay in *Cry1* expression is required for 24 hour cycling (95). Post-translational regulation of CRY stability also helps to create necessary delays in abundance that contribute to the 24-hour period of the clock. In the nucleus, CRY1 and CRY2 stability is regulated by the Skp1-Cul1-F-box protein FBXL3, which ubiquitinates cryptochromes to induce proteasomal degradation (96-98). The related protein FBXL21 was shown to ubiquitinate CRY1 and CRY2 in the cytoplasm (99). Interestingly, FBXL21 activity was found to antagonize the more efficient activity of the nuclear E3 ligase FBXL3 to fine-tune CRY protein levels. The small molecule KL001 was shown to bind directly to CRYs and prevent this ubiquitin-dependent degradation, demonstrating for the first time that CRYs could be valuable targets for clock-based therapeutics. KL001 binds in the FAD binding pocket to compete with FBXL3 binding, resulting in the stabilization of CRY protein levels and lengthening of the circadian period (100, 101). Clearly, the ability to fine-tune CRY protein levels is important for an accurate and robust cellular clock, and also represents a powerful example of a pharmacological strategy to manipulate clock function.

1.5.3 Mechanism of transcriptional repression by cryptochrome

Over the last decade, studies have begun to provide some insight into how cryptochromes inhibit CLOCK:BMAL1-driven transcription. Genetic screens performed concurrently by several groups led to the identification of mutations on both CLOCK and BMAL1 that disrupted the ability of CRY to repress transcription (102, 103); a similar study by the Green lab also identified critical residues on cryptochromes (104). Further investigations into cryptochrome function demonstrated distinct functions of CRY1 and CRY2 that exist at the biochemical level, showing that only CRY1 is capable of generating cell-autonomous circadian rhythms in fibroblasts and in tissues outside the SCN, while CRY2 cannot (85, 105). The molecular basis by which a few modest changes in amino acid identity between mammalian CRY1 and CRY2 confers the ability to cycle is not currently understood.

In the late phase of repression, cryptochromes interact directly with CLOCK:BMAL1 on DNA. Aziz Sancar's group first showed this with purified clock proteins, demonstrating their ability to interact both on and off E-box elements in DNA *in vitro* (94). A genetic screen in mammalian cells identified that mutations in the PAS-B domain of CLOCK and C-terminal transactivation domain of BMAL1 are important for CRY repression (102). Subsequent biophysical studies showed that transcriptional repression by CRY1 occurs through competition with transcriptional coactivators for binding the unstructured C-terminal transactivation domain of BMAL1; notably, mutations

that altered the balance of repressor and activator binding on BMAL1 were critical for establishing proper period length (106). In this way, cryptochromes achieve repression of CLOCK:BMAL1 by sequestering the transactivation domain that is needed for activity (103). Cryptochromes utilize multivalent interactions with both CLOCK and BMAL1 to make stable complexes that allow them to repress activity efficiently when expressed to near-stoichiometric levels with the transcription factor (107). Notably, introducing only a few point mutations on CLOCK PAS-B as well as the BMAL1 transactivation domain eliminated the ability of CRY1 to repress CLOCK:BMAL1 activity (106).

1.5.4 Transcriptional regulation by CRYs

While our understanding of circadian regulation of transcription has steadily grown over the last fifteen years, until recently, it has not been clear whether the activity of circadian transcriptional regulators was strictly limited to regulation of CLOCK:BMAL1, or whether their influence reaches beyond this complex. Koike et al. addressed this with a large-scale chromatin immunoprecipitation sequencing (ChIP-seq) study that examined patterns of recruitment for the six core clock proteins genome-wide in mouse liver over the course of an entire day (92). This study cataloged daily patterns in recognition and circadian transcriptional control, not only for the core clock proteins, but also for Pol II and other epigenetic markers, to clearly demonstrate genome-wide control of the transcriptional landscape by the clock. In addition to providing valuable information about the phase distribution of DNA binding by

circadian regulators, this study also identified a large number of sites that are uniquely bound by each of the clock proteins analyzed. For example, CRY1 was found at over 16,000 sites throughout the genome, nearly one-third of which were unique to CRY1 (amongst all the clock proteins), and CRY2 was found at over 10,000 sites (one-fifth of which were unique to CRY2) (92). These data strongly suggest that cryptochromes also work outside the core clock transcription-translation loop to regulate transcription throughout the genome. It will be exciting to see how cryptochromes provide temporal regulation to pathways traditionally considered outside the purview of clock-mediated transcription.

1.6 New roles for cryptochromes

1.6.1 Communication of temporal information by cryptochromes

While it is well established that cryptochromes are essential for circadian timekeeping, the involvement of CRYs in numerous additional signaling pathways is just beginning to be elucidated (108, 55). As core clock genes, the expression of cryptochromes follows a rhythmic, circadian pattern of accumulation in nearly every tissue. This universal and time-dependent accumulation of CRY has the potential to impart circadian control on the regulation of downstream pathways throughout the body. In this way, CRY proteins act as a type of time-telling second messenger between the core clock and other cellular processes in which they participate. Many of the signaling pathways that CRYs are known to regulate aside from CLOCK:BMAL1 play key

roles in the maintenance of cellular homeostasis such as metabolism, inflammation and DNA damage (109-112). These pathways help to maintain cellular and genomic integrity by sensing the current status of the cell (i.e. metabolic, genotoxic stress) and responding to maintain homeostasis (Figure 1-3). In some interesting cases, the stability of CRY proteins is conversely regulated by metabolic and DNA damage signals, helping to form feedback loops that mediate crosstalk between systems (110, 113). Eliminating cryptochrome-mediated crosstalk through knockdown or genetic ablation of CRYs has been shown in some cases to have deleterious effects (114). However, the mechanisms by which cryptochromes directly regulate pathways outside of the clock are often not fully understood, especially in cancer (115). Here, we discuss a few known regulatory roles of cryptochromes outside of the regulation of CLOCK:BMAL1 activity.

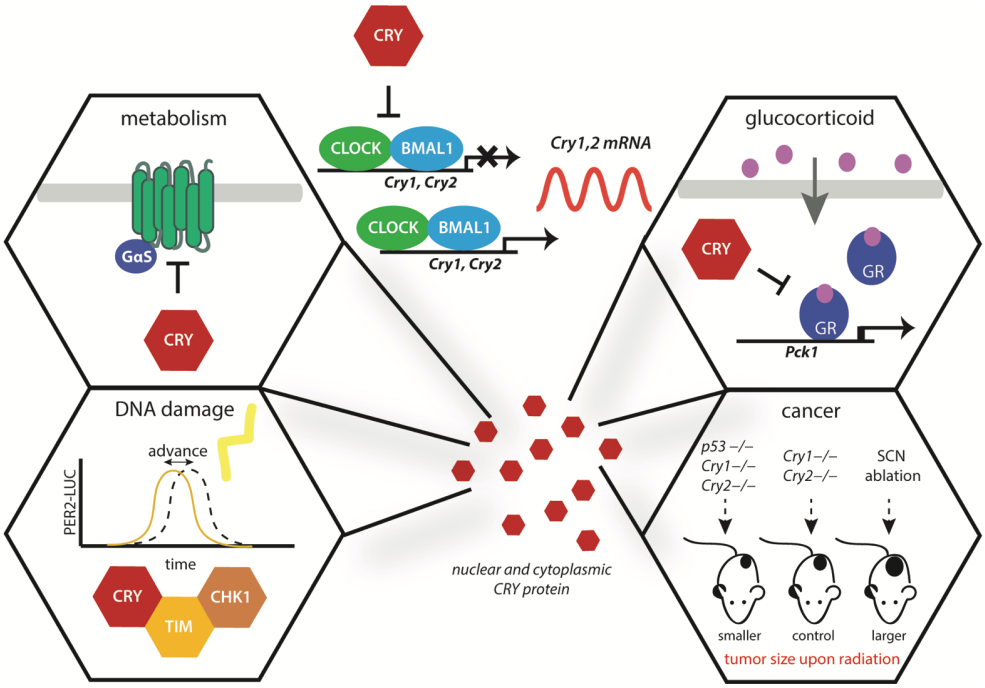

Figure 1-3. Roles of CRY outside of CLOCK:BMAL1 regulation.

In mammals, CRYs negatively regulate CLOCK:BMAL1 activity to generate a ~24 hour clock that regulates ~40% of the genome (88). CRY is also reported to regulate GPCR signaling and downstream metabolism through interaction with the Gsα subunit to block glucagon-stimulated increases in intracellular cAMP (top left). CRY negatively regulates the glucocorticoid receptor to maintain glucose homeostasis, partly through regulation of Pck1 expression (top right). Interaction of CRY with components of the ATR-mediated DNA damage checkpoint control phase shifting of the clock in response to DNA damage (bottom left). While ablation of the SCN increases tumor formation in mouse models, deletion of cryptochromes extends lifespan after ionizing radiation in a p53 null background (bottom right)

1.6.2 Cryptochromes in metabolism

Epidemiological studies of shift workers show that disruption of circadian rhythms is correlated with increased incidence of metabolic disturbances (116). In rodents, disruption of the molecular circadian clock led to increased insulin resistance and obesity, emphasizing the intricate link between the circadian

clock and metabolism (117). Increasing evidence shows that cryptochromes play a direct role in glucose homeostasis through mechanisms that are often independent of CLOCK:BMAL1-regulated transcription. Both CRY1 and CRY2 interact with the glucocorticoid receptor (GR) to repress glucocorticoid-stimulated changes in transcription (Fig. 3) (110). The importance of glucocorticoid signaling to synchronize circadian clocks in peripheral tissues has long been recognized, and recent studies have revealed that CRYs rhythmically antagonize this pathway (118). Interestingly, CRYs modulate only a subset of GR transcriptional targets; the basis of this selectivity is not yet understood. One of the genes negatively regulated by the GR-CRY1 interaction is the rate-limiting gluconeogenic enzyme, phosphoenolpyruvate carboxykinase 1 (*Pck1*). By directly controlling the expression of this essential regulatory enzyme, CRYs globally regulate metabolism in response to circulating factors and presumably function to limit glucocorticoid-induced hyperglycemia. Other studies have also identified that cryptochromes interact with the heterotrimeric G protein subunit $G_{s\alpha}$ to modulate the cAMP pathway and CREB activity downstream of G-protein coupled receptors during fasting (Fig. 3) (114). Consistent with these collective findings, glucose homeostasis is severely disrupted in *Cry*-deficient mice, further highlighting the importance of cryptochromes in metabolic disease.

1.6.3 DNA damage response

As mentioned previously in this review, CRYs share evolutionary conservation and structural similarity to the DNA damage repair enzyme photolyase. By definition, cryptochromes do not directly repair DNA lesions like photolyase, but they do interface with pathways that modulate the cellular responses to DNA damage (119, 120). In mammals, CRY1 modulates the ATR-mediated DNA damage checkpoint by interacting with the cell cycle protein TIMELESS (TIM) (121). There is a substantial degree of sequence homology between mammalian TIM and its counterpart in *Drosophila*; however, they appear to have evolved different functions in these parallel, yet distinct, mechanisms of timekeeping. *Drosophila* contains two *Tim* paralogs, *Tim1 (Timeless)* and *Tim2* (*Timeout*). While *Drosophila* TIMELESS is a core clock component that works with PER and CRY to control clock timing in flies (122), TIMEOUT acts outside of the central clock to regulate light entrainment of the adult circadian clock and is essential for DNA metabolism and chromosome integrity (123). Mammalian TIMELESS is more similar to *Drosophila* TIMEOUT. Consistent with this, ablation of TIM in mammals resulted in embryonic lethality and thus, it has been difficult to study behavioral rhythmicity and classify it as an essential clock gene (124). To date, mammalian TIM is not considered a central clock component. Instead, TIM mediates DNA damage signaling in the ATR-Chk1 pathway to control cell cycle checkpoints (125-127). In mammals, cryptochromes maintain their ability to interact with TIM, where it competes with

ATR-Chk1 for a binding site on the N-terminus of TIM (109, 128). Knockdown of TIM attenuates the canonical phase advance of the circadian system upon DNA damage insults. Mechanistic studies show that TIM interacts with the CC helix (α22) of CRY1 (109). This helical region of CRY1 is a hotspot for regulation by other proteins, including PER2, FBXL3 and BMAL1 (129, 130, 74, 106). Indeed, Tamanini and colleagues found that co-expression of PER2 abolishes formation of a TIM:CRY1 complex, presumably through competition at the CC helix (109). This competitive mechanism for interactions with CRY1 between TIM and other clock proteins that regulate CRY1 stability could represent one manner in which circadian phase is altered in response to genotoxic stress.

1.6.4 Cryptochromes in cancer

Both epidemiological and animal studies show that disruption of circadian rhythms through environmental stimuli (light at night or shift work) or genetic means can lead to an increase incidence of cancer; however, this is confounded by genetic deletion of various clock components and the subsequent array of cancer phenotypes (131, 132). Circadian disruption appears to play a role in the deregulation of cellular homeostasis and cell cycle control, but the mechanisms by which this occur are still being identified (133). Considering that cryptochromes are necessary for circadian timing and regulate vital metabolic processes as well as the UV-induced DNA damage response, deletion of cryptochromes was expected to increase the risk of

developing cancer. Furthermore, *Cry1 –/–*;*Cry2 –/–* mice show elevated *Wee1* levels in the liver and impaired regeneration, linking cryptochromes and the clock to cell cycle control (134). Surprisingly, *in vivo* studies on *Cry1 –/–*;*Cry2 –/–* mice performed by Sancar and colleagues found that these knockout mice do not show an increase in cancer rate compared to wild-type mice, even after exposure to ionizing radiation (135). Further pursuit of these confounding results found that CRY proteins are actually protective using a p53 mutant background that are more prone to cancer. Deletion of cryptochromes extends the median lifespan of *p53 –/–*;*Cry1 –/–*;*Cry2 –/–* mice by 1.5-fold compared to *p53 –/–* mice (136). Mechanistic studies in these triple knockout fibroblasts demonstrated that they were more susceptible than *p53 –/–* knockout cells to UV-induced apoptosis, implicating cryptochromes in the transmission of p53-independent apoptotic signals in response to DNA damage (136). Furthermore, downregulation of CRYs was found to modulate levels of inflammatory cytokines and the NF-κβ-stimulated transcriptional response that sensitizes cells to apoptosis, linking CRYs to the inflammatory response (111). These studies revealed that reprogrammed regulatory networks involving CRYs in cancer that provide potential for tailored chrono- and chemotherapeutic approaches in p53 null tumors.

While deletion of both cryptochromes is required to render mice arrhythmic due to intercellular coupling the SCN, differences in their clock phenotypes has long suggested that *Cry1* and *Cry2* likely have different

functions. This was demonstrated in recent study that CRY1 and CRY2 have divergent functions in response to DNA damage (113). Lamia and co-workers showed that CRY1 was stabilized by the ubiquitin-specific protease HAUSP following DNA damage insults, while CRY2 was simultaneously destabilized through preferential interaction with its ubiquitin ligase, FBXL3. Accordingly, *Cry1 –/–* cells exhibited an increased response to genotoxic stress, while *Cry2 –/–* cells exhibited a decreased response. These opposing phenotypes suggest that future mechanistic studies are needed to examine independent roles that CRY1 and CRY2 may play, especially as they relate to cancer. Understanding the diverse mechanisms by which cryptochromes work, both inside and outside of the circadian clock, will strengthen our understanding of connection between circadian disruption and disease.

1.7 Summary and Perspectives

The very name of cryptochromes appropriately hints at our cryptic understanding of their many biological functions (137). Since their discovery over twenty years ago in plants, a large part of our understanding of cryptochrome function has been drawn from our knowledge of photolyase structure and function (4). However, it is clear that cryptochromes are a family of functionally diverse proteins in their own right. Some cryptochromes act as photopigments to control circadian photoentrainment and possibly even magnetoreception, while others have apparently lost the ability to sense light

and have been co-opted as transcriptional regulators and participants in intracellular signaling cascades that control circadian timing, metabolism, and cellular responses to DNA damage. As more insight is brought to light about cryptochrome structure and function, we hope to fully realize their far-reaching influence over many aspects of animal behavior and physiology.

1.8 References

1. Sancar, G. B. (2000) Enzymatic photoreactivation: 50 years and counting. Mutat Res 451, 25-37.
2. Brash, D. E., W. A. Franklin, G. B. Sancar, A. Sancar and W. A. Haseltine (1985) Escherichia coli DNA photolyase reverses cyclobutane pyrimidine dimers but not pyrimidine-pyrimidone (6-4) photoproducts. J Biol Chem 260, 11438-11441.
3. Todo, T., H. Takemori, H. Ryo, M. Ihara, T. Matsunaga, O. Nikaido, K. Sato and T. Nomura (1993) A new photoreactivating enzyme that specifically repairs ultraviolet light-induced (6-4)photoproducts. Nature 361, 371-374.
4. Sancar, A. (2003) Structure and function of DNA photolyase and cryptochrome blue-light photoreceptors. Chem Rev 103, 2203-2237.
5. Sancar, A. and J. T. Reardon (2004) Nucleotide excision repair in E. coli and man. Adv Protein Chem 69, 43-71.
6. Chaves, I., R. Pokorny, M. Byrdin, N. Hoang, T. Ritz, K. Brettel, L. O. Essen, G. T. van der Horst, A. Batschauer and M. Ahmad (2011) The cryptochromes: blue light photoreceptors in plants and animals. Annu Rev Plant Biol 62, 335-364.
7. Pittendrigh, C. S. (1993) Temporal organization: reflections of a Darwinian clock-watcher. Annu Rev Physiol 55, 16-54.
8. Czeisler, C. A., J. F. Duffy, T. L. Shanahan, E. N. Brown, J. F. Mitchell, D. W. Rimmer, J. M. Ronda, E. J. Silva, J. S. Allan, J. S. Emens, D. J. Dijk and

R. E. Kronauer (1999) Stability, precision, and near-24-hour period of the human circadian pacemaker. Science 284, 2177-2181.

9. Emerson, K. J., W. E. Bradshaw and C. M. Holzapfel (2008) Concordance of the circadian clock with the environment is necessary to maximize fitness in natural populations. Evolution 62, 979-983.

10. Konopka, R. J. and S. Benzer (1971) Clock mutants of Drosophila melanogaster. Proceedings of the National Academy of Sciences of the United States of America 68, 2112-2116.

11. Bargiello, T. A., F. R. Jackson and M. W. Young (1984) Restoration of circadian behavioural rhythms by gene transfer in Drosophila. Nature 312, 752-754.

12. Zehring, W. A., D. A. Wheeler, P. Reddy, R. J. Konopka, C. P. Kyriacou, M. Rosbash and J. C. Hall (1984) P-element transformation with period locus DNA restores rhythmicity to mutant, arrhythmic Drosophila melanogaster. Cell 39, 369-376.

13. Hardin, P. E. (2011) Molecular genetic analysis of circadian timekeeping in Drosophila. Advances in genetics 74, 141-173.

14. Helfrich-Forster, C., C. Winter, A. Hofbauer, J. C. Hall and R. Stanewsky (2001) The circadian clock of fruit flies is blind after elimination of all known photoreceptors. Neuron 30, 249-261.

15. Zimmerman, W. F. and T. H. Goldsmith (1971) Photosensitivity of the circadian rhythm and of visual receptors in carotenoid-depleted Drosophila. Science 171, 1167-1169.

16. Plautz, J. D., M. Kaneko, J. C. Hall and S. A. Kay (1997) Independent photoreceptive circadian clocks throughout Drosophila. Science 278, 1632-1635.

17. Stanewsky, R., M. Kaneko, P. Emery, B. Beretta, K. Wager-Smith, S. A. Kay, M. Rosbash and J. C. Hall (1998) The cryb mutation identifies cryptochrome as a circadian photoreceptor in Drosophila. Cell 95, 681-692.

18. Mealey-Ferrara, M. L., A. G. Montalvo and J. C. Hall (2003) Effects of combining a cryptochrome mutation with other visual-system variants on entrainment of locomotor and adult-emergence rhythms in Drosophila. J Neurogenet 17, 171-221.

19. Busza, A., M. Emery-Le, M. Rosbash and P. Emery (2004) Roles of the two Drosophila CRYPTOCHROME structural domains in circadian photoreception. Science 304, 1503-1506.

20. Partch, C. L., M. W. Clarkson, S. Ozgur, A. L. Lee and A. Sancar (2005) Role of structural plasticity in signal transduction by the cryptochrome blue-light photoreceptor. Biochemistry 44, 3795-3805.

21. Shalitin, D., H. Yang, T. C. Mockler, M. Maymon, H. Guo, G. C. Whitelam and C. Lin (2002) Regulation of Arabidopsis cryptochrome 2 by blue-light-dependent phosphorylation. Nature 417, 763-767.

22. Fedele, G., E. W. Green, E. Rosato and C. P. Kyriacou (2014) An electromagnetic field disrupts negative geotaxis in Drosophila via a CRY-dependent pathway. Nat Commun 5, 4391.

23. Ceriani, M. F., T. K. Darlington, D. Staknis, P. Mas, A. A. Petti, C. J. Weitz and S. A. Kay (1999) Light-dependent sequestration of TIMELESS by CRYPTOCHROME. Science 285, 553-556.

24. Rosato, E., V. Codd, G. Mazzotta, A. Piccin, M. Zordan, R. Costa and C. P. Kyriacou (2001) Light-dependent interaction between Drosophila CRY and the clock protein PER mediated by the carboxy terminus of CRY. Curr Biol 11, 909-917.

25. Dissel, S., V. Codd, R. Fedic, K. J. Garner, R. Costa, C. P. Kyriacou and E. Rosato (2004) A constitutively active cryptochrome in Drosophila melanogaster. Nat Neurosci 7, 834-840.

26. Koh, K., X. Zheng and A. Sehgal (2006) JETLAG resets the Drosophila circadian clock by promoting light-induced degradation of TIMELESS. Science 312, 1809-1812.

27. Ozturk, N., C. P. Selby, Y. Annayev, D. Zhong and A. Sancar (2011) Reaction mechanism of Drosophila cryptochrome. Proceedings of the National Academy of Sciences of the United States of America 108, 516-521.

28. Peschel, N., S. Veleri and R. Stanewsky (2006) Veela defines a molecular link between Cryptochrome and Timeless in the light-input pathway to Drosophila's circadian clock. Proceedings of the National Academy of Sciences of the United States of America 103, 17313-17318.

29. VanVickle-Chavez, S. J. and R. N. Van Gelder (2007) Action spectrum of Drosophila cryptochrome. J Biol Chem 282, 10561-10566.

30. Ozturk, N., S. J. VanVickle-Chavez, L. Akileswaran, R. N. Van Gelder and A. Sancar (2013) Ramshackle (Brwd3) promotes light-induced ubiquitylation of Drosophila Cryptochrome by DDB1-CUL4-ROC1 E3 ligase complex. Proceedings of the National Academy of Sciences of the United States of America 110, 4980-4985.

31. Cashmore, A. R., J. A. Jarillo, Y. J. Wu and D. Liu (1999) Cryptochromes: blue light receptors for plants and animals. Science 284, 760-765.

32. Deisenhofer, J. (2000) DNA photolyases and cryptochromes. Mutat Res 460, 143-149.

33. Sancar, A. (2000) Cryptochrome: the second photoactive pigment in the eye and its role in circadian photoreception. Annu Rev Biochem 69, 31-67.

34. Ozturk, N., S. H. Song, C. P. Selby and A. Sancar (2008) Animal type 1 cryptochromes. Analysis of the redox state of the flavin cofactor by site-directed mutagenesis. J Biol Chem 283, 3256-3263.

35. Song, S. H., N. Ozturk, T. R. Denaro, N. O. Arat, Y. T. Kao, H. Zhu, D. Zhong, S. M. Reppert and A. Sancar (2007) Formation and function of flavin anion radical in cryptochrome 1 blue-light photoreceptor of monarch butterfly. J Biol Chem 282, 17608-17612.

36. Hoang, N., E. Schleicher, S. Kacprzak, J. P. Bouly, M. Picot, W. Wu, A. Berndt, E. Wolf, R. Bittl and M. Ahmad (2008) Human and Drosophila cryptochromes are light activated by flavin photoreduction in living cells. PLoS biology 6, e160.

37. Czarna, A., A. Berndt, H. R. Singh, A. Grudziecki, A. G. Ladurner, G. Timinszky, A. Kramer and E. Wolf (2013) Structures of Drosophila cryptochrome and mouse cryptochrome1 provide insight into circadian function. Cell 153, 1394-1405.

38. Levy, C., B. D. Zoltowski, A. R. Jones, A. T. Vaidya, D. Top, J. Widom, M. W. Young, N. S. Scrutton, B. R. Crane and D. Leys (2013) Updated structure of Drosophila cryptochrome. Nature 495, E3-4.

39. Zoltowski, B. D., A. T. Vaidya, D. Top, J. Widom, M. W. Young and B. R. Crane (2011) Structure of full-length Drosophila cryptochrome. Nature 480, 396-399.

40. Ozturk, N., C. P. Selby, D. Zhong and A. Sancar (2014) Mechanism of photosignaling by Drosophila cryptochrome: role of the redox status of the flavin chromophore. J Biol Chem 289, 4634-4642.

41. Vaidya, A. T., D. Top, C. C. Manahan, J. M. Tokuda, S. Zhang, L. Pollack, M. W. Young and B. R. Crane (2013) Flavin reduction activates Drosophila cryptochrome. Proceedings of the National Academy of Sciences of the United States of America 110, 20455-20460.

42. Conrad, K. S., C. C. Manahan and B. R. Crane (2014) Photochemistry of flavoprotein light sensors. Nature chemical biology 10, 801-809.

43. Ozturk, N., C. P. Selby, S. H. Song, R. Ye, C. Tan, Y. T. Kao, D. Zhong and A. Sancar (2009) Comparative photochemistry of animal type 1 and type 4 cryptochromes. Biochemistry 48, 8585-8593.

44. Gegear, R. J., A. Casselman, S. Waddell and S. M. Reppert (2008) Cryptochrome mediates light-dependent magnetosensitivity in Drosophila. Nature 454, 1014-1018.

45. Muller, P. and M. Ahmad (2011) Light-activated cryptochrome reacts with molecular oxygen to form a flavin-superoxide radical pair consistent with magnetoreception. J Biol Chem 286, 21033-21040.

46. Qin, S., H. Yin, C. Yang, Y. Dou, Z. Liu, P. Zhang, H. Yu, Y. Huang, J. Feng, J. Hao, J. Hao, L. Deng, X. Yan, X. Dong, Z. Zhao, T. Jiang, H. W. Wang, S. J. Luo and C. Xie (2016) A magnetic protein biocompass. Nat Mater 15, 217-226.

47. Niessner, C., S. Denzau, E. P. Malkemper, J. C. Gross, H. Burda, M. Winklhofer and L. Peichl (2016) Cryptochrome 1 in Retinal Cone Photoreceptors Suggests a Novel Functional Role in Mammals. Sci Rep 6, 21848.

48. Watari, R., C. Yamaguchi, W. Zemba, Y. Kubo, K. Okano and T. Okano (2012) Light-dependent structural change of chicken retinal Cryptochrome4. J Biol Chem 287, 42634-42641.

49. Hsu, D. S., X. Zhao, S. Zhao, A. Kazantsev, R. P. Wang, T. Todo, Y. F. Wei and A. Sancar (1996) Putative human blue-light photoreceptors hCRY1 and hCRY2 are flavoproteins. Biochemistry 35, 13871-13877.

50. Todo, T., H. Ryo, K. Yamamoto, H. Toh, T. Inui, H. Ayaki, T. Nomura and M. Ikenaga (1996) Similarity among the Drosophila (6-4)photolyase, a human photolyase homolog, and the DNA photolyase-blue-light photoreceptor family. Science 272, 109-112.

51. Foster, R. G., I. Provencio, D. Hudson, S. Fiske, W. De Grip and M. Menaker (1991) Circadian photoreception in the retinally degenerate mouse (rd/rd). J Comp Physiol A 169, 39-50.

52. Freedman, M. S., R. J. Lucas, B. Soni, M. von Schantz, M. Munoz, Z. David-Gray and R. Foster (1999) Regulation of mammalian circadian behavior by non-rod, non-cone, ocular photoreceptors. Science 284, 502-504.

53. Wee, R., A. M. Castrucci, I. Provencio, L. Gan and R. N. Van Gelder (2002) Loss of photic entrainment and altered free-running circadian rhythms in math5-/- mice. J Neurosci 22, 10427-10433.

54. Miyamoto, Y. and A. Sancar (1998) Vitamin B2-based blue-light photoreceptors in the retinohypothalamic tract as the photoactive pigments for setting the circadian clock in mammals. Proceedings of the National Academy of Sciences of the United States of America 95, 6097-6102.

55. van der Horst, G. T., M. Muijtjens, K. Kobayashi, R. Takano, S. Kanno, M. Takao, J. de Wit, A. Verkerk, A. P. Eker, D. van Leenen, R. Buijs, D. Bootsma, J. H. Hoeijmakers and A. Yasui (1999) Mammalian Cry1 and Cry2 are essential for maintenance of circadian rhythms. Nature 398, 627-630.

56. Vitaterna, M. H., C. P. Selby, T. Todo, H. Niwa, C. Thompson, E. M. Fruechte, K. Hitomi, R. J. Thresher, T. Ishikawa, J. Miyazaki, J. S. Takahashi and A. Sancar (1999) Differential regulation of mammalian period genes and circadian rhythmicity by cryptochromes 1 and 2. Proceedings of the National Academy of Sciences of the United States of America 96, 12114-12119.

57. Hirayama, J., H. Nakamura, T. Ishikawa, Y. Kobayashi and T. Todo (2003) Functional and structural analyses of cryptochrome. Vertebrate CRY regions responsible for interaction with the CLOCK:BMAL1 heterodimer and its nuclear localization. J Biol Chem 278, 35620-35628.

58. Shearman, L. P., S. Sriram, D. R. Weaver, E. S. Maywood, I. Chaves, B. Zheng, K. Kume, C. C. Lee, G. T. van der Horst, M. H. Hastings and S. M. Reppert (2000) Interacting molecular loops in the mammalian circadian clock. Science 288, 1013-1019.

59. Thompson, C. L., W. S. Blaner, R. N. Van Gelder, K. Lai, L. Quadro, V. Colantuoni, M. E. Gottesman and A. Sancar (2001) Preservation of light signaling to the suprachiasmatic nucleus in vitamin A-deficient mice. Proceedings of the National Academy of Sciences of the United States of America 98, 11708-11713.

60. Thompson, C. L., C. P. Selby, R. N. Van Gelder, W. S. Blaner, J. Lee, L. Quadro, K. Lai, M. E. Gottesman and A. Sancar (2004) Effect of vitamin A depletion on nonvisual phototransduction pathways in cryptochromeless mice. Journal of biological rhythms 19, 504-517.

61. Selby, C. P., C. Thompson, T. M. Schmitz, R. N. Van Gelder and A. Sancar (2000) Functional redundancy of cryptochromes and classical photoreceptors for nonvisual ocular photoreception in mice. Proceedings of the National Academy of Sciences of the United States of America 97, 14697-14702.

62. Sexton, T., E. Buhr and R. N. Van Gelder (2012) Melanopsin and mechanisms of non-visual ocular photoreception. J Biol Chem 287, 1649-1656.

63. Provencio, I., G. Jiang, W. J. De Grip, W. P. Hayes and M. D. Rollag (1998) Melanopsin: An opsin in melanophores, brain, and eye. Proceedings of the National Academy of Sciences of the United States of America 95, 340-345.

64. Berson, D. M., F. A. Dunn and M. Takao (2002) Phototransduction by retinal ganglion cells that set the circadian clock. Science 295, 1070-1073.

65. Hattar, S., H. W. Liao, M. Takao, D. M. Berson and K. W. Yau (2002) Melanopsin-containing retinal ganglion cells: architecture, projections, and intrinsic photosensitivity. Science 295, 1065-1070.

66. Panda, S., T. K. Sato, A. M. Castrucci, M. D. Rollag, W. J. DeGrip, J. B. Hogenesch, I. Provencio and S. A. Kay (2002) Melanopsin (Opn4) requirement for normal light-induced circadian phase shifting. Science 298, 2213-2216.

67. Ruby, N. F., T. J. Brennan, X. Xie, V. Cao, P. Franken, H. C. Heller and B. F. O'Hara (2002) Role of melanopsin in circadian responses to light. Science 298, 2211-2213.

68. Panda, S., I. Provencio, D. C. Tu, S. S. Pires, M. D. Rollag, A. M. Castrucci, M. T. Pletcher, T. K. Sato, T. Wiltshire, M. Andahazy, S. A. Kay, R.

N. Van Gelder and J. B. Hogenesch (2003) Melanopsin is required for non-image-forming photic responses in blind mice. Science 301, 525-527.

69. Van Gelder, R. N., R. Wee, J. A. Lee and D. C. Tu (2003) Reduced pupillary light responses in mice lacking cryptochromes. Science 299, 222.

70. Emanuel, A. J. and M. T. Do (2015) Melanopsin tristability for sustained and broadband phototransduction. Neuron 85, 1043-1055.

71. Sexton, T. J., M. Golczak, K. Palczewski and R. N. Van Gelder (2012) Melanopsin is highly resistant to light and chemical bleaching in vivo. J Biol Chem 287, 20888-20897.

72. Owens, L., E. Buhr, D. C. Tu, T. L. Lamprecht, J. Lee and R. N. Van Gelder (2012) Effect of circadian clock gene mutations on nonvisual photoreception in the mouse. Invest Ophthalmol Vis Sci 53, 454-460.

73. Ozgur, S. and A. Sancar (2003) Purification and properties of human blue-light photoreceptor cryptochrome 2. Biochemistry 42, 2926-2932.

74. Xing, W., L. Busino, T. R. Hinds, S. T. Marionni, N. H. Saifee, M. F. Bush, M. Pagano and N. Zheng (2013) SCF(FBXL3) ubiquitin ligase targets cryptochromes at their cofactor pocket. Nature 496, 64-68.

75. Foley, L. E., R. J. Gegear and S. M. Reppert (2011) Human cryptochrome exhibits light-dependent magnetosensitivity. Nat Commun 2, 356.

76. Selby, C. P. and A. Sancar (2006) A cryptochrome/photolyase class of enzymes with single-stranded DNA-specific photolyase activity. Proceedings of the National Academy of Sciences of the United States of America 103, 17696-17700.

77. Partch, C. L. and A. Sancar (2005) Photochemistry and photobiology of cryptochrome blue-light photopigments: the search for a photocycle. Photochem Photobiol 81, 1291-1304.

78. Yu, X., H. Liu, J. Klejnot and C. Lin (2010) The Cryptochrome Blue Light Receptors. Arabidopsis Book 8, e0135.

79. Rubin, E. B., Y. Shemesh, M. Cohen, S. Elgavish, H. M. Robertson and G. Bloch (2006) Molecular and phylogenetic analyses reveal mammalian-like clockwork in the honey bee (Apis mellifera) and shed new light on the molecular evolution of the circadian clock. Genome Res 16, 1352-1365.

80. Yuan, Q., D. Metterville, A. D. Briscoe and S. M. Reppert (2007) Insect cryptochromes: gene duplication and loss define diverse ways to construct insect circadian clocks. Mol Biol Evol 24, 948-955.

81. Ingram, K. K., A. Kutowoi, Y. Wurm, D. Shoemaker, R. Meier and G. Bloch (2012) The molecular clockwork of the fire ant Solenopsis invicta. PloS one 7, e45715.

82. Park, H. W., S. T. Kim, A. Sancar and J. Deisenhofer (1995) Crystal structure of DNA photolyase from Escherichia coli. Science 268, 1866-1872.

83. Chaves, I., K. Yagita, S. Barnhoorn, H. Okamura, G. T. van der Horst and F. Tamanini (2006) Functional evolution of the photolyase/cryptochrome protein family: importance of the C terminus of mammalian CRY1 for circadian core oscillator performance. Mol Cell Biol 26, 1743-1753.

84. van der Schalie, E. A., F. E. Conte, K. E. Marz and C. B. Green (2007) Structure/function analysis of Xenopus cryptochromes 1 and 2 reveals differential nuclear localization mechanisms and functional domains important for interaction with and repression of CLOCK-BMAL1. Mol Cell Biol 27, 2120-2129.

85. Khan, S. K., H. Xu, M. Ukai-Tadenuma, B. Burton, Y. Wang, H. R. Ueda and A. C. Liu (2012) Identification of a novel cryptochrome differentiating domain required for feedback repression in circadian clock function. J Biol Chem 287, 25917-25926.

86. Harada, Y., M. Sakai, N. Kurabayashi, T. Hirota and Y. Fukada (2005) Ser-557-phosphorylated mCRY2 is degraded upon synergistic phosphorylation by glycogen synthase kinase-3 beta. J Biol Chem 280, 31714-31721.

87. Gao, P., S. H. Yoo, K. J. Lee, C. Rosensweig, J. S. Takahashi, B. P. Chen and C. B. Green (2013) Phosphorylation of the cryptochrome 1 C-terminal tail regulates circadian period length. J Biol Chem 288, 35277-35286.
88. Zhang, R., N. F. Lahens, H. I. Ballance, M. E. Hughes and J. B. Hogenesch (2014) A circadian gene expression atlas in mammals: implications for biology and medicine. Proceedings of the National Academy of Sciences of the United States of America 111, 16219-16224.
89. Gustafson, C. L. and C. L. Partch (2015) Emerging models for the molecular basis of mammalian circadian timing. Biochemistry 54, 134-149.
90. Brown, S. A., J. Ripperger, S. Kadener, F. Fleury-Olela, F. Vilbois, M. Rosbash and U. Schibler (2005) PERIOD1-associated proteins modulate the negative limb of the mammalian circadian oscillator. Science 308, 693-696.
91. Duong, H. A. and C. J. Weitz (2014) Temporal orchestration of repressive chromatin modifiers by circadian clock Period complexes. Nat Struct Mol Biol 21, 126-132.
92. Koike, N., S. H. Yoo, H. C. Huang, V. Kumar, C. Lee, T. K. Kim and J. S. Takahashi (2012) Transcriptional architecture and chromatin landscape of the core circadian clock in mammals. Science 338, 349-354.
93. Stratmann, M., F. Stadler, F. Tamanini, G. T. van der Horst and J. A. Ripperger (2010) Flexible phase adjustment of circadian albumin D site-binding protein (DBP) gene expression by CRYPTOCHROME1. Genes Dev 24, 1317-1328.
94. Ye, R., C. P. Selby, N. Ozturk, Y. Annayev and A. Sancar (2011) Biochemical analysis of the canonical model for the mammalian circadian clock. J Biol Chem 286, 25891-25902.
95. Ukai-Tadenuma, M., R. G. Yamada, H. Xu, J. A. Ripperger, A. C. Liu and H. R. Ueda (2011) Delay in feedback repression by cryptochrome 1 is required for circadian clock function. Cell 144, 268-281.

96. Busino, L., F. Bassermann, A. Maiolica, C. Lee, P. M. Nolan, S. I. Godinho, G. F. Draetta and M. Pagano (2007) SCFFbxl3 controls the oscillation of the circadian clock by directing the degradation of cryptochrome proteins. Science 316, 900-904.

97. Godinho, S. I., E. S. Maywood, L. Shaw, V. Tucci, A. R. Barnard, L. Busino, M. Pagano, R. Kendall, M. M. Quwailid, M. R. Romero, J. O'Neill, J. E. Chesham, D. Brooker, Z. Lalanne, M. H. Hastings and P. M. Nolan (2007) The after-hours mutant reveals a role for Fbxl3 in determining mammalian circadian period. Science 316, 897-900.

98. Siepka, S. M., S. H. Yoo, J. Park, W. Song, V. Kumar, Y. Hu, C. Lee and J. S. Takahashi (2007) Circadian mutant Overtime reveals F-box protein FBXL3 regulation of cryptochrome and period gene expression. Cell 129, 1011-1023.

99. Yoo, S. H., J. A. Mohawk, S. M. Siepka, Y. Shan, S. K. Huh, H. K. Hong, I. Kornblum, V. Kumar, N. Koike, M. Xu, J. Nussbaum, X. Liu, Z. Chen, Z. J. Chen, C. B. Green and J. S. Takahashi (2013) Competing E3 ubiquitin ligases govern circadian periodicity by degradation of CRY in nucleus and cytoplasm. Cell 152, 1091-1105.

100. Hirota, T., J. W. Lee, P. C. St John, M. Sawa, K. Iwaisako, T. Noguchi, P. Y. Pongsawakul, T. Sonntag, D. K. Welsh, D. A. Brenner, F. J. Doyle, 3rd, P. G. Schultz and S. A. Kay (2012) Identification of small molecule activators of cryptochrome. Science 337, 1094-1097.

101. Nangle, S., W. Xing and N. Zheng (2013) Crystal structure of mammalian cryptochrome in complex with a small molecule competitor of its ubiquitin ligase. Cell Res 23, 1417-1419.

102. Sato, T. K., R. G. Yamada, H. Ukai, J. E. Baggs, L. J. Miraglia, T. J. Kobayashi, D. K. Welsh, S. A. Kay, H. R. Ueda and J. B. Hogenesch (2006) Feedback repression is required for mammalian circadian clock function. Nat Genet 38, 312-319.

103. Kiyohara, Y. B., S. Tagao, F. Tamanini, A. Morita, Y. Sugisawa, M. Yasuda, I. Yamanaka, H. R. Ueda, G. T. van der Horst, T. Kondo and K. Yagita (2006) The BMAL1 C terminus regulates the circadian transcription feedback loop. Proceedings of the National Academy of Sciences of the United States of America 103, 10074-10079.

104. McCarthy, E. V., J. E. Baggs, J. M. Geskes, J. B. Hogenesch and C. B. Green (2009) Generation of a novel allelic series of cryptochrome mutants via mutagenesis reveals residues involved in protein-protein interaction and CRY2-specific repression. Mol Cell Biol 29, 5465-5476.

105. Evans, J. A., H. Pan, A. C. Liu and D. K. Welsh (2012) Cry1-/- circadian rhythmicity depends on SCN intercellular coupling. Journal of biological rhythms 27, 443-452.

106. Xu, H., C. L. Gustafson, P. J. Sammons, S. K. Khan, N. C. Parsley, C. Ramanathan, H. W. Lee, A. C. Liu and C. L. Partch (2015) Cryptochrome 1 regulates the circadian clock through dynamic interactions with the BMAL1 C terminus. Nat Struct Mol Biol 22, 476-484.

107. Lee, Y., R. Chen, H. M. Lee and C. Lee (2011) Stoichiometric relationship among clock proteins determines robustness of circadian rhythms. J Biol Chem 286, 7033-7042.

108. Kume, K., M. J. Zylka, S. Sriram, L. P. Shearman, D. R. Weaver, X. Jin, E. S. Maywood, M. H. Hastings and S. M. Reppert (1999) mCRY1 and mCRY2 are essential components of the negative limb of the circadian clock feedback loop. Cell 98, 193-205.

109. Engelen, E., R. C. Janssens, K. Yagita, V. A. Smits, G. T. van der Horst and F. Tamanini (2013) Mammalian TIMELESS is involved in period determination and DNA damage-dependent phase advancing of the circadian clock. PloS one 8, e56623.

110. Lamia, K. A., S. J. Papp, R. T. Yu, G. D. Barish, N. H. Uhlenhaut, J. W. Jonker, M. Downes and R. M. Evans (2011) Cryptochromes mediate rhythmic repression of the glucocorticoid receptor. Nature 480, 552-556.

111. Lee, J. H. and A. Sancar (2011) Circadian clock disruption improves the efficacy of chemotherapy through p73-mediated apoptosis. Proceedings of the National Academy of Sciences of the United States of America 108, 10668-10672.

112. Narasimamurthy, R., M. Hatori, S. K. Nayak, F. Liu, S. Panda and I. M. Verma (2012) Circadian clock protein cryptochrome regulates the expression of proinflammatory cytokines. Proceedings of the National Academy of Sciences of the United States of America 109, 12662-12667.

113. Papp, S. J., A. L. Huber, S. D. Jordan, A. Kriebs, M. Nguyen, J. J. Moresco, J. R. Yates and K. A. Lamia (2015) DNA damage shifts circadian clock time via Hausp-dependent Cry1 stabilization. Elife 4.

114. Zhang, E. E., Y. Liu, R. Dentin, P. Y. Pongsawakul, A. C. Liu, T. Hirota, D. A. Nusinow, X. Sun, S. Landais, Y. Kodama, D. A. Brenner, M. Montminy and S. A. Kay (2010) Cryptochrome mediates circadian regulation of cAMP signaling and hepatic gluconeogenesis. Nat Med 16, 1152-1156.

115. Sancar, A., L. A. Lindsey-Boltz, T. H. Kang, J. T. Reardon, J. H. Lee and N. Ozturk (2010) Circadian clock control of the cellular response to DNA damage. FEBS Lett 584, 2618-2625.

116. Wang, X. S., M. E. Armstrong, B. J. Cairns, T. J. Key and R. C. Travis (2011) Shift work and chronic disease: the epidemiological evidence. Occup Med (Lond) 61, 78-89.

117. Shi, S. Q., T. S. Ansari, O. P. McGuinness, D. H. Wasserman and C. H. Johnson (2013) Circadian disruption leads to insulin resistance and obesity. Current biology : CB 23, 372-381.

118. Reddy, A. B., E. S. Maywood, N. A. Karp, V. M. King, Y. Inoue, F. J. Gonzalez, K. S. Lilley, C. P. Kyriacou and M. H. Hastings (2007) Glucocorticoid

signaling synchronizes the liver circadian transcriptome. Hepatology 45, 1478-1488.

119. Kang, T. H., L. A. Lindsey-Boltz, J. T. Reardon and A. Sancar (2010) Circadian control of XPA and excision repair of cisplatin-DNA damage by cryptochrome and HERC2 ubiquitin ligase. Proceedings of the National Academy of Sciences of the United States of America 107, 4890-4895.

120. Kang, T. H. and A. Sancar (2009) Circadian regulation of DNA excision repair: implications for chrono-chemotherapy. Cell Cycle 8, 1665-1667.

121. Lee, T. H., J. M. Park, S. H. Leem and T. H. Kang (2014) Coordinated regulation of XPA stability by ATR and HERC2 during nucleotide excision repair. Oncogene 33, 19-25.

122. Rosato, E., E. Tauber and C. P. Kyriacou (2006) Molecular genetics of the fruit-fly circadian clock. Eur J Hum Genet 14, 729-738.

123. Benna, C., S. Bonaccorsi, C. Wulbeck, C. Helfrich-Forster, M. Gatti, C. P. Kyriacou, R. Costa and F. Sandrelli (2010) Drosophila timeless2 is required for chromosome stability and circadian photoreception. Current biology : CB 20, 346-352.

124. Gotter, A. L., T. Manganaro, D. R. Weaver, L. F. Kolakowski, Jr., B. Possidente, S. Sriram, D. T. MacLaughlin and S. M. Reppert (2000) A time-less function for mouse timeless. Nat Neurosci 3, 755-756.

125. Chou, D. M. and S. J. Elledge (2006) Tipin and Timeless form a mutually protective complex required for genotoxic stress resistance and checkpoint function. Proceedings of the National Academy of Sciences of the United States of America 103, 18143-18147.

126. Unsal-Kacmaz, K., T. E. Mullen, W. K. Kaufmann and A. Sancar (2005) Coupling of human circadian and cell cycles by the timeless protein. Mol Cell Biol 25, 3109-3116.

127. Yoshizawa-Sugata, N. and H. Masai (2007) Human Tim/Timeless-interacting protein, Tipin, is required for efficient progression of S phase and DNA replication checkpoint. J Biol Chem 282, 2729-2740.
128. Kang, T. H. and S. H. Leem (2014) Modulation of ATR-mediated DNA damage checkpoint response by cryptochrome 1. Nucleic Acids Res 42, 4427-4434.
129. Nangle, S. N., C. Rosensweig, N. Koike, H. Tei, J. S. Takahashi, C. B. Green and N. Zheng (2014) Molecular assembly of the period-cryptochrome circadian transcriptional repressor complex. Elife 3, e03674.
130. Schmalen, I., S. Reischl, T. Wallach, R. Klemz, A. Grudziecki, J. R. Prabu, C. Benda, A. Kramer and E. Wolf (2014) Interaction of circadian clock proteins CRY1 and PER2 is modulated by zinc binding and disulfide bond formation. Cell 157, 1203-1215.
131. Papagiannakopoulos, T., M. R. Bauer, S. M. Davidson, M. Heimann, L. Subbaraj, A. Bhutkar, J. Bartlebaugh, M. G. Vander Heiden and T. Jacks (2016) Circadian Rhythm Disruption Promotes Lung Tumorigenesis. Cell Metab.
132. Davis, S. and D. K. Mirick (2006) Circadian disruption, shift work and the risk of cancer: a summary of the evidence and studies in Seattle. Cancer Causes Control 17, 539-545.
133. Takahashi, J. S., H. K. Hong, C. H. Ko and E. L. McDearmon (2008) The genetics of mammalian circadian order and disorder: implications for physiology and disease. Nat Rev Genet 9, 764-775.
134. Matsuo, T., S. Yamaguchi, S. Mitsui, A. Emi, F. Shimoda and H. Okamura (2003) Control mechanism of the circadian clock for timing of cell division in vivo. Science 302, 255-259.
135. Gauger, M. A. and A. Sancar (2005) Cryptochrome, circadian cycle, cell cycle checkpoints, and cancer. Cancer Res 65, 6828-6834.

136. Ozturk, N., J. H. Lee, S. Gaddameedhi and A. Sancar (2009) Loss of cryptochrome reduces cancer risk in p53 mutant mice. Proceedings of the National Academy of Sciences of the United States of America 106, 2841-2846.
137. J., G. (1979) Blue light of photoreception. Photochemistry and Photobiology 30, 749-754.
138. Clamp, M., J. Cuff, S. M. Searle and G. J. Barton (2004) The Jalview Java alignment editor. Bioinformatics 20, 426-427.

2 CHAPTER 2 — FORMATION OF A REPRESSIVE COMPLEX IN THE MAMMALIAN CIRCADIAN CLOCK IS MEDIATED BY THE SECONDARY POCKET OF CRY1

2.1 Abstract

The basic helix-loop-helix PAS domain (bHLH-PAS) transcription factor CLOCK:BMAL1 sits at the core of the mammalian circadian transcription/translation feedback loop. Precise control of CLOCK:BMAL1 activity by coactivators and repressors establishes the ~24 hour periodicity of gene expression. Formation of a repressive complex, defined by the core clock proteins CRY1:CLOCK:BMAL1, plays an important role controlling the switch from repression to activation each day. Here we show that CRY1 binds directly to the PAS domain core of CLOCK:BMAL1, driven primarily by interaction with the CLOCK PAS-B domain. Integrative modeling and solution x-ray scattering studies unambiguously position a key loop of the CLOCK PAS-B domain in the secondary pocket of CRY1, analogous to the antenna chromophore-binding pocket of photolyase. CRY1 docks onto the transcription factor alongside the PAS domains, extending above the DNA-binding bHLH domain. Single point mutations at the interface on either CRY1 or CLOCK disrupt formation of the ternary complex, highlighting the importance of this interface for direct regulation of CLOCK:BMAL1 activity by CRY1.

2.2 Introduction

Circadian rhythms allow animals to coordinate behavior and physiology

with the environmental light/dark cycle (1). While a host of cellular processes contribute to the generation of ~24-hour timing at the molecular level (i.e. transcriptional, post-transcriptional, translational, post-translational), the mammalian transcription factor CLOCK:BMAL1 sits at the core of integrated transcription-translation feedback loops that regulate the rhythmic expression of over 40% of the genome throughout the body (2). In support of its central role, the loss of *Bmal1* renders mice arrhythmic in the absence of external time cues, the only single clock gene deletion to do so in mice (3). Disruption of circadian rhythms has been linked to altered cellular homeostasis and disease, yet we still lack fundamental insight into basic mechanisms of clock function, including how core clock proteins interact with each other to control the ~24-hour periodicity of gene expression (4).

Recent studies have suggested the presence of several regulatory complexes of core clock proteins that form throughout the day to establish a dynamic balance of CLOCK:BMAL1 activation and repression. In the morning, CLOCK:BMAL1 is bound at E-box sites on DNA with its coactivator CBP/p300, driving expression of the core clock repressors *Per* and *Cry* along with other clock-controlled output genes. Repression begins early in the evening, defined by large hetero-multimeric PER:CRY complexes bound to CLOCK:BMAL1 (5-7). The structural basis for formation of these complexes, and whether they occur primarily on or off DNA, is still not well understood (8). Based on ChIP-Seq studies, these complexes appear to remodel or reform over time, evolving

to a late repressive complex where CRY1 is bound to CLOCK:BMAL1 on DNA, apparently independently of PER (7).These findings suggest that cryptochromes can work both together and separately from PER to repress CLOCK:BMAL1 activity (8-10). We showed that tuning affinity of CRY1 for the transactivation domain (TAD) of BMAL1 controls circadian period by competing with the coactivator CBP/p300 (11). CRY1 also binds to CLOCK, although it is not yet understood how multivalent interactions with CLOCK:BMAL1 contribute to CRY1 function. Therefore, understanding the molecular basis for recruitment of regulators to CLOCK:BMAL1 will shed light on mechanisms that are crucial for establishing the ~24-hour periodicity of the circadian clock.

Here, we set out to identify how CRY1 interacts with CLOCK:BMAL1 to form a stable ternary complex. We found that the photolyase homology region (PHR) of CRY1 binds directly to the second of two tandem PAS domains (PAS-B) of CLOCK and identified single point mutations on CRY1 and CLOCK PAS-B that eliminate complex formation. Using these data to guide HADDOCK modeling, we found that CLOCK PAS-B docks directly into the secondary pocket of the CRY1 PHR. This pocket is evolutionarily conserved with photolyase, where it serves as the binding site for an antenna chromophore that is important for repair of UV-induced DNA damage (12). Small angle x-ray scattering (SAXS) studies of CRY1, CLOCK:BMAL1, and the CRY1:CLOCK:BMAL1 ternary complex highlight structural dynamics of these complexes and validate our low resolution model of the ternary complex.

Together, these data illustrate how CRY1 exploits a conserved binding pocket to form a ternary complex with CLOCK:BMAL1 that maintains the transcription factor in a repressed state to close the circadian feedback loop.

2.3 Results

2.3.1 CRY1 interacts directly with the CLOCK:BMAL1 PAS domain core

The repressive activity of CRY1 is essential to generate circadian rhythms (13-15); one way that CRY1 does this is by binding the BMAL1 TAD to sequester it from coactivators (11, 16). However, CRY1 has only moderate affinity (K_d ~1 μM) for the isolated TAD (11, 17), suggesting that it makes at least one other interaction with CLOCK:BMAL1 that allows it to serve as a potent repressor when expressed to near stoichiometric levels (18). Previous studies suggest the CLOCK PAS-B domain is important for repression by CRY1 (11, 19, 20), but evidence for a direct interaction is lacking. To further explore the biochemical basis for interactions between CRY1 and CLOCK:BMAL1, we purified the core photolyase homology region of mouse CRY1 (PHR) and a tandem PAS domain heterodimer (comprising PAS-A and PAS-B domains, PAS-AB) of mouse CLOCK:BMAL1 (Figure 2-1A). Using size exclusion chromatography to follow complex formation, we found that the CRY1 PHR directly bound the PAS-AB core of CLOCK:BMAL1 to form a ternary complex (Figure 2-1B). Further dissection of this interaction revealed that the CLOCK PAS-B domain alone was sufficient to bind CRY1 PHR. Moreover, while BMAL1 PAS-B shares the same protein fold as CLOCK PAS-

B, it did not interact with CRY1, highlighting the specificity of this interaction (Figure 2-1C).

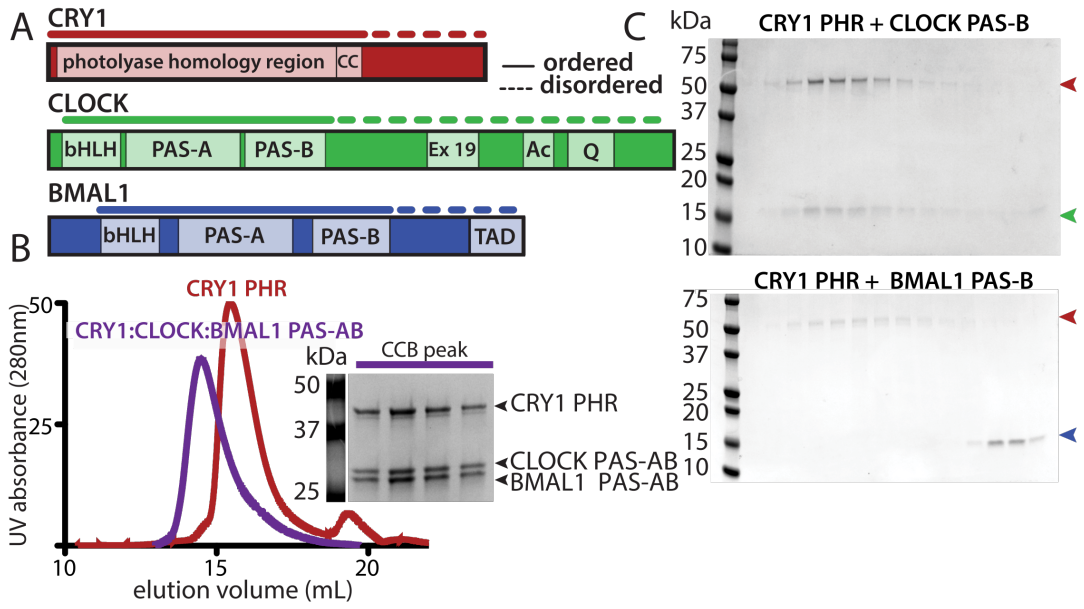

Figure 2-1 CRY interacts directly with CLOCK:BMAL1 PAS domain core.

(A) Domain schematic of CRY1, CLOCK and BMAL1. Solid lines indicate regions used in this current study. (B) Size exclusion chromatography (SEC) analysis of complex formation with CRY1 PHR alone or mixed with the CLOCK:BMAL1 tandem PAS-AB domain dimer. Proteins were mixed and incubated at 4°C overnight and then injected on a S200 10/300 GL column. The peak fraction of CRY1 PHR with CLOCK:BMAL1 PAS-AB was analyzed by SDS-PAGE (CCB peak) and stained by Coomassie. (C) SEC analysis of CRY1 PHR with CLOCK PAS-B (top) or BMAL1 PAS-B (bottom) in isolation. Identical fractions (12 – 18.5 mL on a S200 10/300GL column, 0.5 mL each) were analyzed by SDS-PAGE gel electrophoresis and stained by Coomassie. Red arrow indicates CRY1 PHR, green arrow indicates CLOCK PAS-B and blue arrow indicates BMAL1 PAS-B.

Several residues in the HI loop (connecting the Hβ and Iβ strands) of CLOCK PAS-B are important for CRY1-mediated repression of

CLOCK:BMAL1 (11, 19, 20). The entire HI loop is freely accessible in the crystal structure of the CLOCK:BMAL1 bHLH-PAS dimer, protruding out from the PAS-B dimer interface (Figure 2-2A) (21). To test the role of the HI loop in binding CRY1, we made a W362A substitution in CLOCK PAS-B and tested its ability to bind CRY1 using a GST pull-down experiment. This single point mutation disrupted formation of the stoichiometric CRY1:CLOCK PAS-B complex (Figure 2-2B). We then explored the importance of W362 for the CRY1:CLOCK interaction in the context of a larger, tandem PAS domain dimer. While GST-BMAL1 PAS-AB was able to pull down similar amounts of wild-type and W362A CLOCK PAS-AB, CRY1 was only present in a ternary complex with wild-type CLOCK PAS-AB (Figure 2-2C). Furthermore, a CLOCK:BMAL1 PAS-AB dimer possessing the W362A mutation no longer co-migrated with CRY1 on size-exclusion chromatography (Figure 2-2D). Collectively, these data demonstrate that stable association of CRY1 with the CLOCK:BMAL1 PAS domain core is predicated on a single, solvent-accessible tryptophan on CLOCK PAS-B.

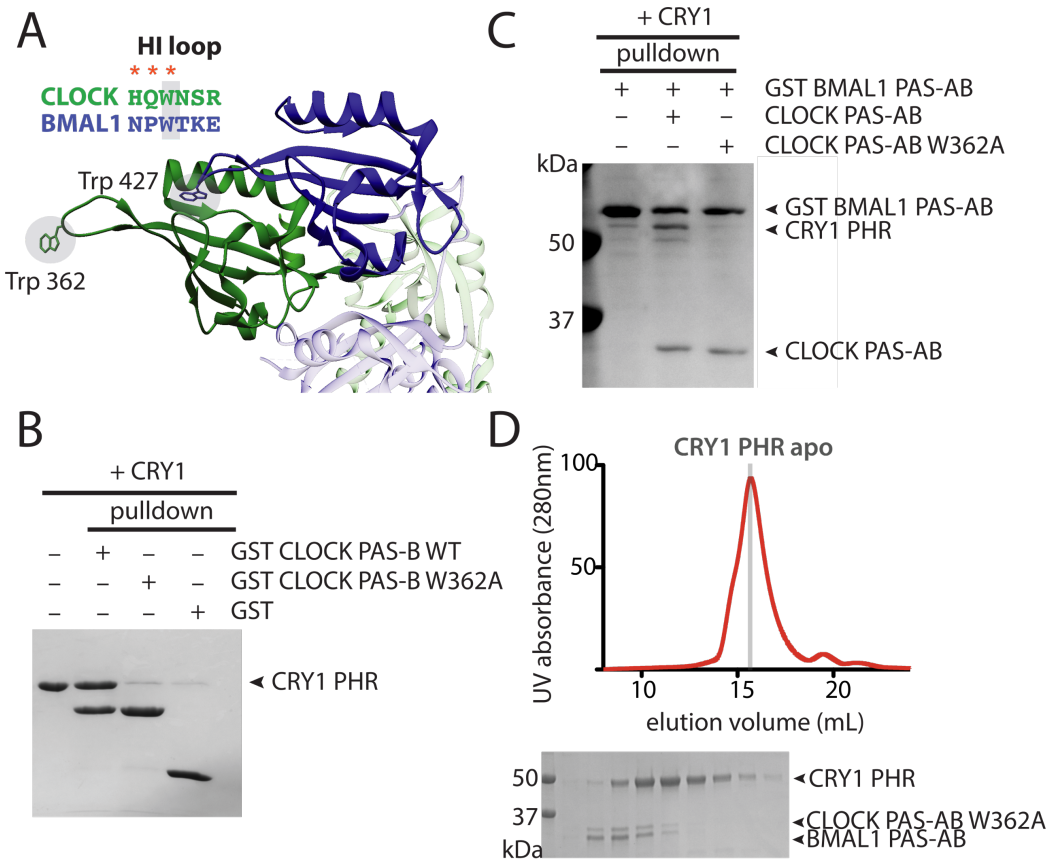

Figure 2-2. A single point mutation disrupts CRY1:CLOCK:BMAL1 complex formation.

(A) PAS-B domains of CLOCK:BMAL1 (PDB: 4F3L; CLOCK, green, BMAL1, blue) with conserved tryptophan in HI loop shown in sticks. Red asterisks indicate mutations in CLOCK that disrupt CRY1 repression of CLOCK:BMAL1. Adjacent PAS-A domains are shown in light blue (BMAL1) and light green (CLOCK). (B) GST pull-down assay of GST-CLOCK PAS-B and GST-CLOCK PAS-B W362A with CRY1 PHR. (C) GST pull-down assay of GST-BMAL1 PAS-AB alone, in the presence of CLOCK PAS-AB or CLOCK PAS-AB W362A with CRY1 PHR. (D) S200 10/300 GL SEC analysis of complex formation with CRY1 PHR and the PAS-AB dimer with W362A CLOCK mutation.

2.3.2 The CLOCK PAS-B domain docks into the CRY1 secondary pocket

To better understand the nature of the CRY1:CLOCK PAS-B interface, we generated a computational model of the complex using HADDOCK (High Ambiguity Driven protein-protein DOCKing) (22, 23). HADDOCK utilizes residues identified from experimental studies to guide selection of probable protein-protein interfaces and then performs rigid body docking and simulated annealing protocols to provide clusters of hits that are ranked by energetic considerations and their similarity to one another. Based on previous mutagenesis data and our own studies here, we used the following residues as active restraints, defined by their importance for binding and solvent accessibility: CRY1: G106, R109, E383, E382 (17, 24) and CLOCK PAS-B: G332, H360, Q361, W362, E367 (Figure 2-3A) (11, 19, 20). The CRY1 restraints cluster around the secondary pocket in the PHR, which is structurally conserved with photolyase where it serves as a chromophore binding pocket (12). The existing crystal structure of mouse CRY1 lacks a short, flexible loop adjacent to this pocket (17), so we solved a structure of the mouse CRY1 PHR (1.8 Å resolution) in a new space group with the goal of visualizing this loop (PDB: 5T5X,Table 2-1 Statistics of data collection and refinement). While our new structure also lacked density for this loop, it was of higher resolution so we used it along with the CLOCK PAS-B domain (isolated from PDB: 4F3L) for HADDOCK modeling. Clusters were ranked using electrostatic, van der Waals, and ambiguous interaction restraint energy terms. All four clusters docked the

HI loop of CLOCK PAS-B into secondary pocket of CRY1 in similar orientations (Supplementary Figure 2-1A), with the top cluster populated by the greatest number of models (118) and the best overall HADDOCK score (Table 2-2).

Table 2-1 Statistics of data collection and refinement

Data	
Space group	P1
Unit cell dimensions (a,b,c) (Å), (α, β, γ)(º)	46.63, 51.03, 54.17 71.62, 84.12, 88.89
Resolution Range (Å) (highest shell)	51.15-1.80 (1.83-1.80)
Wavelength (Å)	0.999
Total observations	138880 (7431)
Unique reflections	38528 (2114)
Completeness (%)	93.5 (85.9)
R_{merge}	11.0 (47.2)
CC1/2	0.98(0.74)
<I/σ>	45.4 (4.6)
Redundancy	3.6 (3.5)
Refinement	
No. of Reflection	35812
R_{work} %/ R_{free} %	16.8/23.1
Number of atoms	
Protein	3829
Ligand/ion	1

Water	455
Average B-factor (Wilson)	20.5
RMSD Bond length (Å)	0.013
RMSD Bond angle	1.35

Details of structure for apo mouse cryptochrome 1 PDB: 5T5X. Values reported in parentheses are for higher resolution shell.

Table 2-2 HADDOCK cluster statistics

Output statistics for CRY1 PHR (PDB: 5T5X) docking with CLOCK PAS-B (PDB: 4F3L, CLOCK PAS-B) using HADDOCK 2.2.

	Cluster 1	Cluster 2	Cluster 3	Cluster 4
HADDOCK score	-147.3	-131.6	-109.5	-132.1
Cluster size	118	43	15	13
RMSD lowest-energy structure	12.7 ± 0.2	13.3 ± 0.2	11.0 ± 0.8	2.8 ± 2.0
Van der Walls energy	-47.4 ± 3.8	-47.4 ± 4.1	-40.1 ± 7.3	-51.9 ± 9.9
Electrostatic energy	-289.5 ± 42.7	-243.0 ± 31.0	-213.8 ± 52.9	-206.9 ± 18.3
Desolvation energy	-44.5 ± 7.6	-36.7 ± 5.9	-30.9 ± 7.7	-41.0 ± 7.2
Restraints violation energy	24.1 ± 25.04	11.5 ± 14.27	43.7 ± 11.91	22.2 ± 17.36
Buried surface area	1944.5 ± 83.2	1869.0 ± 46.2	1446.6 ± 114.9	1839.6 ± 105.4
Z-score	-1.3	-0.1	1.5	-0.1

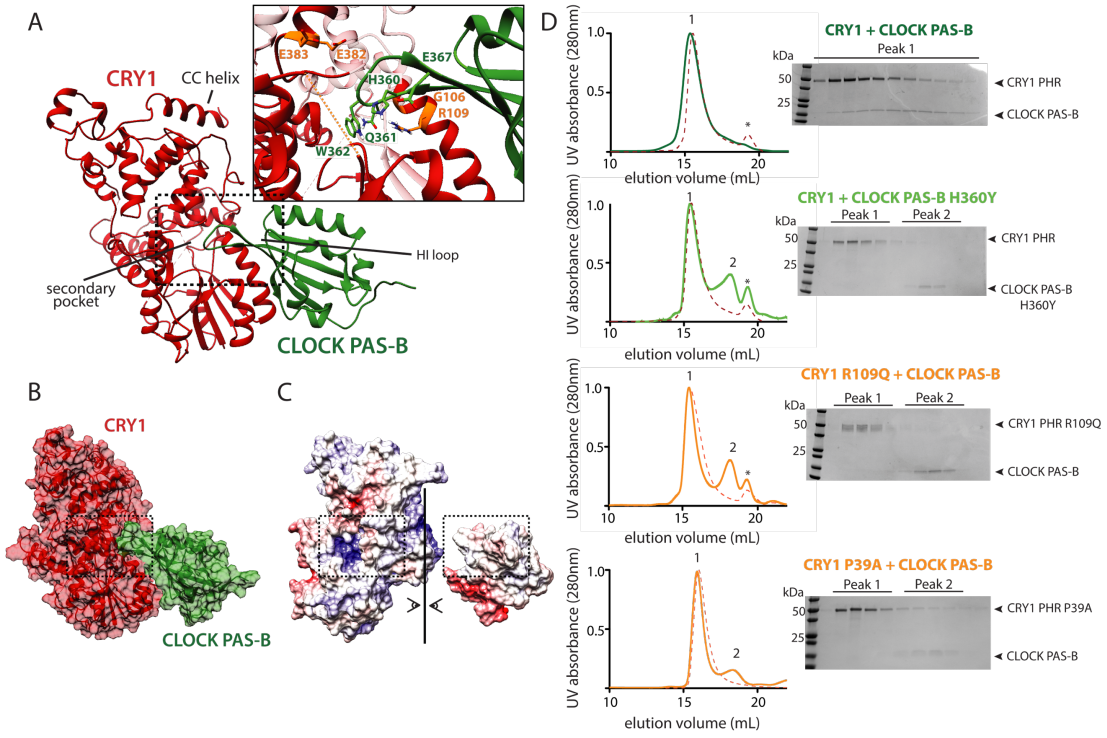

Figure 2-3 CLOCK PAS-B docks into secondary pocket of CRY1.

(A) Representative PDB from top HADDOCK cluster (cluster 1). Active residues used to guide the docking are shown in orange (CRY1) and light green (CLOCK). CRY1 PHR unstructured secondary pocket loop is shown in an orange dashed line. See Table S2 for details on HADDOCK cluster statistics. (B) Surface representation of CRY1:CLOCK PAS-B HADDOCK model. (C) Electrostatic representation of CRY1:CLOCK PAS-B HADDOCK model. Surface potential maps were generated using the Adaptive Poisson-Boltzmann Solver (APBS) in UCSF Chimera (43). The secondary pocket of CRY1 and HI loop of CLOCK PAS-B are highlighted in the dashed box analogous to panel A. (D) SEC analysis of the CRY1:CLOCK PAS-B interaction with mutants. Proteins were mixed and incubated at ~30 min. at 4°C and then injected on a S200 10/300 GL column. Top, wild-type CRY1 PHR and CLOCK PAS-B. Asterisk, slight UV-absorbing contaminant. Numbers above peaks correspond to fractions analyzed by SDS-PAGE and Coomassie stain at right. Top middle, wild-type CRY1 PHR and CLOCK PAS-B H360Y mutant. Bottom middle, CRY1 PHR R109Q mutant with wild-type CLOCK PAS-B. Bottom, CRY1 PHR P39A mutant with wild-type CLOCK PAS-B. Residue P39 is located in the disordered loop shown in orange

dashed line in panel A. Elution profiles of CRY1 PHR WT or mutant alone are shown in each respective panel in the red dashed line.

A representative model from the top cluster is characterized by a large buried surface area (1994.5 ± 83.2 $Å^2$) mediated by burial of the HI loop and additional sites of contact between the β-sheet of CLOCK PAS-B and CRY1 (Figure 2-3B and Supplementary Figure 2-1B). We also noted complementary electrostatic contacts at the interface (Figure 2-3C). To test this model experimentally, we made additional point mutations at the observed interface. CLOCK PAS-B H360Y and two mutations in CRY1 (P39A and R109Q) each disrupted formation of a CRY1:CLOCK PAS-B complex as shown by loss of CLOCK PAS-B co-migration with CRY1 (peak 1) and the presence of a new peak for the isolated CLOCK PAS-B domain (peak 2) by size exclusion chromatography (Figure 2-3D). This is consistent with the inability of CRY1 R109Q to co-immunoprecipitate with CLOCK:BMAL1 and reconstitute circadian rhythms in cell-based cycling assays (24). Additionally, mutations that eliminate CRY1:CLOCK PAS-B complex formation *in vitro* also significantly reduce repressive activity of full-length mCRY1 in steady-state luciferase reporter assays (Supplementary Figure 2-2), demonstrating that these phenotypes are mediated by a direct interaction between CRY1 and the CLOCK:BMAL1 complex at the secondary pocket.

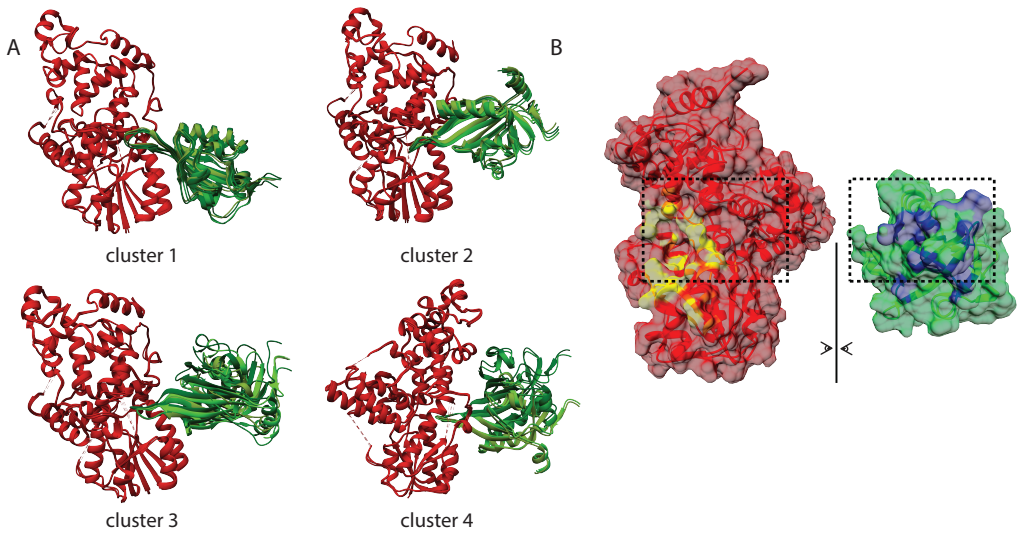

Supplementary Figure 2-1. CRY1:CLOCK PAS-B HADDOCK modeling

(A) All docking solutions from HADDOCK 2.2 analysis of CRY1:CLOCK PAS-B interaction. Clusters are ranked numerically according to lowest HADDOCK scoring. See Table S2 for details of cluster scoring. (B) Buried surface area representation of CRY1 and CLOCK PAS-B for top HADDOCK cluster 1 PDB using built-in chimera tools. Buried surface of CRY1 shown in yellow and CLOCK PAS-B in blue. Buried surface area calculated by HADDOCK: 1944.5 ± 83.2 $Å^2$

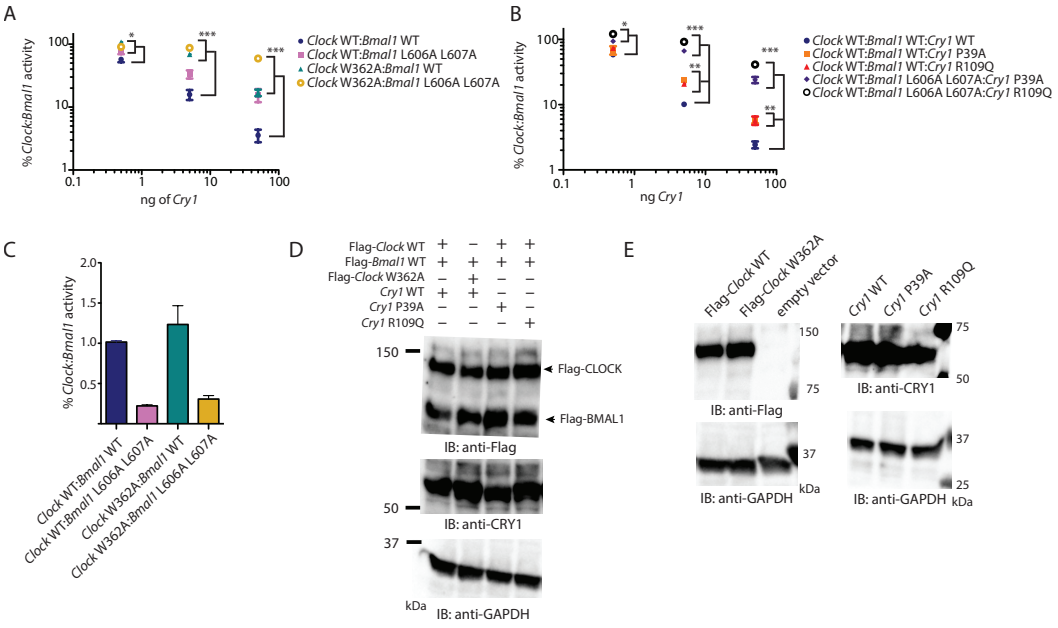

Supplementary Figure 2-2. Point mutations in CLOCK PAS-B and CRY1 secondary pocket reduce repression of *Clock:Bmal1* by *Cry1*

(A) Per1-Luc assay with increasing amounts of plasmids encoding mCry1 (0.5, 5 and 50 ng) with Clock WT or Clock W362A and Bmal1 WT or L606A L607A (100 ng each). Relative activity normalized to Clock:Bmal1 (WT or mut) without mCry1 co-transfected set to 100. (B) Per1-Luc assay with increasing amounts of mCry1 WT or point mutants (P39A and R109Q) with Clock WT and Bmal1 WT or L606A L607A. L606A and L607A mutations in the transactivation domain of Bmal1 reduce repression by mCry1 and synergistically reduce repression when paired with mutations in CLOCK PAS-B and the CRY1 secondary pocket. * $P < 0.05$; ** $P < 0.01$; ***$P < 0.001$ compared by two-tailed t-test. (C) Comparison of relative activity of *Clock:Bmal1* constructs used in *Per1*-luciferase assay. The basal activity of the mutants are shown relative to wild-type *Clock:Bmal1* activity set to 1.0. (D) HEK293T cells were transfected with plasmid ratios used in *Per1*-luciferase assay (100 ng each Flag-*Clock* and Flag-*Bmal1*, and *Cry1* plasmid as indicated, scaled 4X for increase in culture dish area). Relative protein expression levels are shown by western blotting using indicated antibodies. GAPDH is shown as a loading control. (E) HEK293T cells were transfected with 1µg of the indicated plasmid. Relative protein expression levels are shown by western blotting using indicated antibodies.

2.3.3 Solution scattering studies highlight flexibility of clock protein complexes

To examine the behavior of the late circadian repressive complex in more detail, we employed the solution-based technique of small angle x-ray scattering (SAXS). We first performed SAXS analysis on the isolated CRY1 PHR and CLOCK:BMAL1 bHLH PAS-AB heterodimer individually to provide insight into their behavior before assembling the ternary complex. Scattering data were collected at several concentrations; both CRY1 PHR and CLOCK:BMAL1 bHLH PAS-AB samples were well-behaved, showing no radiation damage or aggregation as demonstrated by Guinier analysis (Supplementary Figure 2-3). The mass and radius of gyration determined from our analysis of the SAXS data agreed with values calculated from the crystal structures of CRY1 and CLOCK:BMAL1 bHLH PAS-AB. We then used the SAXS profile calculation server FoXS to generate a theoretical scattering profile of CRY1 PHR based on our crystal structure (Figure 2-4A) (25). Comparison of the theoretical scattering profile to the experimental data provided a fit within the noise (χ = 1.13), indicating that CRY1 PHR maintains a compact structure in solution that is similar to its crystal structure. Moreover, our crystal structure of CRY1 PHR fit well into a corresponding solution envelope consistent with the pairwise distribution function (Figure 2-4B and Figure 2-5A).

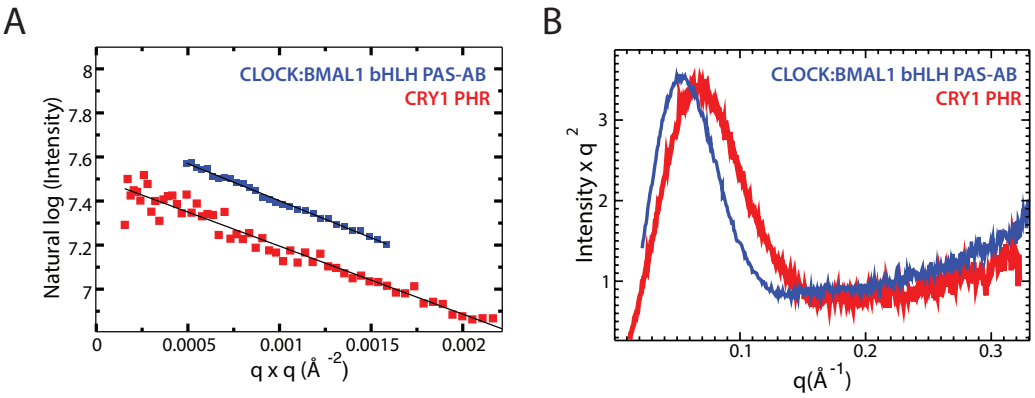

Supplementary Figure 2-3. Small angle x-ray scattering profile of CRY1 and CLOCK:BMAL1 bHLH PAS-AB.

(A) Guinier analysis of both CLOCK:BMAL1 bHLH PAS-AB and CRY1 PHR show no aggregation indicated by the linear dependence of log(I(q)) vs. q2. SAXS calculated molecular weight for CRY1 PHR: 45 kDa, CLOCK:BMAL1 bHLH PAS-AB: 78 kDa. (B) Kratky plot of CLOCK:BMAL1 dimer and CRY PHR show mostly folded character and an elongated shape.

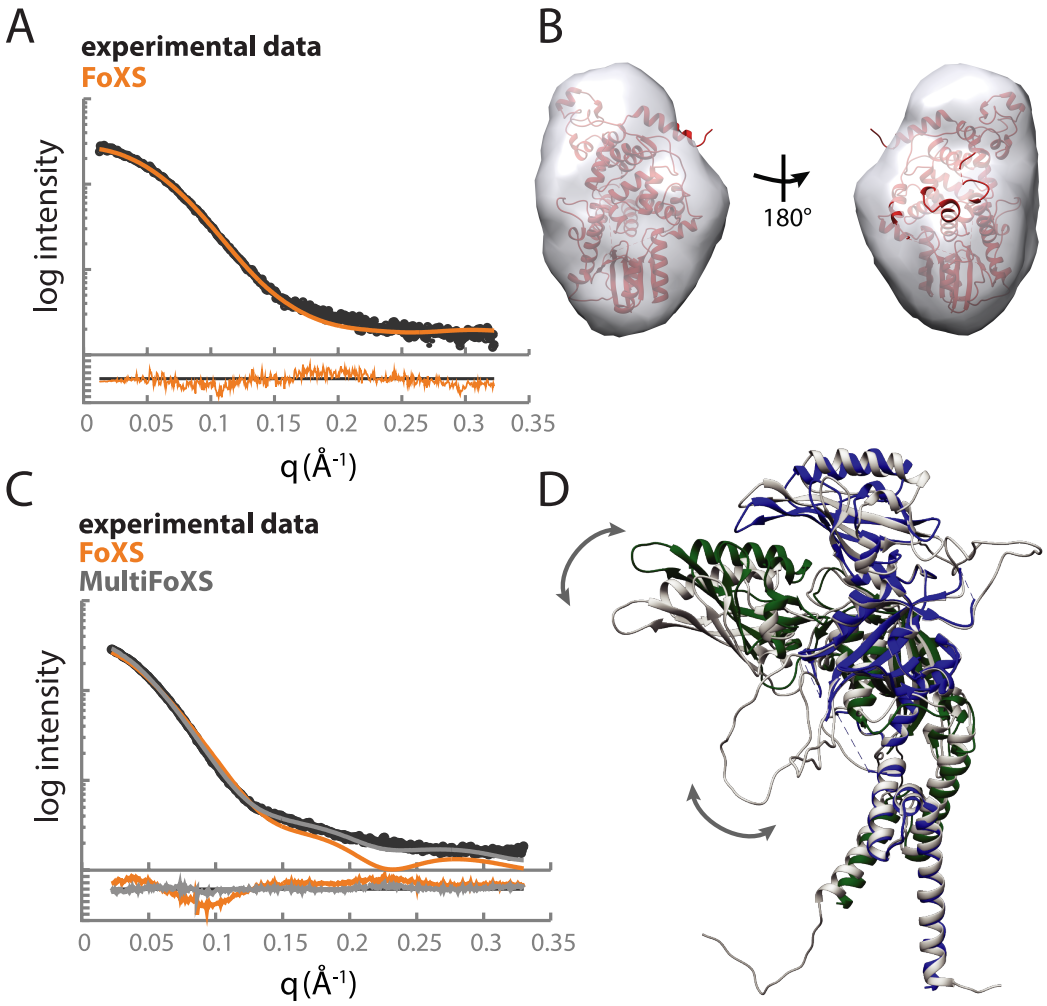

Figure 2-4 CRY1 PHR is compact and CLOCK:BMAL1 bHLH-PAS-AB dimer is highly flexible in solution.

(A) Solution x-ray scattering profile for CRY1 PHR (black) compared to the theoretical scattering profile for CRY1 PHR (PDB: 5T5X) calculated by the FoXS server (orange). Residuals for the fit are shown below with an overall $\chi = 1.13$. (B) The crystal structure of CRY1 PHR fit into the solution envelope generated from the SAXS data. (C) Solution x-ray scattering profile for the CLOCK:BMAL1 PAS-AB dimer (black) compared to the theoretical scattering profile calculated from PDB: 4F3L by the FoXS server (orange). Multi-state modeling of flexible regions within the dimer was performed with HingeProt paired with MultiFoXS. (D) A representative PDB from the top MultiFoXS hit that includes flexible loops not visible in the crystal structure (gray) aligned

with PDB: 4F3L using the PAS-A domain of BMAL1; CLOCK, green; BMAL1, blue. Arrows indicate regions of predicted flexibility.

By contrast, the experimental scattering profile of the CLOCK:BMAL1 bHLH PAS-AB heterodimer was not well fit by the theoretical scattering profile calculated from its crystal structure (FoXS, χ = 5.93) (Figure 2-4C). The PAS-A domains of CLOCK and BMAL1 both possess long, flexible loops that are not observed in the crystal structure (12% and 26% of the sequence, respectively) (21). To better describe the motions of these dynamic regions, we used MODELLER v9.15 to build in the missing fragments (26) and MultiFoXS to sample a range of possible conformations constrained by the SAXS data. As a result, we found conformations that fit the experimental scattering profile within the noise (χ = 1.43) (Figure 2-4D) (27, 28). The top structural ensemble resulting from this analysis highlighted two main findings: 1) the loops absent from the crystal structure are highly flexible in solution and contribute significantly to the scattering profile of the PAS domain core, and 2) the interface between CLOCK and BMAL1 PAS-B domains may be dynamic. Our best fits were obtained using a model where the PAS-B domains were able to sample an undocked state, suggesting that the PAS-B domains may exist in more than one state in solution. Given that multiple regions within the PAS domain core of CLOCK:BMAL1 are known to be important for its function (21, 29), characterization of their dynamic behavior in solution could begin to shed

light on their role in regulation of DNA binding and/or CLOCK:BMAL1 transcriptional activity.

2.3.4 Low resolution model of the CRY1:CLOCK:BMAL1 ternary complex

The use of SAXS to guide and validate computational models of protein complexes can be a powerful tool with high-resolution structures in hand for individual components (30). To generate a low resolution model for the ternary complex, we purified the CRY1 PHR together with the CLOCK:BMAL1 bHLH PAS-AB dimer as a stable ternary complex by size exclusion chromatography and collected SAXS data (Figure 2-5). Analysis of the scattering profiles confirmed the presence of all three molecules consistent with the molecular weight of the ternary complex (Supplementary Figure 2-4A-C). Furthermore, the ternary complex showed a maximum particle size (D_{max}) of 195 Å, much longer than either CRY1 or CLOCK:BMAL1 alone (86 Å and 115 Å, respectively) (Figure 2-5A). The elongated D_{max} of the ternary complex suggests that CRY1 extends out from the CLOCK:BMAL1 bHLH PAS-AB dimer.

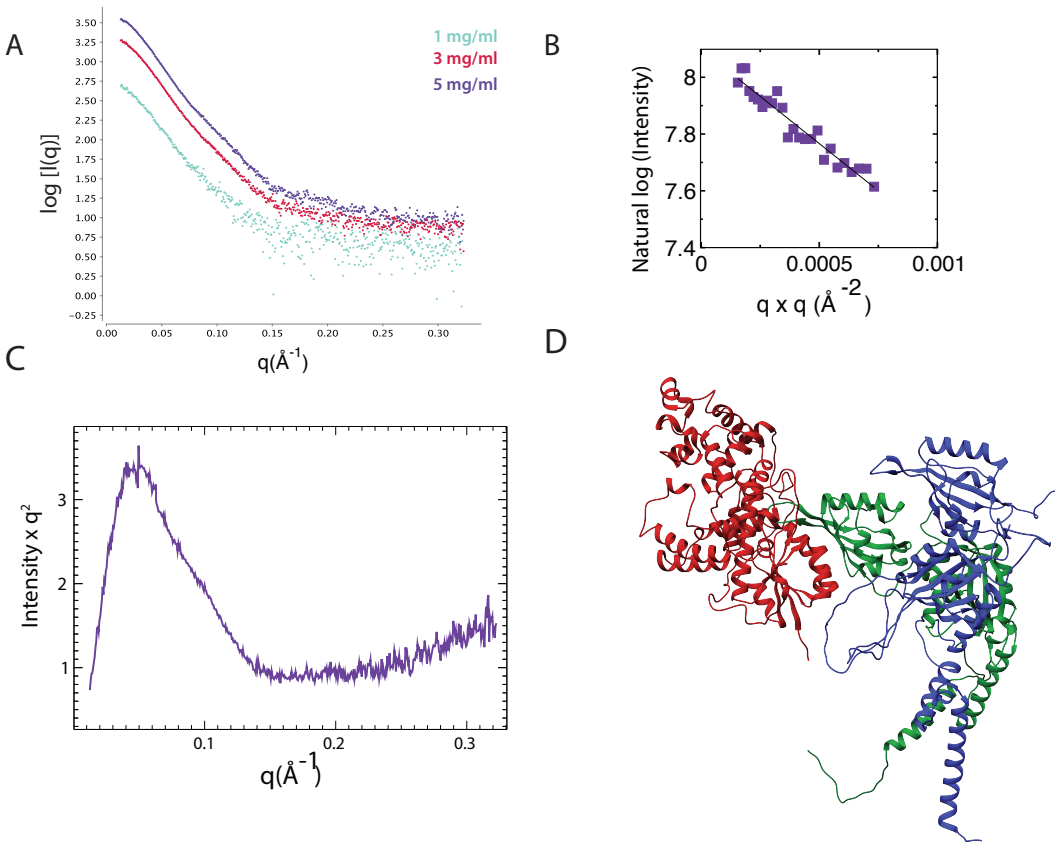

Supplementary Figure 2-4. Small angle x-ray scattering profile of the CRY1:CLOCK:BMAL1 repressive complex.

(A) Scattering traces of CRY1:CLOCK:BMAL1 ternary complex (CCB) at different concentrations are shown. These scattering plots were merged to generate the dataset as the input for FoXSDock. (B) Guinier analysis of CCB shows little or no aggregation of sample. SAXS calculated molecular weight of the ternary complex is 113 kDa. (C) Kratky plot shows the CCB complex indicates a folded mass with an elongated shape. (D) PDB of FoXSDock HADDOCK driven model that is amongst the top 20 nearly degenerate docking structures, $\chi = 2.74$.

We assessed models for the ternary complex using two methods. First, we used FoXSDock, which combines experimental data and analysis of calculated energies at predicted interfaces to best fit the SAXS profile of a

complex from two known structures. In agreement with the long D_{max}, the top FoXSDock model of the ternary complex (χ = 2.22) placed CRY1 alongside the PAS-AB core, docked at the CLOCK PAS-B interface (Figure 2-5B and *C*). Importantly, each of the statistically degenerate top ensembles independently placed CRY1 at the CLOCK PAS-B interface. However, there was some ambiguity in the positioning of CRY1 using the SAXS data alone, as the experimental scattering profile was equally fit by several orientations of CRY1 bound to the HI loop protrusion in CLOCK PAS-B. We then examined how well our HADDOCK model fit the data when aligned onto the bHLH PAS-AB dimer via the CLOCK PAS-B domain. As shown in Figure 2-5B, both methods provided reasonable fits to the experimental data, as shown by the overlay of a representative model of HADDOCK (FoXSDock HADDOCK χ = 2.74, Supplementary Figure 2-4D) with the best-scored SAXS-driven model (FoXSDock SAXS). Importantly, both of these models orient CRY1 such that its coiled-coil (CC) helix sits on the top of the ternary complex, available to make interactions with the BMAL1 TAD and other clock proteins that target this critical interface (Fig. 5*C*) (11, 24, 31, 32). Therefore, the integration of biochemistry, SAXS and computational modeling provide the first low resolution models of the CRY1:CLOCK:BMAL1 ternary complex.

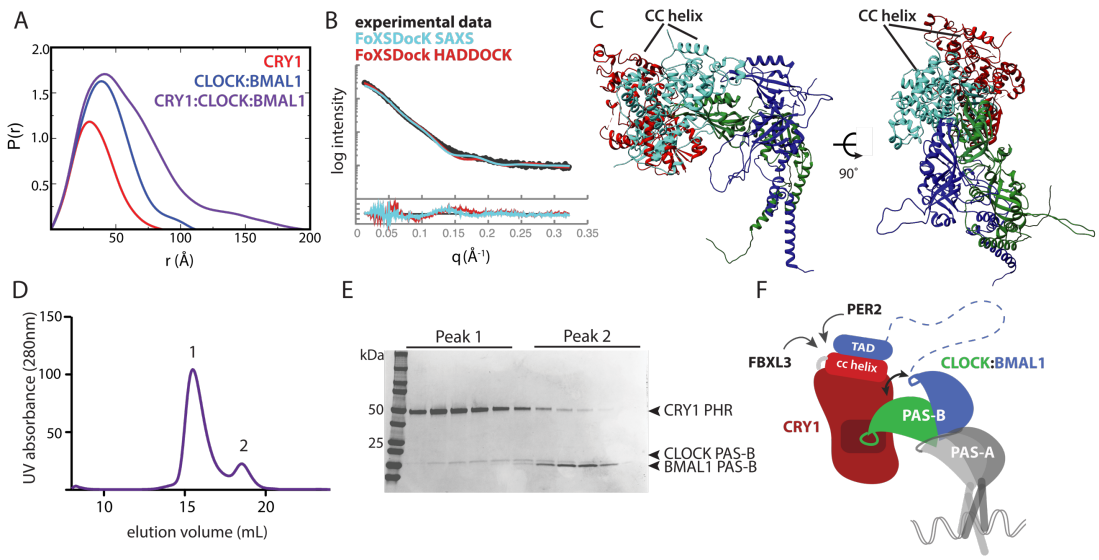

Figure 2-5. A model for the CRY1:CLOCK:BMAL1 repressive complex.

(A) Pairwise distribution function of complexes in the current study. CRY1 PHR, D_{max} = 86 Å (red); CLOCK:BMAL1 bHLH-PAS-AB dimer, D_{max}, 115 Å (blue); CRY1:CLOCK:BMAL1 ternary complex, D_{max}, 195 Å (purple). (B) Solution x-ray scattering curve for the ternary complex (black). Docking of CRY1 onto CLOCK:BMAL1 was restrained by the SAXS profile using FoXSDock. The model with the best combined SAXS and energy score is shown in light blue (χ = 2.22). The FoXSDock HADDOCK structure (red) is among these top scoring models that most closely represent the CRY1 PHR:CLOCK PAS-B HADDOCK model. (C) Top FoXSDock model (light blue) aligned with the HADDOCK model from Figure 2-3 using the CLOCK PAS-B domain. (D) SEC analysis of CRY1 PHR mixed with CLOCK:BMAL1 PAS-B heterodimer. Proteins were mixed and incubated at ~30 min. at 4°C and then injected on a S200 10/300 GL column. (E) Peak fractions were analyzed by SDS-PAGE and stained with Coomassie. (F) Cartoon model of the late repressive CRY1:CLOCK:BMAL1 repressive complex.

As with our SAXS studies of the CLOCK:BMAL1 heterodimer, scattering data for the ternary complex were best fit by a model where the PAS-B domains of CLOCK and BMAL1 were no longer tightly bound to each other, with the heterodimer maintained by interactions between the N-terminal PAS-A

domains (Figure 2-2C) and bHLH domains (Figure 2-5B). To test whether CRY1 binding influences the association of CLOCK and BMAL1 PAS-B domains with one another, we performed binding assays using the heterodimer of isolated PAS-B domains. The PAS-B domains of CLOCK and BMAL1 form a complex that co-migrates by size exclusion chromatography (Supplementary Figure 2-5). Using NMR and size exclusion chromatography, we confirmed that the PAS-B domains maintain a parallel, stacked orientation in isolation similar to that observed in the bHLH PAS-AB structure (21) (Figure 2-5A-*E*). We then asked if binding of CRY1 would influence the interaction between CLOCK and BMAL1 PAS-B domains in the dimer. Size exclusion chromatography of CRY1 with a preformed CLOCK:BMAL1 PAS-B dimer demonstrated that binding of CLOCK PAS-B to CRY1 disrupted its interaction with BMAL1 PAS-B (Figure 2-5D and *E*). Altogether, these data indicate that CRY1 binding to CLOCK:BMAL1 may influence the architecture of the PAS domain core.

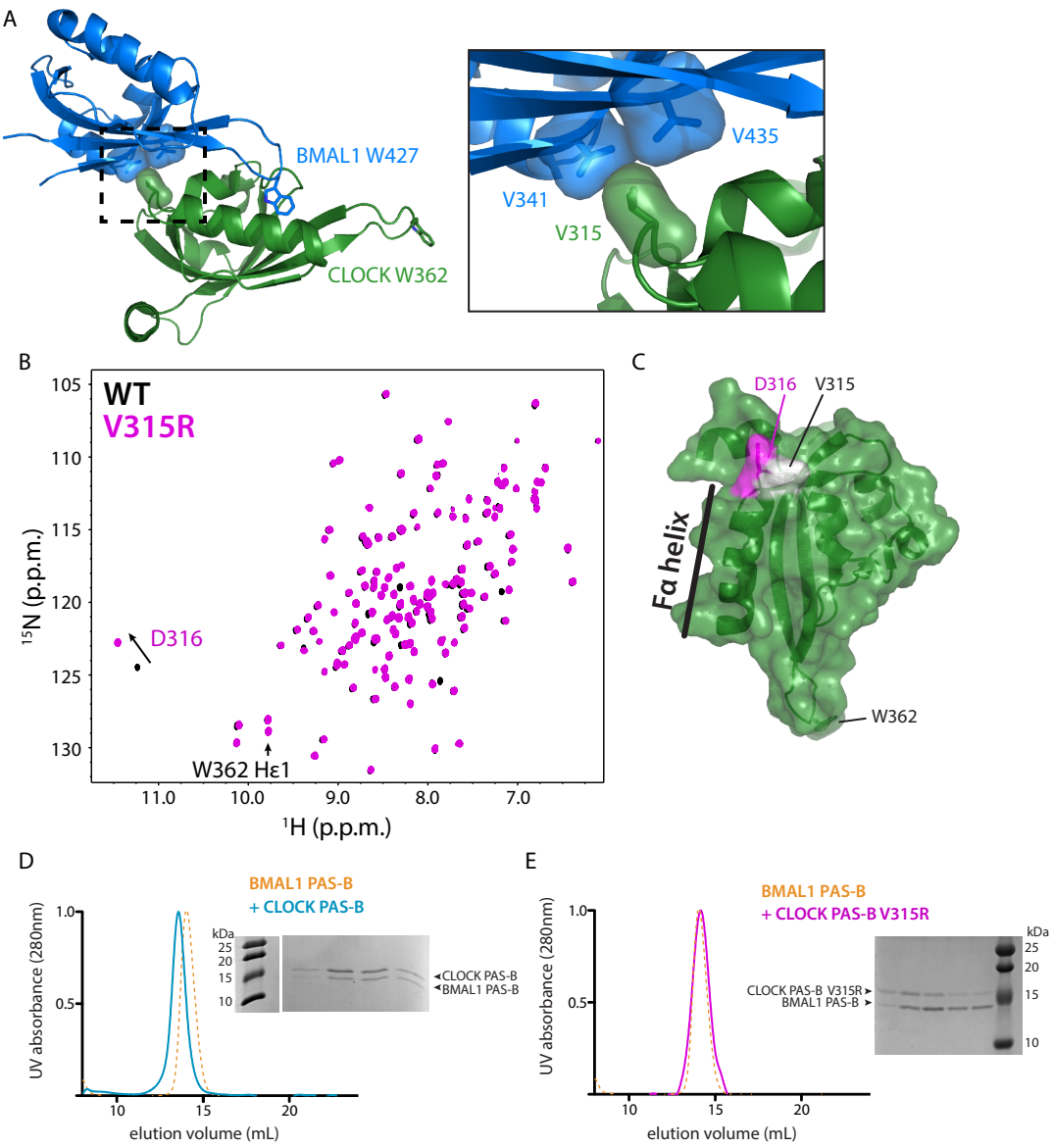

Supplementary Figure 2-5. CLOCK PAS-B and BMAL1 PAS-B form a native dimer in solution.

(A) Residue V315 in the Fα-helix of CLOCK PAS-B is at the native CLOCK:BMAL1 PAS-B interface in the bHLH PAS-AB dimer structure (PDB: 4F3L). Introduction of a charge V315R is predicted to disrupt native PAS-B dimer formation. (B) 15N HSQC of CLOCK PAS-B WT (black) and CLOCK PAS-B V315R mutant (pink). Peaks are well-dispersed indicative of a well-folded PAS domain protein. D316 shows a minor shift as it is located in close proximity to the mutation (See Panel C). (C) CLOCK PAS-B domain

highlighting residues assigned in the 5N HSQC spectra in Panel B. (D) Superdex 75 10/300 GL analytical size exclusion analysis of BMAL1 PAS-B and CLOCK PAS-B heterodimerization. Co-elution and a shift in elution volume indicate PAS-B dimer formation. BMAL1 PAS-B alone UV trace is shown in yellow dash. CLOCK:BMAL1 PAS-B dimer trace is displayed in solid blue. Peak fractions analyzed by SDS-PAGE gel electrophoresis. (E) CLOCK PAS-B V315R mutant no longer binds BMAL1 PAS-B. Size exclusion analysis on Superdex 75 10/300 GL of BMAL1 PAS-B and CLOCK PAS-B V315R no longer results in a gel shift or co-elution of the proteins. CLOCK PAS-B V315R incubated 1:1 with BMAL1 PAS-B is shown by the pink solid UV trace.

2.4 Discussion

Although it has been nearly two decades since the identification of cryptochromes and discovery of their essential role in circadian rhythms, it is still not clear how cryptochromes interact with CLOCK:BMAL1 to inhibit their activity and close the transcription/translation feedback loop of the clock (33). Probing the molecular details of transcription factor-regulator interactions in the clock is important, because they control 24-hour timekeeping and generate a vast network of clock-controlled genes that confer circadian timing to physiology and behavior. Here we show that CRY1 interacts directly with the CLOCK:BMAL1 PAS-AB core. We previously demonstrated that multivalent interactions with CLOCK PAS-B and the BMAL1 TAD are required for repression by CRY1 (11, 19). We suggest that CRY1 binding to the PAS-B domain of CLOCK keeps the repressor stably bound to the transcription factor, facilitating its sequestration of the BMAL1 TAD from coactivators (Figure 2-5F). In this way, multivalent interactions contribute to the potency of CRY1 as an

essential circadian repressor even when expressed at approximately stoichiometric levels with CLOCK:BMAL1 (18).

We identify a gain-of-function interaction at the secondary pocket of mouse CRY1 and demonstrate that it is required to bind CLOCK:BMAL1. This pocket is a remnant of cryptochromes' evolutionary relationship with the DNA damage repair enzyme, photolyase (17, 34). Photolyases use this pocket to bind an antenna chromophore that harvests photons in low light conditions, transferring the energy to a flavin molecule buried deep within the catalytic pocket to repair UV-induced thymine dimers (35). The photolyase homology region (PHR) of cryptochromes shares a high degree of structural similarity with photolyases, yet mammalian cryptochromes no longer repair DNA, and presumably have need for an antenna chromophore. We found that the bulky aromatic sidechain of CLOCK W362 is buried within the secondary pocket, exhibiting some similarity to light-harvesting chromophores that dock into the analogous pocket in photolyase. Due to the potent ability of the CLOCK W362A mutation to disrupt CRY1 binding, we propose that it could be a useful tool to specifically uncouple the direct regulation of CLOCK:BMAL1 by CRY1 in cells, allowing the functional dissection of different repressive complexes on CLOCK:BMAL1 that appear throughout the evening (7, 36).

PAS domains play crucial roles in the regulation of bHLH-PAS transcription factors by mediating interactions between bHLH-PAS partners and recruitment of regulatory proteins (37, 38). We focused here on the role

that the CLOCK PAS-B domain HI loop plays in binding CRY1, but HI loops in the PAS-B domains of other clock proteins also play central roles in establishing clock protein complexes. For example, HI loop tryptophans in PERIOD proteins mediate their PAS domain-dependent hetero- and homodimerization (39, 40), while the analogous tryptophan in BMAL1 PAS-B embeds itself within an internal pocket in CLOCK PAS-B to stabilize the PAS-B dimer (21). Our analysis of the SAXS data shows that the CLOCK:BMAL1 PAS-B interface likely samples open and closed states in solution. We also showed that CRY1 binding further stabilizes the open state by disrupting dimerization of PAS-B domains. Small molecules that bind to the internal pocket of the related hypoxia-inducible factor 2α PAS-B domain allosterically regulate protein interactions at the PAS-B domain (41), suggesting that CRY1 binding could act similarly to regulate docking of BMAL1 through the central pocket of CLOCK. These data highlight the potential importance of protein dynamics and allosteric regulation in controlling the architecture of clock protein complexes.

The combination of static, high-resolution structures from x-ray crystallography with solution studies of proteins by NMR and SAXS is needed to fully describe the role of flexibility in regulating formation of protein complexes. By studying the structural dynamics of the core bHLH PAS-AB dimer of CLOCK:BMAL1 in solution, we pave the way to study new, highly flexible regions of the transcription factor that control circadian rhythms. For

example, our best-fit SAXS models indicate that long, flexible loops in the PAS-A domains, not observed in the crystal structure, are highly dynamic and sample a large area around the core PAS domain dimer. This flexibility could play a role in regulating CLOCK:BMAL1 function, as the longest of these loops, located within the BMAL1 PAS-A domain, is modified by sumoylation to control CLOCK:BMAL1 activity (29). These data also lay the foundation for future studies on the role of the disordered CRY1 C-terminal extension, which controls circadian period and amplitude (42). Understanding the structural basis for mutual exclusivity or synergy of clock protein interactions will provide a framework to elucidate the mechanistic underpinnings of the transcription-based mammalian circadian clock.

2.5 Materials and Methods

2.5.1 Recombinant protein expression and purification.

Using the baculovirus expression system (Invitrogen) His_6-tagged mouse CRY1 PHR was expressed in Sf9 suspension insect cells (Expression Systems). His_6-tagged mouse CLOCK bHLH PAS-AB domains (residues 26 - 384) and native mouse BMAL1 bHLH PAS-AB (residues 68 - 453) were cloned into pFastBac HTb and pFastBac1 vectors, respectively. CLOCK PAS-B (residues 261–395), CLOCK PAS-AB (residues 93-395), and BMAL1 PAS-B (residues 329 – 441) were expressed in *E. coli* Rosetta2 (DE3) cells as a fusion to the solubilizing tags His_6-NusA and His_6-B1 domain of *Streptococcal* protein G (GB1).

For His_6-tagged mouse CRY1 PHR (amino acids 1–491) Sf9 suspension cells were infected with a P3 virus at 1.5 x 10^6 cells/mL and grown for 72 hours. Following brief centrifugation at 4K rpm, cells were resuspended in 50 mM Tris pH 7.5, 200 mM NaCl, 20 mM imidazole, 10% glycerol, 0.2% triton x-100, 0.1% NP40, 0.4% Tween-20, 5 mM β-mercaptoethanol and EDTA-free protease inhibitors (Pierce). Cells were lysed using a microfluidizer followed by brief sonication for 15 sec. on/30 sec. off for 3 pulses at 40% amplitude. Lysate was clarified at 37K rpm, 4°C for 1 hour. The protein was then isolated by Ni^{2+}-nitrilotriacetic acid affinity chromatography (QIAGEN) followed by ion exchange and size-exclusion chromatography. The protein was isolated by Ni^{2+}-nitrilotriacetic acid affinity chromatography (QIAGEN). The eluted protein was further purified by ion exchange and size-exclusion chromatography into 20 mM HEPES (pH 7.5), 125 mM NaCl, 5% glycerol and 2 mM TCEP.

Sf9 insect cells (Expression systems) co-expressing 6xHis tagged mouse CLOCK and BMAL1 bHLH PASAB for 65 hours were lysed by sonication in lysis buffer containing 50mM Na2HPO4 pH 8.0, 300 mM NaCl, 10% v/v glycerol, 15mM imidazole, 2.5mM CHAPS, 5mM β-mercaptoethanol and EDTA-free protease inhibitors (Thermo). The clarified cell lysate was applied onto a NiNTA Agarose column (Qiagen) and bound protein was eluted with a gradient of 15mM-500mM imidazole. Pooled fractions were buffer exchanged into 20mM Tris pH 8.0, 200mM NaCl,10% v/v glycerol, 1mM DTT. His tag was removed by treatment with TEV Protease overnight at 4°C. The

CLOCK:BMAL1 bHLH PASAB complex was further purified using a heparin column followed by a size exclusion chromatography into 20 mM Hepes pH 7.5, 300mM NaCl, 5% v/v glycerol and 1mM DTT.

For CLOCK PAS-B, CLOCK PAS-AB and BMAL1 PAS-B expressed in Rosetta (DE3) cells; protein expression was induced with 0.5 mM IPTG at an OD_{600} of 0.8, and grown for an additional 16 h at 18 °C. Soluble protein was purified by Ni^{2+}-nitrilotriacetic acid affinity chromatography (QIAGEN), followed by cleavage of the tag with His_6-TEV protease overnight at 4°C. Subsequent Ni^{2+}-nitrilotriacetic acid affinity chromatography was performed to remove the protease and cleaved tag. The protein was further purified by size-exclusion chromatography on a Superdex 75 16/60 prep grade column (GE Healthcare) equilibrated with 20 mM HEPES pH 7.5, 125 mM NaCl, 5% glycerol and 2 mM TCEP. Point mutations in CRY1 PHR, CLOCK PAS-B and CLOCK PAS-AB were introduced by site-directed mutagenesis and validated by sequencing.

BMAL1 PAS-AB (residues 136-441) was expressed in *E. coli* SoluBL21 cells as a fusion to the solubilizing tag Glutathione S-Transferase (GST). Protein was expressed via the method described above. Soluble protein was purified by GST affinity chromatography (GE Healthcare), followed by cleavage of the tag with His_6-TEV protease overnight at 4°C. Subsequent Ni^{2+}-nitrilotriacetic acid and GST affinity chromatography were performed to remove the protease and cleaved tag. The protein was further purified by size-exclusion chromatography as described above.

2.5.2 Analytical size-exclusion chromatography.

For analysis of complex formation by size-exclusion chromatography (SEC), purified proteins were injected on a Superdex 200 10/300 GL or Superdex 75 10/300 GL analytical column at 10-50 μM (~250μL, 1:1 molar ratio) in 20 mM HEPES pH 7.5, 125 mM NaCl, 5% glycerol and 2 mM TCEP. Proteins were incubated for ~30 min. or overnight and analyzed by SEC. All size-exclusion columns were calibrated with a low-molecular-weight gel filtration standards kit (GE Healthcare Life Sciences). The content of each peak was evaluated by SDS-PAGE and Coomassie staining.

2.5.3 Transcriptional reporter assays and western blotting.

Per1-Luc reporter gene assays investigating repression by CRY1 were performed as before (11). Briefly, the following plasmids were transfected in duplicate into HEK293T cells in a 48-well plate using LT-1 transfection reagent (Mirus): 5 ng pGL3 *Per1-Luc* reporter, 100 ng each pSG5 mouse Flag-*Bmal1* and pSG5 mouse His_6Flag-*Clock*, and pcDNA3 mouse *Cry1* (untagged) in increasing amounts as indicated; empty pcDNA4 vector was used to normalize total plasmid levels to 800 ng DNA/well. Cells were harvested 30 hours after transfection using Passive Lysis Buffer (NEB) and luciferase activity assayed using Bright-Glo luciferin reagent (Promega). Each reporter assay was repeated three independent times. To compare expression of Flag-tagged *Clock*, *Bmal1* and untagged *Cry1* genes, cells were lysed in 50mM HEPES pH 7.5, 150mM NaCl, 1mM EDTA, 5% glycerol and 1% Triton X-100. Immunoblotting was done with the HRP-conjugated rabbit polyclonal OctA-Probe antibody (D-8) (Santa Cruz Biotechnology cat. no. sc-

807), rabbit polyclonal anti-CRY1 (H-84) (Santa Cruz Biotechnology cat. no. sc-33177) or mouse monoclonal GAPDH (G-9) (Santa Cruz Biotechnology, sc-365-062). HRP-conjugated secondary antibodies were used at 1:10,000 (Santa Cruz Biotechnology) in TBST. Western signal was detected using Clarity ECL reagent (Bio-Rad) and visualized on a ChemiDoc XRS+ imager (Bio-Rad).

2.5.4 HADDOCK modeling.

The CLOCK PAS-B molecule (residues 261 – 384) used in the modeling was generated from the CLOCK:BMAL1 bHLH-PAS-AB structure (PDB:4F3L). The CRY1 input molecule used was our 1.8Å resolution structure (PDB: 5T5X) After generating the protein components; the structures were docked as a complex using the HADDOCK 2.2 server (22). The protocol for docking and refinement was executed using the default parameter sets on the server and defining passive residues automatically around the active residues.

2.5.5 GST pulldown assays.

GST CLOCK PAS-B and GST BMAL1 PAS-AB were expressed in *E. coli* as described above. Soluble proteins were purified using GS4B resin (GE Healthcare). GST-tagged proteins were eluted with 10 mM glutathione and peak elution was desalted into 20 mM HEPES pH 7.5, 125 mM NaCl, 5% glycerol and 2 mM TCEP. GST pulldowns contained 1 μM GST-tagged protein (bait) and 5 μM CRY1 (prey) and ~10 μL glutathione agarose in a 200 μL reaction volume. After rotation at 4°C overnight, reactions were washed 3 times

with the above buffer and eluted with 6X SDS. Samples were boiled for ~ 5 min. and loaded on an SDS-PAGE gel for visualization by Coomassie stain.

2.5.6 Small angle x-ray scattering (SAXS).

SAXS data were collected on the SIBYLS beamline (12.3.1) at the Advanced Light Source (Lawrence Berkeley National Laboratory). Multiple exposures of three concentrations (1, 3, and 5 mg/mL) of freshly purified protein were taken to check for concentration dependence of scattering and radiation damage (neither was detected). Briefly, data were merged using PRIMUS, and the radius of gyration was determined using the Guinier approximation. The pair-distance distribution function [P(r)] and maximal particle size (D_{max}) were generated in GNOM, and the output data were used by GASBOR to calculate 10 independent solution envelopes that were averaged together using DAMAVER. The improved model of the solution structure was used in UCSF Chimera to fit into the averaged solution envelope.

SAXS modeling was performed using a combination of programs: FoXS (43), MultiFoXS (28) and FoXSDock (25, 44). Conformational sampling of the CLOCK:BMAL1 bHLH PAS-AB was done by MultiFoXS starting from the crystal structure (PDB: 4F3L) with missing fragments built by MODELLER (26). HingeProt (27) was used to determine the hinge regions within the CLOCK:BMAL1 heterodimer with PDB: 4F3L as the input. The input to FoXSDock was the HADDOCK active residues as the binding site and (Fig. 3) the SAXS profile of the CRY1:CLOCK:BMAL1 bHLH PAS-AB complex. The

entire sequences of CRY1 and CLOCK:BMAL1 bHLH PAS-AB subject to crystallography and SAXS, including vector artifacts after TEV cleavage, were used in the modeling (21).

2.5.7 X-ray crystallography.

CRY1 protein was purified as described above. The protein was concentrated to 5 mg/mL and crystallized by hanging-drop vapor diffusion at 22°C. Crystals formed in a 1:1 ratio of protein to precipitant in 0.1 M MES pH 6.8, 10 mM EDTA, 15% (vol/vol) PEG3350. Crystals were frozen in the proper well buffer with 20% (vol/vol) PEG400 as a cryoprotectant. Data were collected at the Advanced Light Source, Lawrence Berkeley National Laboratory at Beamline (BL5.0.1). Diffraction spots were integrated using MOSFLM (45), and data were merged and scaled using Scala (46). Phases were first solved for by molecular replacement with a previous apo CRY1 structure (PDB: 4K0R) using Phaser (47). The structure was built with Coot and refined with PHENIX (48, 49). Coordinates and structure factors have been deposited in PDB (PDB ID: 5T5X).

2.5.8 Nuclear magnetic resonance (NMR).

NMR experiments were conducted at 25°C. on a Varian INOVA 600-MHz spectrometer equipped with 1H, 13C, 15N triple resonance, Z-axis pulsed field gradient probes. All NMR data were processed using NMRPipe/NMRDraw (50). Chemical shift assignments were made by mutation and by analogy to a far downfield-shifted peak found in all PAS domain HSQC spectra (51, 52) for

the residue that sits at the top of the helical dipole for the Fα helix (D316 in CLOCK PAS-B). 1H-15N HSQC spectra were collected on 100 μM 15N CLOCK PAS-B WT or V315R mutant in 50 mM Tris, pH 7.5, 50 mM NaCl, 2 mM TCEP, 10% (vol/vol) D_2O. HSQC data were visualized with NMRViewJ (53).

2.6 References

1. Partch CL, Green CB, & Takahashi JS (2014) Molecular architecture of the mammalian circadian clock. Trends in cell biology 24(2):90-99.
2. Zhang R, Lahens NF, Ballance HI, Hughes ME, & Hogenesch JB (2014) A circadian gene expression atlas in mammals: implications for biology and medicine. Proceedings of the National Academy of Sciences of the United States of America 111(45):16219-16224.
3. Bunger M, et al. (2000) Mop3 is an essential component of the master circadian pacemaker in mammals. Cell 103(7):1009-1017.
4. Takahashi J, Hong H-K, Ko C, & McDearmon E (2008) The genetics of mammalian circadian order and disorder: implications for physiology and disease. Nature reviews. Genetics 9(10):764-775.
5. Brown S, et al. (2005) PERIOD1-associated proteins modulate the negative limb of the mammalian circadian oscillator. Science 308(5722):693-696.
6. Kim JY, Kwak PB, & Weitz CJ (2014) Specificity in Circadian Clock Feedback from Targeted Reconstitution of the NuRD Corepressor. Molecular cell 56(6):738-748.
7. Koike N, et al. (2012) Transcriptional architecture and chromatin landscape of the core circadian clock in mammals. Science 338(6105):349-354.

8. Ye R, et al. (2014) Dual modes of CLOCK:BMAL1 inhibition mediated by Cryptochrome and Period proteins in the mammalian circadian clock. Genes & development 28(18):1989-1998.
9. Chen R, et al. (2009) Rhythmic PER abundance defines a critical nodal point for negative feedback within the circadian clock mechanism. Molecular cell 36(3):417-430.
10. Ye R, Selby C, Ozturk N, Annayev Y, & Sancar A (2011) Biochemical analysis of the canonical model for the mammalian circadian clock. The Journal of biological chemistry 286(29):25891-25902.
11. Xu H, et al. (2015) Cryptochrome 1 regulates the circadian clock through dynamic interactions with the BMAL1 C terminus. Nat Struct Mol Biol 22(6):476-484.
12. Sancar A (2003) Structure and function of DNA photolyase and cryptochrome blue-light photoreceptors. Chemical reviews 103(6):2203-2237.
13. van der Horst G, et al. (1999) Mammalian Cry1 and Cry2 are essential for maintenance of circadian rhythms. Nature 398(6728):627-630.
14. Kume K, et al. (1999) mCRY1 and mCRY2 are essential components of the negative limb of the circadian clock feedback loop. Cell 98(2):193-205.
15. Vitaterna M, et al. (1999) Differential regulation of mammalian period genes and circadian rhythmicity by cryptochromes 1 and 2. Proceedings of the National Academy of Sciences of the United States of America 96(21):12114-12119.
16. Czarna A, et al. (2011) Quantitative analyses of cryptochrome-mBMAL1 interactions: mechanistic insights into the transcriptional regulation of the mammalian circadian clock. The Journal of biological chemistry 286(25):22414-22425.
17. Czarna A, et al. (2013) Structures of Drosophila cryptochrome and mouse cryptochrome1 provide insight into circadian function. Cell 153(6):1394-1405.

18. Lee Y, Chen R, Lee H-m, & Lee C (2011) Stoichiometric relationship among clock proteins determines robustness of circadian rhythms. The Journal of biological chemistry 286(9):7033-7042.
19. Sato T, et al. (2006) Feedback repression is required for mammalian circadian clock function. Nature genetics 38(3):312-319.
20. Zhao W-N, et al. (2007) CIPC is a mammalian circadian clock protein without invertebrate homologues. Nature cell biology 9(3):268-275.
21. Huang N, et al. (2012) Crystal structure of the heterodimeric CLOCK:BMAL1 transcriptional activator complex. Science 337(6091):189-194.
22. van Zundert GC, et al. (2016) The HADDOCK2.2 Web Server: User-Friendly Integrative Modeling of Biomolecular Complexes. Journal of molecular biology 428(4):720-725.
23. Dominguez C, Boelens R, & Bonvin AM (2003) HADDOCK: a protein-protein docking approach based on biochemical or biophysical information. Journal of the American Chemical Society 125(7):1731-1737.
24. Nangle SN, et al. (2014) Molecular assembly of the period-cryptochrome circadian transcriptional repressor complex. Elife 3:e03674.
25. Schneidman-Duhovny D, Hammel M, & Sali A (2010) FoXS: a web server for rapid computation and fitting of SAXS profiles. Nucleic acids research 38(Web Server issue):W540-544.
26. Webb B & Sali A (2014) Comparative Protein Structure Modeling Using MODELLER. Current protocols in bioinformatics / editoral board, Andreas D. Baxevanis ... [et al.] 47:5 6 1-32.
27. Emekli U, Schneidman-Duhovny D, Wolfson HJ, Nussinov R, & Haliloglu T (2008) HingeProt: automated prediction of hinges in protein structures. Proteins 70(4):1219-1227.
28. Schneidman-Duhovny D, Hammel M, Tainer JA, & Sali A (2016) FoXS, FoXSDock and MultiFoXS: Single-state and multi-state structural modeling of

proteins and their complexes based on SAXS profiles. Nucleic acids research 44(W1):W424-429.

29. Cardone L, et al. (2005) Circadian clock control by SUMOylation of BMAL1. Science 309(5739):1390-1394.

30. Putnam CD, Hammel M, Hura GL, & Tainer JA (2007) X-ray solution scattering (SAXS) combined with crystallography and computation: defining accurate macromolecular structures, conformations and assemblies in solution. Q Rev Biophys 40(3):191-285.

31. Schmalen I, et al. (2014) Interaction of circadian clock proteins CRY1 and PER2 is modulated by zinc binding and disulfide bond formation. Cell 157(5):1203-1215.

32. Xing W, et al. (2013) SCF(FBXL3) ubiquitin ligase targets cryptochromes at their cofactor pocket. Nature 496(7443):64-68.

33. Michael AK, Fribourgh, J.L., Van Gelder, R. N., Partch, C.L. (2016) Animal cryptochromes: divergent roles in light perception, circadian timekeeping and beyond. Photochemistry and photobiology In press.

34. Selby CP & Sancar A (2012) The second chromophore in Drosophila photolyase/cryptochrome family photoreceptors. Biochemistry 51(1):167-171.

35. Zhong D (2015) Electron transfer mechanisms of DNA repair by photolyase. Annu Rev Phys Chem 66:691-715.

36. Gustafson CL & Partch CL (2015) Emerging models for the molecular basis of Mammalian circadian timing. Biochemistry 54(2):134-149.

37. Partch CL & Gardner KH (2010) Coactivator recruitment: a new role for PAS domains in transcriptional regulation by the bHLH-PAS family. Journal of cellular physiology 223(3):553-557.

38. Partch CL & Gardner KH (2011) Coactivators necessary for transcriptional output of the hypoxia inducible factor, HIF, are directly recruited by ARNT PAS-B. Proceedings of the National Academy of Sciences of the United States of America 108(19):7739-7744.

39. Hennig S, et al. (2009) Structural and functional analyses of PAS domain interactions of the clock proteins Drosophila PERIOD and mouse PERIOD2. PLoS biology 7(4).

40. Kucera N, et al. (2012) Unwinding the differences of the mammalian PERIOD clock proteins from crystal structure to cellular function. Proceedings of the National Academy of Sciences of the United States of America 109(9):3311-3316.

41. Scheuermann TH, et al. (2013) Allosteric inhibition of hypoxia inducible factor-2 with small molecules. Nat Chem Biol 9(4):271-276.

42. Khan S, et al. (2012) Identification of a novel cryptochrome differentiating domain required for feedback repression in circadian clock function. The Journal of biological chemistry 287(31):25917-25926.

43. Pettersen EF, et al. (2004) UCSF Chimera--a visualization system for exploratory research and analysis. J Comput Chem 25(13):1605-1612.

44. Schneidman-Duhovny D, Hammel M, Tainer JA, & Sali A (2013) Accurate SAXS profile computation and its assessment by contrast variation experiments. Biophysical journal 105(4):962-974.

45. Schneidman-Duhovny D, Hammel M, & Sali A (2011) Macromolecular docking restrained by a small angle X-ray scattering profile. J Struct Biol 173(3):461-471.

46. Leslie AG (2006) The integration of macromolecular diffraction data. Acta Crystallogr D Biol Crystallogr 62(Pt 1):48-57.

47. Collaborative Computational Project N (1994) The CCP4 suite: programs for protein crystallography. Acta Crystallogr D Biol Crystallogr 50(Pt 5):760-763.

48. McCoy AJ (2007) Solving structures of protein complexes by molecular replacement with Phaser. Acta Crystallogr D Biol Crystallogr 63(Pt 1):32-41.

49. Emsley P & Cowtan K (2004) Coot: model-building tools for molecular graphics. Acta Crystallogr D Biol Crystallogr 60(Pt 12 Pt 1):2126-2132.

50. Adams PD, et al. (2010) PHENIX: a comprehensive Python-based system for macromolecular structure solution. Acta Crystallogr D Biol Crystallogr 66(Pt 2):213-221.
51. Delaglio F, et al. (1995) NMRPipe: a multidimensional spectral processing system based on UNIX pipes. Journal of biomolecular NMR 6(3):277-293.
52. Card PB, Erbel PJ, & Gardner KH (2005) Structural basis of ARNT PAS-B dimerization: use of a common beta-sheet interface for hetero- and homodimerization. Journal of molecular biology 353(3):664-677.
53. Erbel PJ, Card PB, Karakuzu O, Bruick RK, & Gardner KH (2003) Structural basis for PAS domain heterodimerization in the basic helix--loop--helix-PAS transcription factor hypoxia-inducible factor. Proceedings of the National Academy of Sciences of the United States of America 100(26):15504-15509.
54. Johnson B (2004) Using NMRView to visualize and analyze the NMR spectra of macromolecules. Methods in molecular biology (Clifton, N.J.) 278:313-352.

3 CHAPTER 3 — BHLH-PAS PROTEINS: FUNCTIONAL SPECIFICATION THROUGH MODULAR DOMAIN ARCHITECTURE

3.1 Abstract

The basic helix-loop-helix PER-ARNT-SIM (bHLH-PAS) family of transcription factors respond to a wide range of external stimuli to regulate diverse biological processes ranging from development to circadian rhythms. These proteins selectively heterodimerize through relatively well conserved bHLH and PAS domains, while differences in C-terminal regulatory domains confer opposing activities to either stimulate or repress transcription. The evolution of modular regulatory domains and the ability to selectively dimerize with different subunits within the family allows fine-tuning of gene expression through temporal and tissue-specific expression of bHLH-PAS subunits.

3.2 Introduction

The bHLH-PAS family of transcription factors is well conserved in metazoans from *C. elegans* to humans (1). These proteins play an integral role in maintaining cellular health by acting as environmental sensors that respond to a wide range of external stimuli such as oxygen (hypoxia), harmful chemicals (xenobiotic), and light (circadian) (2–4). This review will examine how the modularity of this protein family enables diversity in recognition of cellular signaling cues and subsequent regulation of transcriptional activity. Pairwise interactions between the DNA-binding bHLH and PAS domains establish the general architecture of the heterodimeric transcription factors, while C-terminal

regulatory motifs control activity of the complexes. The function of bHLH-PAS proteins has been elaborated throughout evolution through domain shuffling amongst the regulatory motifs to confer new functionality. This review will also discuss how the activity of bHLH-PAS transcription factors is differentially attenuated in a tissue-specific manner by evolutionarily related proteins to regulate development and the cellular response to environmental stimulus.

3.3 Discussion

3.3.1 The PAS domain

The ability of the bHLH-PAS family to sense and respond to diverse cellular cues can be attributed in many ways to their PAS domain. The PAS fold is the distinguishing feature of bHLH-PAS proteins, showing the highest degree of evolutionary conservation between even distantly related members of the family. The canonical PAS domain consists of a five-stranded antiparallel β-sheet flanked by α-helices that, despite sharing a rather small, globular fold, can bind a wide array of chemically diverse cofactors and ligands (5)(6).

In PAS-mediated signal transduction pathways in prokaryotes and lower eukaryotes, the binding of small molecules within a hydrophilic cavity buried within the PAS domain typically modulates protein activity to initiate a cellular signaling response (7,8). However, in metazoan bHLH-PAS proteins, the ability to couple intrinsic ligand binding with transcriptional regulation appears to have been retained only in the aryl hydrocarbon receptor (AhR) pathway. The

second of two tandem PAS domains (PAS-B) in AhR binds polycyclic aromatic hydrocarbons such as dioxin to serve as a xenobiotic detector (9). Ligand binding induces translocation of AhR to the nucleus where it interacts with its obligate heterodimeric partner ARNT (aryl hydrocarbon receptor nuclear translocator) to initiate activation of a vast transcriptional program involved in detoxification of xenobiotics (10). To date, no other bHLH-PAS proteins have been shown to co-purify with endogenous ligands, leaving it open to speculation whether they may be regulated by small molecule metabolites. Despite this apparent lack of regulation *in vivo*, high-resolution x-ray crystal structures of mammalian bHLH-PAS proteins reveal the presence of buried, solvated cavities located within the PAS domains (11–13). The localization of hydrophilic cavities within mammalian PAS domains suggests that they may have the capacity to bind ligands internally. Moreover, targeted screening of PAS domains from HIF-2α and its obligate heterodimeric partner ARNT have led to the discovery of selective, high affinity exogenous small molecules that bind within the PAS domains to regulate protein interaction, suggesting that they may have potential applications for therapeutic modulation of bHLH-PAS function (12,14). The ability to target specific bHLH-PAS transcription factors with PAS-binding small molecules and elicit tight control over gene expression pathways highlights the importance of gaining additional mechanistic information into this family of proteins.

PAS domains also mediate protein-protein interactions that occur through several distinct interfaces on the small, globular fold (5). PAS domains typically use their exposed ☙-sheet to dimerize with other PAS domains, but recently the opposing α-helical surface has been shown to mediate heterotypic interactions with other PAS domains and regulatory proteins (13,15,16). Proteins in the bHLH-PAS family predominantly use specific interactions between tandem PAS domains (denoted PAS-A and PAS-B) to form stable, heterodimeric transcription factor complexes. Mutation of PAS domains decreases complex formation to regulate transcriptional activity and can even alter selectivity of subunits for their heterodimeric partners (13,17) Therefore, PAS-mediated dimerization not only dictates selectivity for bHLH-PAS subunits for one another, but also facilitates DNA binding by forming the dimeric bHLH domain. (13,18)

3.3.2 Modularity within the bHLH-PAS family

If structural conservation within the PAS domains allows heterodimerization within the bHLH-PAS family, the C-terminal regulatory domains contain transactivation (TAD) or repressor domains that control their activity. Although members of the family share a relatively high degree of sequence similarity within the bHLH and PAS domains, a sequence alignment clearly segregates genes together into clusters that regulate the same pathway (Figure 3-1). These findings highlight the importance of letting conservation guide identification of functional subclasses within bHLH-PAS proteins and

provide insight into potential mechanisms of regulation (10). While the N-terminus of this protein family is structured by the presence of bHLH and PAS domains, the C-terminus tends to be intrinsically disordered with only short regions of predicted secondary structure, a common feature of transcription factors that serve as scaffolds for assembly of the eukaryotic transcriptional machinery(13,19). The C-terminal regulatory domains also show a higher degree of divergence among family members and confer functional constraints by interacting with pathway-specific transcriptional regulators and controlling stability of the complex. For example, the stability of HIF-1α is regulated by oxygen concentration through conserved prolines in the oxygen-dependent degradation domain (ODD) and an asparagine in the TAD. Under normoxic conditions, proline hydroxylation association of HIF1-α with the von Hippel-Lindau E3 ubiquitin ligase, which targets HIF-1α for proteosome-mediated degradation (20).

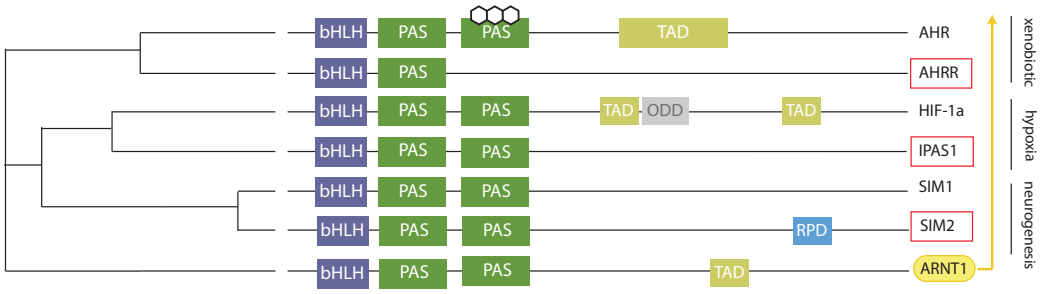

Figure 3-1 bHLH-PAS transcription factors are evolutionarily related and have homologous repressors with internal deletions.

Many of the important bHLH-PAS signaling pathways are regulated by paralog repressors that share high sequence homology (line length within cladogram represents evolutionary distance) with the activator, but lack a domain that the positive element possesses. SIM2 represses the neurogenesis pathway and lacks a transactivation domain (TAD). IPAS1 attenuates the hypoxia response, but lacks a transactivation domain and cannot form a DNA-bound complex. AhRR cannot bind xenobiotics as AhR can (denoted with the chemical symbol) and therefore represses AhR:ARNT activity by competing for ARNT binding. Yellow dashed line indicates that ARNT1 acts as the obligate heterodimeric partner these pathways.

In mammals, two bHLH-PAS transcription factors within the family, ARNT and BMAL1 (Brain and Muscle ARNT-Like 1) act as general factors that heterodimerize with multiple partners to control all of bHLH-PAS signaling. The functional specificity of ARNT or BMAL1 is conferred by the dimerization partner with which they interact, allowing for tissue- or pathway-specific regulation of target genes (21). The non-redundant roles of ARNT and BMAL1 proteins in mediating interactions with diverse partners suggest that complex mechanisms may exist for crosstalk between signaling pathways. The extent to which inter-pathway regulation plays a role in transcriptional regulation is still

not well understood; however, there is some evidence that HIF-1α can compete with AhR for recruitment of ARNT to interfere with the dioxin signaling pathway (22). The overlap between pathways and potential crosstalk presents the intriguing potential for another level of transcriptional control to be driven by local protein concentration, stoichiometry and affinity of these complexes, and should be explored further.

3.3.3 Evolutionarily related repressors of bHLH-PAS transcription factors

When comparing bHLH-PAS proteins across signaling pathways, one interesting trend emerges: within each pathway, there is often a homologous repressor that shares modular domain architecture with an activator (23–25). The repressors either lack domain(s) necessary for activation or possess an additional domain with repressive activity. Examples of how the bHLH-PAS protein family exploits gene duplication and domain shuffling to add additional layers of transcriptional regulation are discussed below.

The mammalian SIM1/2 proteins are homologs of the *Drosophila melanogaster* gene single-minded (sim) and regulate gene expression during development (26). SIM1 and SIM2 share a high degree of sequence similarity (~90%) within the PAS domains, however, they have highly divergent C-termini (27,28). Both proteins heterodimerize through similar PAS-mediated interactions with their cognate partner, ARNT; however, due to differences in their C-termini, the heterodimers have opposing activities on transcriptional

regulation. The SIM1:ARNT complex activates target genes, while SIM2, with its distinct C-terminal sequence that contains two repressive domains, quenches the transactivation domain of ARNT to inhibit gene expression (Figure 3-2) (29).

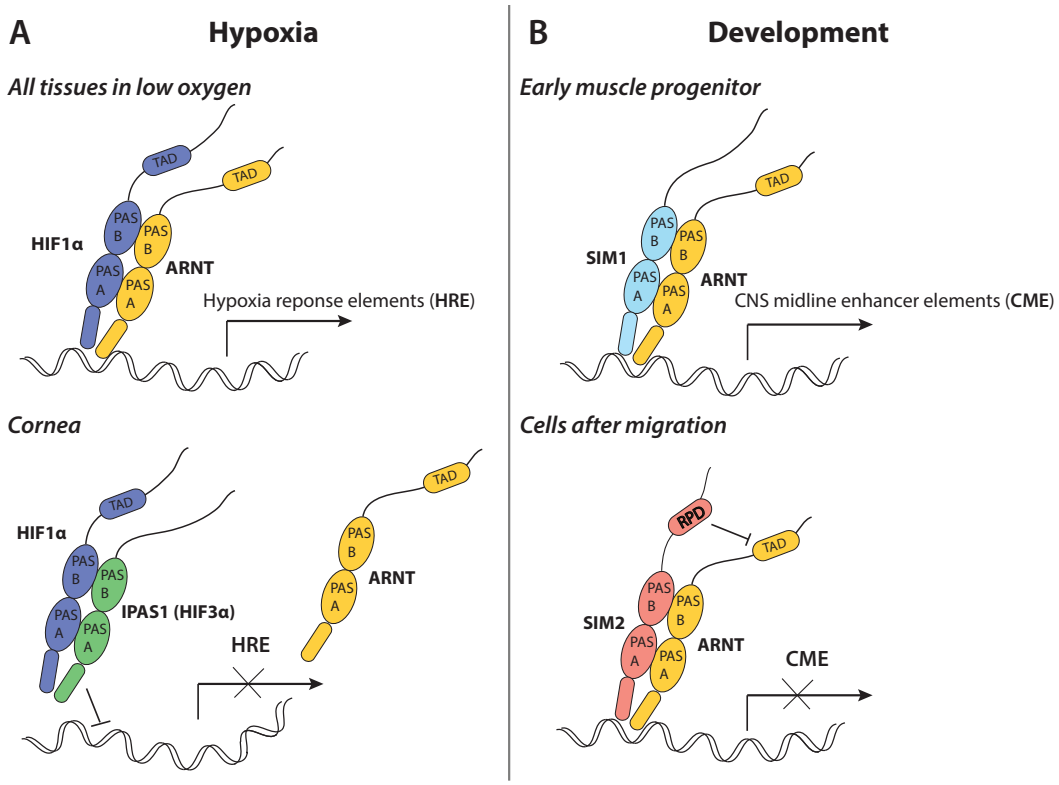

Figure 3-2. Tissue-specific expression of bHLH-PAS transcriptional repressors provides cell-type specific responses to external stimuli and cell fate control.

(A) In almost all hypoxic mammalian tissues, HIF-1α forms a heterodimer with ARNT to activate hypoxia response genes, including genes involved in neovascularization. Selective upregulation of IPAS1 in the cornea inhibits the transcriptional activity of HIF-1α:ARNT by binding to HIF-1α and sequestering the protein. This tissue-specific regulation prevents detrimental neovascularization within the cornea in mammals. (B) During mouse embryonic development early muscle progenitor cells show high expression of SIM1, which can bind ARNT and activate genes. As development progresses, SIM1 expression is downregulated and SIM2 expression dominates to form an inactive transcriptional complex with ARNT to attenuate expression of SIM2 target genes.

The hypoxia-inducible factor-1 (HIF-1) is an oxygen-labile protein that mediates adaptive responses to reduced oxygen availability by

heterodimerizing with ARNT to bind DNA and activate genes involved in glycolysis and angiogenesis, promoting survival in low-oxygen conditions (30,31). Beside HIF-1α, there are two additional members of the HIF bHLH-PAS superfamily: HIF-2α, also known as endothelial PAS domain protein 1 (EPAS1), and HIF-3α (32,33). A novel transcriptional repressor of this pathway has been identified that is a splicing variant of the HIF-3α locus, referred to as inhibitory PAS domain protein 1 (IPAS1). This alternative splicing event produces a truncated protein product that does not contain a transactivation domain. IPAS1 competes with ARNT to form a complex with HIF-1α, forming an abortive IPAS1:HIF-1α complex that cannot bind DNA at hypoxia response elements. In this way, splicing variants can generate repressors to attenuate the cellular response to hypoxia (34). In healthy tissue, the HIF1α:ARNT complex plays a beneficial role in human physiology and development; however, this adaptation also increases oxygen supply to hypoxic microenvironments in tumors to permit proliferation and tumorigenesis (35). Understanding how the activity HIF1α:ARNT complex is modulated endogenously by the repressor IPAS1 will further our understanding of the mechanisms in place that regulate the escape from oxygen sensitivity in cancer progression.

Exposure to harmful chemicals that humans encounter in the environment, such as dioxin, results in the expression of xenobiotic response

genes to break down these toxic compounds. This response is mediated in part at the transcriptional level by the AhR:ARNT complex (3). Dioxin and other halogenated aromatic hydrocarbons bind to the PAS-B domain of the transcription factor AHR, breaking up the interaction with AHR and the chaperone protein, Hsp90 that retains AHR in the cytoplasm (36). After this, AhR is free to enter the nucleus and form a heterodimer with ARNT to bind DNA, recruit transcriptional coactivators and activate xenobiotic response genes. The activity of AhR:ARNT is adjusted by the aryl hydrocarbon receptor repressor (AhRR) that binds to ARNT in a ligand-independent manner and sequesters the protein away from AhR (37). AhRR shares a high degree of similarity with AhR (PAS-A, 59.7%; C-terminus, 19.7%) and uses this molecular mimicry to form an inactive transcriptional complex that downregulates the xenobiotic pathway (25). While studies suggest that AhRR may act as a tumor suppressor, the functional significance of this negative regulation remains to be fully elucidated (38). However, it has been postulated that AhRR is upregulated in delicate tissues such as the germline, to protect against toxic metabolites generated by the breakdown of these polycyclic aromatic hydrocarbons.

3.3.4 Tissue-specific regulation of gene expression

Each cell type demands the ability to differentially regulate gene expression and cellular responsiveness to external cues, suggesting that mechanisms exist to modulate the output of environmentally sensitive bHLH-PAS signaling pathways in a tissue-specific manner. This is accomplished at

the molecular level by distinct expression patterns of transcriptional activators and repressors, which allows for fine-tuning of the cellular response to global inputs, such as low oxygen concentration or xenobiotic exposure, depending upon the identity and needs of the cell.

One of the most well understood examples of tissue-specific regulation of bHLH-PAS signaling pathways occurs in the cornea. During sleep, closure of the eyelid creates a hypoxic environment within cells of the cornea. Despite continual exposure to low oxygen levels that would normally stimulate HIF-1α dependent gene expression to increase neovascularization, the cornea remains completely avascular, which is necessary for vision (39,40). Selective downregulation of the hypoxia pathway in the cornea can be attributed to the unique expression pattern of the HIF-1α-related repressor, IPAS1 (Figure 3-2) (24). Exposure of the corneal epithelium to hypoxia results in a rapid HIF-dependent induction of IPAS1 mRNA and repression of HIF-1α:ARNT activity by sequestering HIF-1α from ARNT in an abortive HIF-1α:IPAS1 complex incapable of binding DNA (41). Repression by IPAS1 in hypoxic conditions specifically in the cornea is believed to play an important role in preventing neovascularization in the cornea and blindness (24).

In addition to their participation in pathways that respond to environmental stimuli, many bHLH-PAS proteins also play a direct role in development and cell fate determination (42). The *Drosophila* the bHLH-PAS

protein Tango, the ortholog of the mammalian ARNT protein, regulates specific stages of development. Like ARNT, Tango is broadly expressed throughout tissues and forms a heterodimer with SIM to control development of the central nervous system midline cells. However, Tango also forms a heterodimer with its bHLH-PAS partner Trachealess to control proper development and tubulogenesis within tracheal cells and the salivary duct. (43). Because expression of sim and Trachealess is restricted to the cell lineages that they control, they possess the ability to regulate specific developmental programs through selective expression of their specific target genes upon binding to their shared partner, Tango. In mammals, SIM proteins have similar functions that control embryonic development and cell differentiation. *In situ* hybridization studies in mouse embryos show largely non-overlapping expression patterns of mSIM1 and mSIM2, with mSIM1 being expressed in early limb muscle precursor cells and selective SIM2 expression in cells after migration (Figure 3-2B). (44)

While many studies have quantified mRNA expression levels of bHLH-PAS genes across different tissues, the mechanisms controlling these differential expression patterns remain to be elucidated and deserve further study. With the advent of genome-wide techniques that allow for identification of transcription factor binding sites and chromatin modifications that dictate the epigenetic state of the cell. These studies will illustrate the roles that bHLH-

PAS proteins play in controlling cell- and tissue-specific gene expression and how these pathways respond to environmental insults.

3.4 Conclusion

Nature has tinkered with the bHLH-PAS family, using the PAS domain module as a building block to establish the foundation of a specific transcription factor architecture that is accessorized with regulatory motifs that modulate activity. bHLH-PAS transcription factors exemplify the concept of functional expansion through modular domain shuffling in molecular evolution, using the well-conserved PAS fold to bring together stimulus-responsive proteins with their partners, while conserved domains and motifs outside of the PAS fold have been swapped to activate or repress the pathway. Over 29,000 PAS domain-containing proteins have been identified from archaebacteria to humans (SMART database), most of which likely sense environmental cues to act within transcriptional networks. We are just beginning to understand the intricacies of these proteins and the pathways they act within. Additional studies need to be done to further characterize these proteins using sequence conservation paired with bioinformatic analyses of predicted regulatory motifs that will help inform biological function of paralogs and other related genes. Moreover, the capability to determine protein expression, DNA binding and transcriptional regulation genome-wide by these proteins in response to external stimuli will help us better understand tissue-specific regulation of

bHLH-PAS proteins and their biological role in keeping mammals healthy and in tune with their environment.

3.5 References

1. Taylor BL, Zhulin IB. PAS domains: internal sensors of oxygen, redox potential, and light. Microbiol. Mol. Biol. Rev. 1999;63:479–506.
2. Wang GL, Jiang BH, Rue EA, Semenza GL. Hypoxia-inducible factor 1 is a basic-helix-loop-helix-PAS heterodimer regulated by cellular O2 tension. Proc. Natl. Acad. Sci. U. S. A. 1995;92:5510–4.
3. Hahn ME. The aryl hydrocarbon receptor: a comparative perspective. Comp Biochem. C.Pharmacol.Toxicol.Endocrinol. [Internet]. 1998;121:23–53. Available from: D:\MORE DOCS\pdf Reviews\AH receptor Hahn.pdf
4. Gekakis N, Staknis D, Nguyen HB, Davis FC, Wilsbacher LD, King DP, et al. Role of the CLOCK protein in the mammalian circadian mechanism. Science. 1998;280:1564–9.
5. Möglich A, Ayers RA, Moffat K. Structure and signaling mechanism of Per-ARNT-Sim domains. Structure. 2009;17:1282–94.
6. Hefti MH, Françoijs K-J, de Vries SC, Dixon R, Vervoort J. The PAS fold. A redefinition of the PAS domain based upon structural prediction. Eur. J. Biochem. 2004;271:1198–208.
7. Sevvana M, Vijayan V, Zweckstetter M, Reinelt S, Madden DR, Herbst-Irmer R, et al. A ligand-induced switch in the periplasmic domain of sensor histidine kinase CitA. J. Mol. Biol. 2008;377:512–23.
8. Harper SM, Neil LC, Gardner KH. Structural basis of a phototropin light switch. Science. 2003;301:1541–4.
9. Bradfield CA, Kende AS, Poland A. Kinetic and equilibrium studies of Ah receptor-ligand binding: use of [125I]2-iodo-7,8-dibromodibenzo-p-dioxin. Mol. Pharmacol. 1988;34:229–37.

10. McIntosh BE, Hogenesch JB, Bradfield CA. Mammalian Per-Arnt-Sim proteins in environmental adaptation. Annu. Rev. Physiol. 2010;72:625–45.
11. Key J, Scheuermann TH, Anderson PC, Daggett V, Gardner KH. Principles of ligand binding within a completely buried cavity in HIF2alpha PAS-B. J. Am. Chem. Soc. 2009;131:17647–54.
12. Scheuermann TH, Tomchick DR, Machius M, Guo Y, Bruick RK, Gardner KH. Artificial ligand binding within the HIF2alpha PAS-B domain of the HIF2 transcription factor. Proc. Natl. Acad. Sci. U. S. A. 2009;106:450–5.
13. Huang N, Chelliah Y, Shan Y, Taylor CA. Crystal Structure of the Heterodimeric CLOCK: BMAL1 Transcriptional Activator Complex. Sci. (New York, NY) [Internet]. 2012; Available from: http://stke.sciencemag.org/cgi/content/abstract/sci\n337/6091/189\npapers2://publication/uuid/CCFFC057-9EA7-49BC-91F1-326C91B907D9
14. Guo Y, Partch CL, Key J, Card PB, Pashkov V, Patel A, et al. Regulating the ARNT/TACC3 axis: multiple approaches to manipulating protein/protein interactions with small molecules. ACS Chem. Biol. [Internet]. 2013;8:626–35. Available from: http://www.ncbi.nlm.nih.gov/pubmed/23240775
15. Partch CL, Gardner KH. Coactivators necessary for transcriptional output of the hypoxia inducible factor, HIF, are directly recruited by ARNT PAS-B. Proc. Natl. Acad. Sci. U. S. A. 2011;108:7739–44.
16. Partch CL, Card PB, Amezcua CA, Gardner KH. Molecular basis of coiled coil coactivator recruitment by the aryl hydrocarbon receptor nuclear translocator (ARNT). J. Biol. Chem. 2009;284:15184–92.
17. Hao N, Whitelaw ML, Shearwin KE, Dodd IB, Chapman-Smith A. Identification of residues in the N-terminal PAS domains important for dimerization of Arnt and AhR. Nucleic Acids Res. 2011;39:3695–709.
18. Erbel PJA, Card PB, Karakuzu O, Bruick RK, Gardner KH. Structural basis for PAS domain heterodimerization in the basic helix--loop--helix-PAS

transcription factor hypoxia-inducible factor. Proc. Natl. Acad. Sci. U. S. A. 2003;100:15504–9.

19. Fuxreiter M, Tompa P, Simon I, Uversky VN, Hansen JC, Asturias FJ. Malleable machines take shape in eukaryotic transcriptional regulation. Nat. Chem. Biol. 2008;4:728–37.

20. Chan DA, Sutphin PD, Yen S-E, Giaccia AJ. Coordinate regulation of the oxygen-dependent degradation domains of hypoxia-inducible factor 1 alpha. Mol. Cell. Biol. 2005;25:6415–26.

21. Labrecque M. The aryl hydrocarbon receptor nuclear translocator (ARNT) family of proteins: Transcriptional modifiers with multi-functional protein interfaces. Curr. Mol. … [Internet]. 2012;13:1047–65. Available from: http://www.ncbi.nlm.nih.gov/pubmed/23116263\nhttp://europepmc.org/abstract/MED/23116263

22. Gu YZ, Hogenesch JB, Bradfield CA. The PAS superfamily: sensors of environmental and developmental signals. Annu. Rev. Pharmacol. Toxicol. 2000;40:519–61.

23. Ema M, Morita M, Ikawa S, Tanaka M, Matsuda Y, Gotoh O, et al. Two new members of the murine Sim gene family are transcriptional repressors and show different expression patterns during mouse embryogenesis. Mol. Cell. Biol. 1996;16:5865–75.

24. Makino Y, Cao R, Svensson K, Bertilsson G, Asman M, Tanaka H, et al. Inhibitory PAS domain protein is a negative regulator of hypoxia-inducible gene expression. Nature. 2001;414:550–4.

25. Mimura J, Ema M, Sogawa K, Fujii-Kuriyama Y. Identification of a novel mechanism of regulation of Ah (dioxin) receptor function. Genes Dev. 1999;13:20–5.

26. Nambu JR, Lewis JO, Wharton KA, Crews ST. The Drosophila single-minded gene encodes a helix-loop-helix protein that acts as a master regulator of CNS midline development. Cell. 1991;67:1157–67.

27. Fan CM, Kuwana E, Bulfone A, Fletcher CF, Copeland NG, Jenkins NA, et al. Expression patterns of two murine homologs of Drosophila single-minded suggest possible roles in embryonic patterning and in the pathogenesis of Down syndrome. Mol. Cell. Neurosci. 1996;7:1–16.

28. Yamaki A, Noda S, Kudoh J, Shindoh N, Maeda H, Minoshima S, et al. The mammalian single-minded (SIM) gene: mouse cDNA structure and diencephalic expression indicate a candidate gene for Down syndrome. Genomics. 1996;35:136–43.

29. Moffett P, Pelletier J. Different transcriptional properties of mSim-1 and mSim-2. FEBS Lett. 2000;466:80–6.

30. Forsythe JA, Jiang BH, Iyer N V, Agani F, Leung SW, Koos RD, et al. Activation of vascular endothelial growth factor gene transcription by hypoxia-inducible factor 1. Mol. Cell. Biol. 1996;16:4604–13.

31. Firth JD, Ebert BL, Pugh CW, Ratcliffe PJ. Oxygen-regulated control elements in the phosphoglycerate kinase 1 and lactate dehydrogenase A genes: similarities with the erythropoietin 3' enhancer. Proc. Natl. Acad. Sci. U. S. A. 1994;91:6496–500.

32. Gu YZ, Moran SM, Hogenesch JB, Wartman L, Bradfield CA. Molecular characterization and chromosomal localization of a third alpha-class hypoxia inducible factor subunit, HIF3alpha. Gene Expr. 1998;7:205–13.

33. Tian H, McKnight SL, Russell DW. Endothelial PAS domain protein 1 (EPAS1), a transcription factor selectively expressed in endothelial cells. Genes Dev. 1997;11:72–82.

34. Jang MS, Park JE, Lee JA, Park SG, Myung PK, Lee DH, et al. Binding and regulation of hypoxia-inducible factor-1 by the inhibitory PAS proteins. Biochem. Biophys. Res. Commun. 2005;337:209–15.

35. Rankin EB, Giaccia AJ. The role of hypoxia-inducible factors in tumorigenesis. Cell Death Differ. 2008;15:678–85.

36. Coumailleau P, Poellinger L, Gustafsson JA, Whitelaw ML. Definition of a minimal domain of the dioxin receptor that is associated with Hsp90 and maintains wild type ligand binding affinity and specificity. J. Biol. Chem. 1995;270:25291–300.

37. Evans BR, Karchner SI, Allan LL, Pollenz RS, Tanguay RL, Jenny MJ, et al. Repression of aryl hydrocarbon receptor (AHR) signaling by AHR repressor: role of DNA binding and competition for AHR nuclear translocator. Mol. Pharmacol. 2008;73:387–98.

38. Zudaire E, Cuesta N, Murty V, Woodson K, Adams L, Gonzalez N, et al. The aryl hydrocarbon receptor repressor is a putative tumor suppressor gene in multiple human cancers. J Clin Invest [Internet]. 2008;118:640–50. Available from: http://www.ncbi.nlm.nih.gov/pubmed/18172554

39. Sack RA, Beaton AR, Sathe S. Diurnal variations in angiostatin in human tear fluid: a possible role in prevention of corneal neovascularization. Curr. Eye Res. 1999;18:186–93.

40. Thakur A, Willcox MD, Stapleton F. The proinflammatory cytokines and arachidonic acid metabolites in human overnight tears: homeostatic mechanisms. J. Clin. Immunol. 1998;18:61–70.

41. Makino Y, Uenishi R, Okamoto K, Isoe T, Hosono O, Tanaka H, et al. Transcriptional up-regulation of inhibitory PAS domain protein gene expression by hypoxia-inducible factor 1 (HIF-1): a negative feedback regulatory circuit in HIF-1-mediated signaling in hypoxic cells. J. Biol. Chem. 2007;282:14073–82.

42. Crews ST, Fan CM. Remembrance of things PAS: regulation of development by bHLH-PAS proteins. Curr. Opin. Genet. Dev. 1999;9:580–7.

43. Ward MP, Mosher JT, Crews ST. Regulation of bHLH-PAS protein subcellular localization during Drosophila embryogenesis. Development. 1998;125:1599–608.

44. Coumailleau P, Duprez D. Sim1 and Sim2 expression during chick and mouse limb development. Int. J. Dev. Biol. 2009;53:149–57

4 CHAPTER 4 — CANCER/TESTIS ANTIGEN PASD1 SILENCES THE CIRCADIAN CLOCK

4.1 Abstract

The circadian clock orchestrates global changes in transcriptional regulation on a daily basis via the bHLH-PAS transcription factor CLOCK:BMAL1. Pathways driven by other bHLH-PAS transcription factors have a homologous repressor that modulates activity on a tissue-specific basis, but none have been identified for CLOCK:BMAL1. We show here that the cancer/testis antigen PASD1 fulfills this role to suppress circadian rhythms. PASD1 is evolutionarily related to CLOCK and interacts with the CLOCK:BMAL1 complex to repress transcriptional activation. Expression of PASD1 is restricted to germline tissues in healthy individuals, but can be induced in cells of somatic origin upon oncogenic transformation. Reducing PASD1 in human cancer cells significantly increases the amplitude of transcriptional oscillations to generate more robust circadian rhythms. Our results describe a function for a germline-specific protein in regulation of the circadian clock and provide a molecular link from oncogenic transformation to suppression of circadian rhythms.

4.2 Introduction

The circadian clock coordinates temporal control of physiology by regulating the expression of at least 40% of the genome on a daily basis (1) . Disruption of circadian rhythms through environmental stimuli (e.g. light at

night) or genetic means can lead to the onset of diseases such as: diabetes, cardiovascular disease, premature aging and cancer (2–5). Understanding the molecular basis of circadian transcriptional regulation in health and disease states offers the opportunity to control vast transcriptional programs that promote health and well-being (6).

The heterodimeric basic helix-loop-helix PER-ARNT-SIM (bHLH-PAS) transcription factor CLOCK:BMAL1 sits at the core of the molecular circadian clock in mammals. CLOCK:BMAL1 drives expression of core clock factors *Period* (*Per)* and *Cryptochrome* (*Cry*), as well as thousands of additional clock-controlled output genes (1, 7). PER and CRY complexes interact with CLOCK:BMAL1 in the nucleus to inhibit transcriptional activation and close the feedback loop, generating intrinsic ~24-hour timing (7–9) This cell-autonomous molecular oscillator is present in nearly every mammalian tissue (10–12) and is regulated by tissue-specific factors to fine-tune circadian output genes according to cell type (13, 14). While the molecular circadian clock is broadly recognized as a systemic transcriptional regulator, factors that provide tissue-specific regulation of the clock and its outputs remain to be elucidated.

CLOCK and BMAL1 belong to the bHLH-PAS family of transcription factors, which share similar domain architecture but regulate diverse processes including adaptation to hypoxia, xenobiotic metabolism and neuronal development (15–18). Homotypic interactions between N-terminal DNA-binding bHLH domains and tandem PAS domains guide formation of specific

heterodimeric transcription factor complexes (19–21). By contrast, bHLH-PAS C-termini interact with regulatory factors that modulate activity of the complexes (22, 23). In CLOCK:BMAL1, the BMAL1 C-terminus harbors the essential transactivation domain (TAD) that recruits coactivators CBP/p300 and cryptochrome repressors (24–26) and a short helical region encoded by CLOCK Exon 19 interacts with the histone methyltransferase MLL1 and a vertebrate-specific repressor CIPC (27, 28). Deletion of Exon 19 prevents proper chromatin targeting of CLOCK:BMAL1 to interfere with circadian transcriptional regulation (29, 30).

One interesting feature shared by bHLH-PAS transcription factors is their regulation by paralogous PAS domain-containing repressors. By definition, each paralog repressor shares significant homology with an activator subunit, but either possesses a repressive domain and/or lacks a domain(s) necessary for activation (17, 31–33). These repressors are often expressed in a highly restricted manner to control the tissue-specificity of transcriptional outputs (34, 35). However, the mechanisms by which the pathway-specific paralogs repress transcriptional activation by their cognate heterodimers, and importantly, how their homology to activator subunits is used to impinge on transcriptional regulation are not well understood.

The dedicated bHLH-PAS family repressor for circadian rhythms has not yet been identified. Here we show that the protein PAS domain containing 1 (PASD1) is evolutionarily related to the circadian transcription factor subunit

CLOCK and interacts with the CLOCK:BMAL1 complex to inhibit transcriptional activation and suppress circadian timekeeping. Furthermore, deletion of one region, highly conserved with CLOCK Exon 19, alleviates repression by PASD1 to suggest that it utilizes molecular mimicry to interfere with CLOCK:BMAL1 function. As a cancer/testis antigen, expression of PASD1 is natively restricted to gametogenic tissues but can be upregulated in somatic tissues as a consequence of oncogenic transformation. Our work suggests that mechanisms to suppress circadian cycling can be hard-wired in a tissue-specific manner and we show here that they can be co-opted in cancer cells to attenuate clock function.

4.3 Results

4.3.1 Identification of a CLOCK paralog in humans

The absence of a paralogous repressor for CLOCK:BMAL1 prompted us to search for human clock protein paralogs that might serve this purpose. Using a PAS domain-based query with the SMART algorithm (36, 37) we discovered an uncharacterized PAS domain-containing protein in humans, PAS domain containing protein 1 (PASD1), that is homologous to CLOCK (Figure 4-1A and Supplementary **Figure 4-1. Human PASD1 has significant sequence homology with CLOCK and lacks a murine homolog.**Supplementary Figure 4-1). In contrast to CLOCK, PASD1 lacks the DNA-binding bHLH domain and the PAS-B domain, both of which are needed to interact with BMAL1 to form a functional heterodimeric transcription factor

(19). Similarity between PASD1 and CLOCK is restricted to the PAS-A domain and a helical region in the C-terminus (Figure 4-1B and Supplementary Figure 4-1A) defined by CLOCK Exon 19, which is essential for CLOCK:BMAL1 function (27, 29, 38). *PASD1* has two splice isoforms (*PASD1v1* and *PASD1v2*) that differ only by extension of the C-terminus (Figure 4-1B) (39). The C-terminus of PASD1 has more predicted secondary structure than CLOCK, with two conserved helical regions designated coiled coil 1 and 2 (CC1 and CC2, Figure 4-1B). Based on these sequence analyses, PASD1 demonstrates two key properties of a pathway-specific bHLH-PAS repressor—homology to a bHLH-PAS activator subunit with the loss of domain(s) critical for transcriptional activation (16, 32, 40).

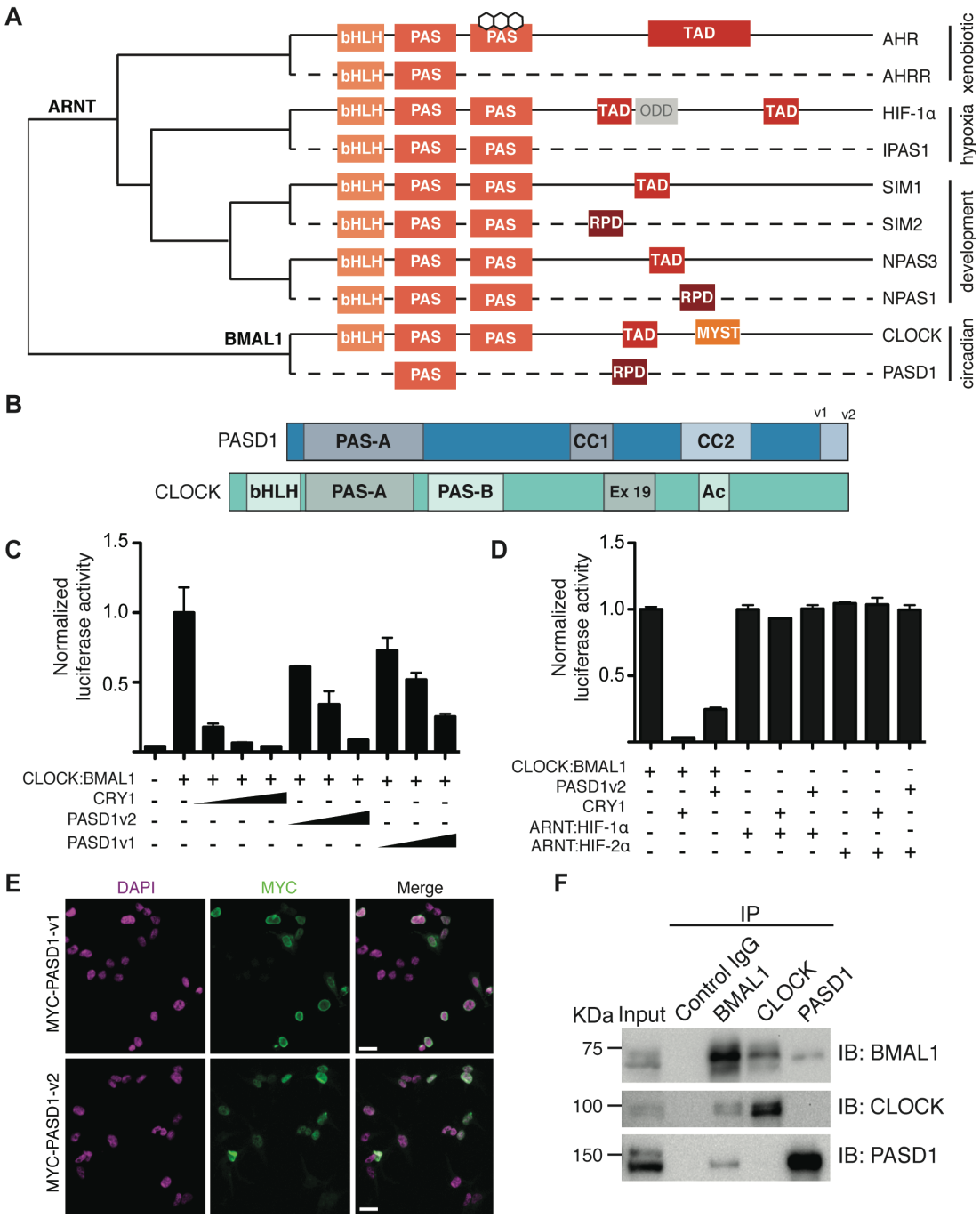

Figure 4-1. Identification of a novel circadian repressor that is homologous to CLOCK.

(A) Cladogram of bHLH-PAS transcription factors showing their evolutionary relationship. Each branch of transcription factors within the bHLH-PAS family has a truncated transcriptional repressor that clusters with its related activator

subunit and shares similar domain architecture. PAS: PER-ARNT-SIM domain; TAD: Transactivation domain; RPD, repression domain; ODD: Oxygen-dependent degradation domain; MYST, histone acetyltransferase motif from the MYST family (79). The cladogram was generated using EMBL-EBI Clustal Omega. Activator subunits have solid lines; repressors have dashed lines. (B) Comparison of human PASD1 and CLOCK domain organization. Gray shading highlights regions of high sequence identity with PASD1. CC1: Coiled-coil domain 1, CC2: Coiled-coil domain 2. (C) Both isoforms of PASD1 inhibit CLOCK:BMAL1 activity in *Per1:luc* reporter gene assays. HEK293T cells were transfected with *Per1:luc*, CLOCK, BMAL1 and increasing amounts of CRY1 or PASD1 plasmid as indicated. (D) CRY1 and PASD1 do not inhibit transactivation of a *VEGF:luc* reporter by the bHLH-PAS homologs HIF-1α:ARNT or HIF-2α:ARNT. HA-tagged P1P2N mutants stabilize expression of HIF-1α or HIF-2α under normoxic conditions (80). (E) HEK293T cells were transiently transfected with MYC-PASD1v1 and MYC-PASD1v2 and subcellular localization was determined by immunofluorescence Scale bar, 20 μm. (F) Co-immunoprecipitation of endogenous BMAL1, CLOCK with PASD1-GFP from U2OS *Per2:dluc* PASD1-GFP cells.

PASD1 is an X-linked gene that is broadly conserved in mammals but absent in murine lineages (Supplementary Figure 4-1B), a property common to X-linked genes involved in spermatogenesis (41). In healthy individuals, PASD1 is only expressed in germline tissues such as the testis (42); however, PASD1 can be found in somatic tissues upon oncogenic transformation (39, 43, 44). PASD1 is therefore designated as a cancer/testis antigen, a classification shared with a large family of proteins that are normally expressed only in the germline and whose expression can provoke immune responses when aberrantly upregulated in neoplastic somatic cells (39, 44, 45). While the immunogenicity and expression of PASD1 in a diverse array of human cancers have been well characterized (46, 47), the cellular function of this protein

remains unknown. These data prompted us to investigate whether PASD1 could represent the dedicated bHLH-PAS family repressor that negatively regulates CLOCK:BMAL1.

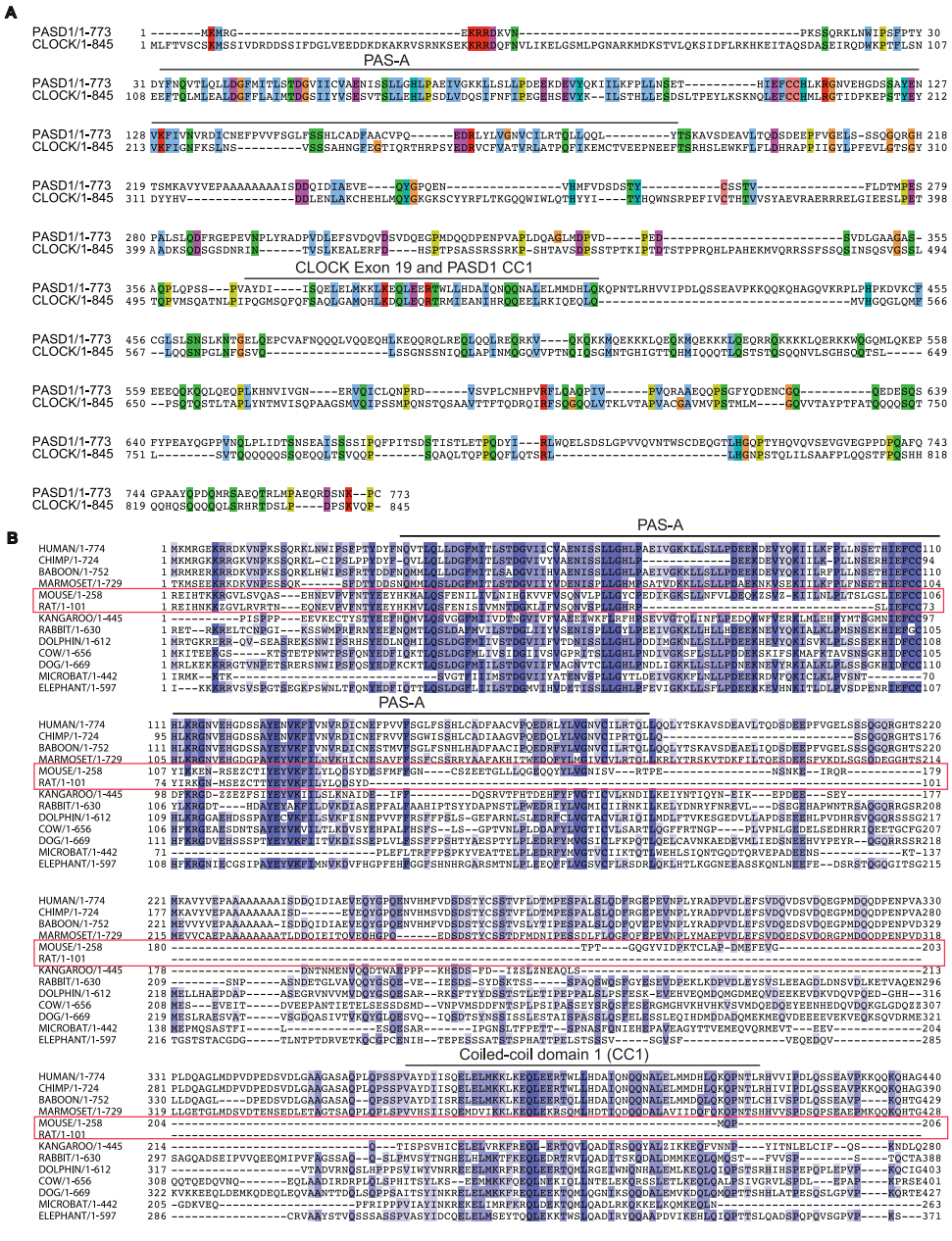

Supplementary Figure 4-1. Human PASD1 has significant sequence homology with CLOCK and lacks a murine homolog.
(A) Clustalx alignment of human PASD1 (NP_775764.2) aligned with human CLOCK using Multiple Alignment Fast Fourier Transform. Regions of high identity between the PAS-A domains (34%) or the Exon 19 of CLOCK and CC1 domain of PASD1 (36%) are highlighted with a thick black line. (B) Multiple sequence alignment of PASD1 proteins across mammals were

generated using the UCSC genome browser Vertebrate Multiz Alignment track and displayed using Jalview. Only residues corresponding to human PASD1 1 – 400 are shown due to space constraints. While the mouse gm1141 (accession: B9EJU1) is annotated as PASD1 in the mouse genome (mm10), it shows very low sequence identity with the PASD1 gene found in mammals. The predicted mouse transcript from the UCSC genome browser Vertebrate Multiz Alignment has a higher degree of identity and is shown here. The red box highlights the putative protein product of the truncated gene in mice and rats.

4.3.2 PASD1 is a nuclear protein that represses transcriptional activation by CLOCK:BMAL1

To determine if PASD1 regulates CLOCK:BMAL1 activity, we conducted a reporter gene assay in human embryonic kidney 293T (HEK293T) cells using the *Per1:luc* luciferase reporter (29). PASD1 had no effect on the *Per1:luc* reporter by itself or in combination with either CLOCK or BMAL1 alone, indicating that it cannot drive transcriptional activation (Supplementary Figure 4-2). Titration of either splice isoform of PASD1 led to dose-dependent repression of CLOCK:BMAL1 activity, similar to the core clock repressor Cryptochrome 1 (Figure 4-1C). Furthermore, both CRY1 and PASD1 demonstrated specificity for CLOCK:BMAL1 as co-expression of either repressor with bHLH-PAS homologs HIF-1α:ARNT or HIF-2α:ARNT had no effect on their transcriptional activation of a hypoxia response element from *VEGF* (Figure 4-1D).

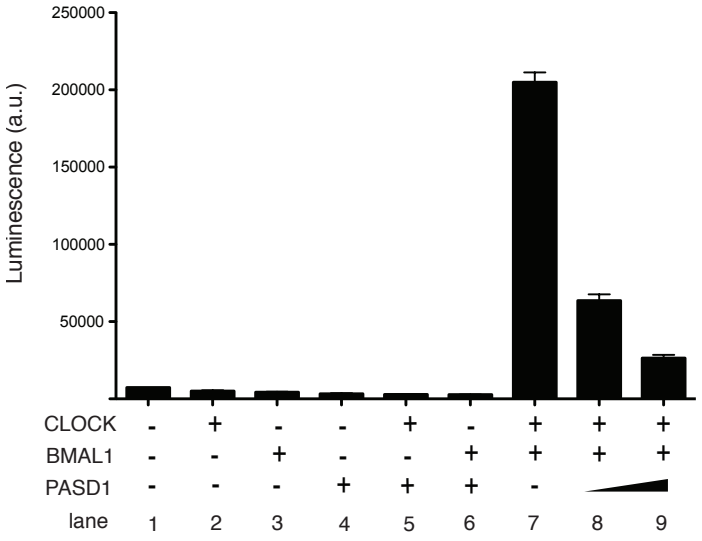

Supplementary Figure 4-2. Co-transfection of PASD1 with CLOCK or BMAL1 does not transactivate the Per1:luc gene.

HEK293T cells were transfected with the Per1:luc reporter gene plasmid alone (lane 1), or with CLOCK, BMAL1 or PASD1 alone as indicated (lanes 2-4). PASD1 cannot drive activation of the Per1:luc reporter gene in combination with either CLOCK or BMAL1 (lanes 5 and 6). Co-transfection of CLOCK and BMAL1 results in 25 - 30 fold activation over the background of the Per1:luc reporter gene alone (lane 7) that is repressed by PASD1 (lanes 8-9). Raw luminescence counts from a representative assay (in triplicate) are shown ± SD.

Regulation of CLOCK:BMAL1 transcriptional activity is likely to occur in the nucleus where the complex is localized. To determine the subcellular localization of PASD1, we transfected HEK293T cells with MYC-tagged versions of both splice isoforms of PASD1 and used immunofluorescence to visualize PASD1. Both MYC-tagged PASD1 splice isoforms are localized exclusively in the nucleus, predominantly at the periphery where

heterochromatin is generally compartmentalized in metazoan cells (48) (Figure 4-1E). To determine if PASD1 interacts with CLOCK:BMAL1, we performed co-immunoprecipitations of each protein from nuclear lysate of a U2OS cell line stably expressing PASD1-GFP. Endogenous BMAL1 precipitated both CLOCK and PASD1-GFP, while CLOCK precipitated low levels of BMAL1 but no detectable PASD1-GFP (Figure 4-1F). PASD1-GFP precipitated BMAL1 but not CLOCK, suggesting that PASD1 may target the CLOCK:BMAL1 complex through interaction with BMAL1. Taken together, these data show that PASD1 is a potent and specific, nuclear repressor of the CLOCK:BMAL1 complex.

Identification of the PASD1 repressive domain

To understand how PASD1 regulates CLOCK:BMAL1 activity, we set out to identify the repressive domain on PASD1. We initially focused our attention on the PASD1 PAS-A domain because it shares a high degree of conservation with CLOCK (Supplementary Figure 4-1A). Moreover, PASD1 residues conserved with CLOCK are predominantly localized at the PAS-A interface of the CLOCK:BMAL1 heterodimer (Figure 4-2A). Mutations in CLOCK PAS-A (L113E/F122R) at this interface diminish interaction with BMAL1 and decrease transactivation by the complex in the *Per1:luc* reporter assay (19). We reasoned that if PASD1 represses CLOCK:BMAL1 by sequestration of the BMAL1 PAS-A domain, then mutation of homologous residues in PASD1 (V36E/M45R) should reduce inhibition of CLOCK:BMAL1 by disrupting the interaction (Figure 4-2B). The CLOCK PAS-A L113E/F122R

mutant caused a significant decrease in *Per1:luc* activation with BMAL1 as previously reported (19), but we saw no effect of the PAS-A V36E/M45R mutation on the ability of PASD1 to repress CLOCK:BMAL1 (Figure 4-2C). Moreover, we determined that both full-length PASD1 and the isolated C-terminus repressed CLOCK:BMAL1 activity to the same degree (Figure 4-2D) and localized to the nucleus (Figure 4-2E), demonstrating that the PASD1 C-terminus is sufficient to repress CLOCK:BMAL1 activity.

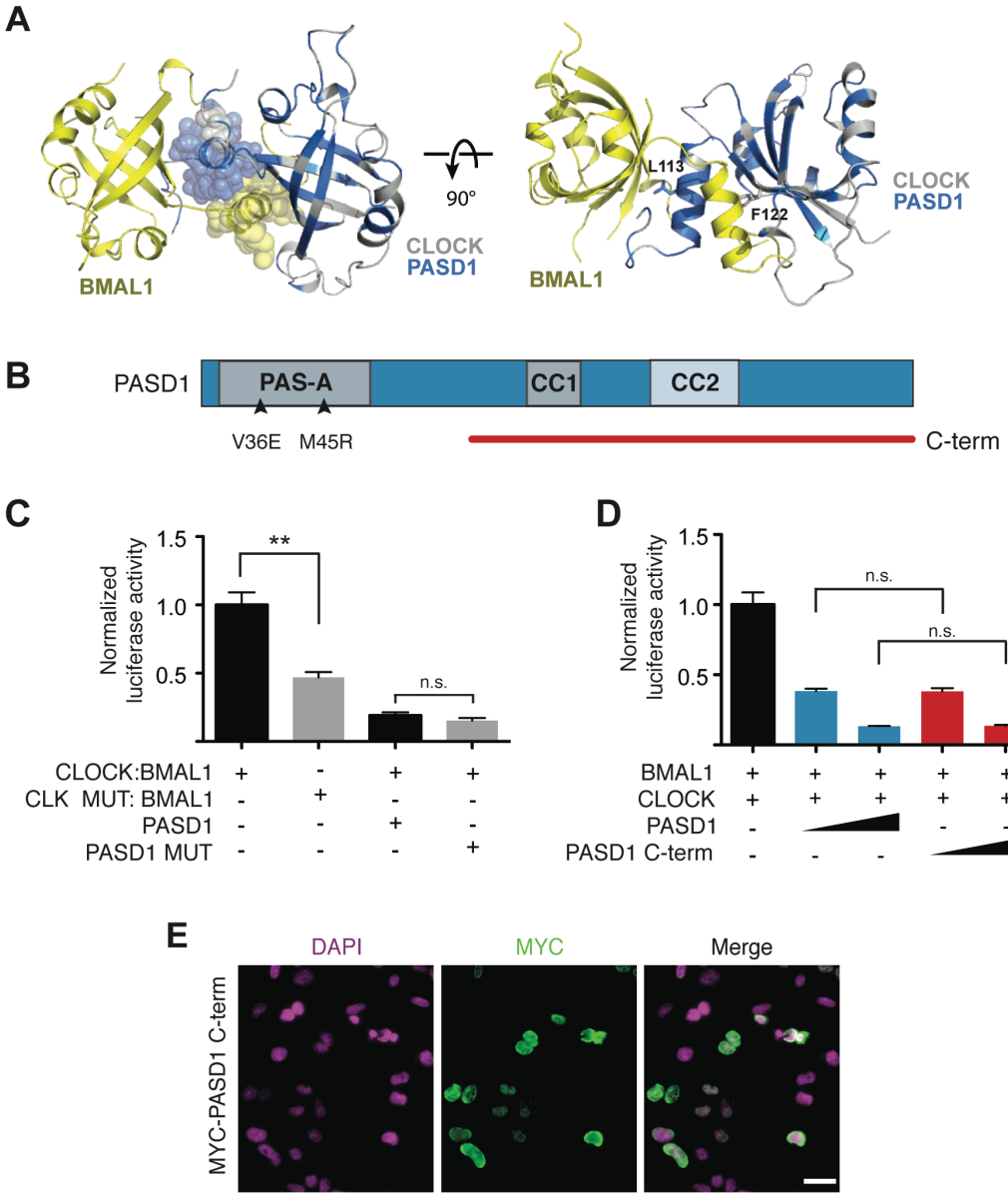

Figure 4-2. The C-terminus of PASD1 is sufficient to repress CLOCK:BMAL1

(A) Mapping of residues conserved between PASD1 and CLOCK onto the CLOCK:BMAL1 PAS-A domain interface (PDB: 4F3L). BMAL1 (yellow), CLOCK residues conserved with PASD1 (blue) and non-conserved residues (white). Location of the CLOCK PAS-A mutations (L113E/F122R) that disrupt the CLOCK:BMAL1 heterodimer and reduce transactivation are shown (19). (B) Schematic of PASD1 expression constructs. Arrowheads indicate point mutations in the PAS-A domain. (C) Mutation of the PASD1 PAS-A β-sheet

interface (V36E/M45R) does not affect repression of CLOCK:BMAL1, while mutation of analogous residues in the PAS-A domain of CLOCK (L113E/F122R) reduces activation of the Per1:luc gene (19). (D) The PASD1 C-terminus is sufficient to repress CLOCK:BMAL1 Per1:luc luciferase expression. Significance was determined by Student's t-test: n.s., not significant. (E) HEK293T cells were transiently transfected with MYC-PASD1v1 C-term and subcellular localization was determined by immunofluorescence. Scale bar, 20 μm.

The other major region of conservation between PASD1 and CLOCK exists within the coiled-coil domain 1 (CC1) in the C-terminus of PASD1, which exhibits significant homology with Exon 19 of CLOCK (Figure 4-3A). This short helical region of CLOCK is important for transcriptional activation and necessary to sustain a robust amplitude of cycling (27, 29, 30), suggesting that its conservation within PASD1 might play a role in its regulation of CLOCK:BMAL1 activity. We deleted the CC1 region from the full-length protein (PASD1ΔCC1) or the isolated C-terminus (C-term ΔCC1) to probe its role in CLOCK:BMAL1 regulation (Figure 4-3B). Although CC1-truncated forms of PASD1 retained nuclear localization and were expressed to the degree as full-length protein (Figure 4-3C and Supplementary Figure 4-3A), repression of CLOCK:BMAL1-driven luciferase activity was significantly impaired (Figure 4-3D). Co-expression of CLOCK and BMAL1 drives their nuclear localization (49, 50). Full-length PASD1 and the C-terminus both interacted with co-expressed CLOCK and BMAL1, and complex formation was visibly reduced with deletion of CC1 (Figure 4-3E and Supplementary Figure 4-3B). Therefore, the CC1 domain of PASD1 is important for interaction with its cognate transcription factor and transcriptional repression.

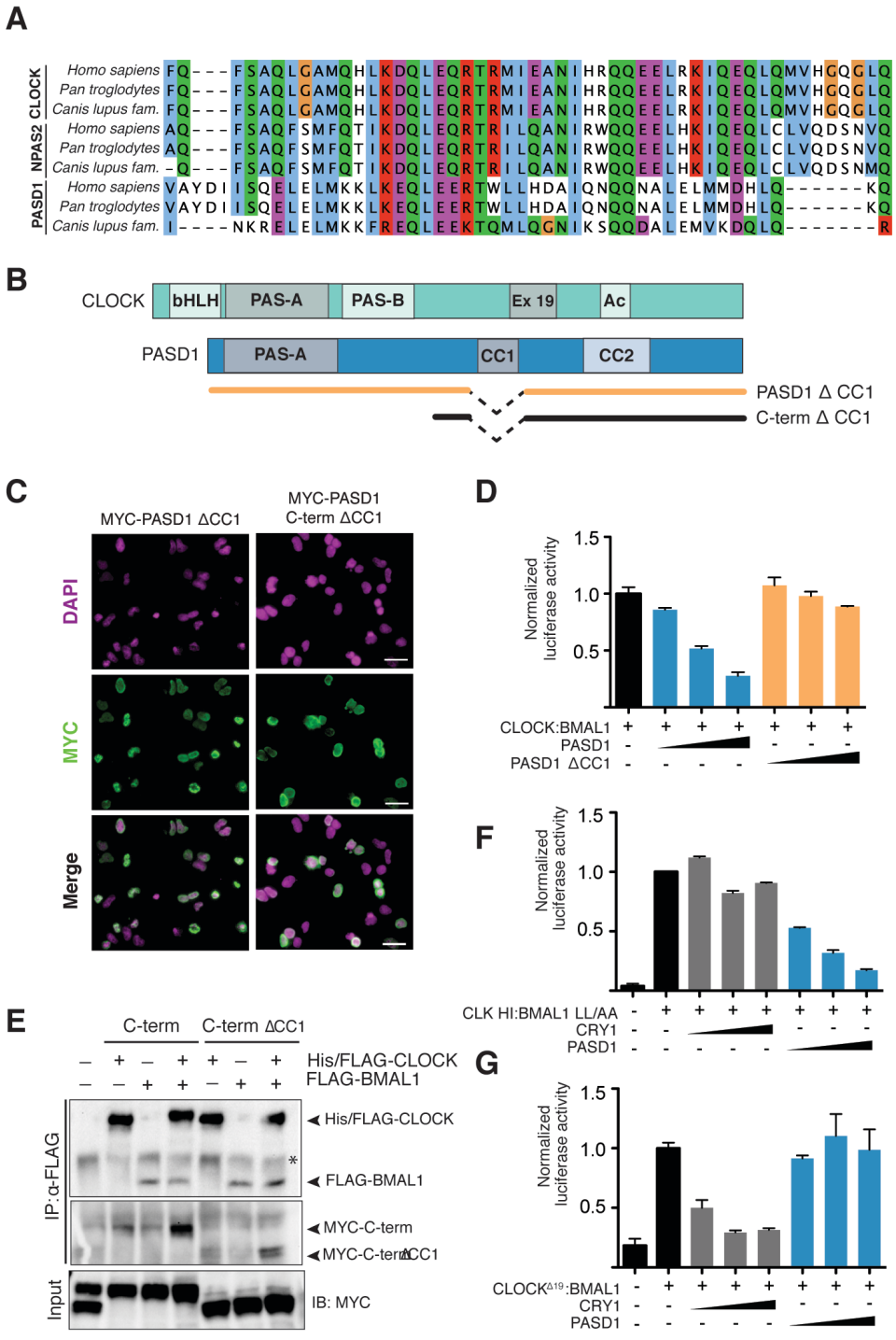

Figure 4-3. PASD1 requires its CC1 domain and Exon 19 of CLOCK to repress CLOCK:BMAL1

(A) TCoffee alignment of CLOCK and NPAS2 Exon 19 domain with PASD1 CC1 domain. (B) Schematic of PASD1 expression constructs used in luciferase assays. (C) Deletion of CC1 domain in the full-length protein or C-terminus does not affect nuclear localization. HEK293T cells were transfected with MYC-tagged constructs and subcellular localization was visualized by immunofluorescence. Scale bar, 20 μm. (D) Deletion of the PASD1 CC1 domain (residues 365-415) relieves repression of CLOCK:BMAL1 activation of the Per1:luc gene. (E) PASD1-MYC tagged C-term ΔCC1 shows decreased interaction when both CLOCK and BMAL1 are precipitated compared to the MYC tagged C-terminus. Asterisk, non-specific protein. (F) Mutation of two residues in the PAS-B domain HI loop of CLOCK (Q361P/W362R; HI) and BMAL1 (L606A/L607A; LL/AA) that significantly reduce repression by CRY1 do not affect PASD1-mediated repression in *Per1:luc* luciferase assays. (G) CRY1 can inhibit transactivation by CLOCKΔ19:BMAL1 but PASD1 cannot. See also **Supplementary Figure** 4-3.

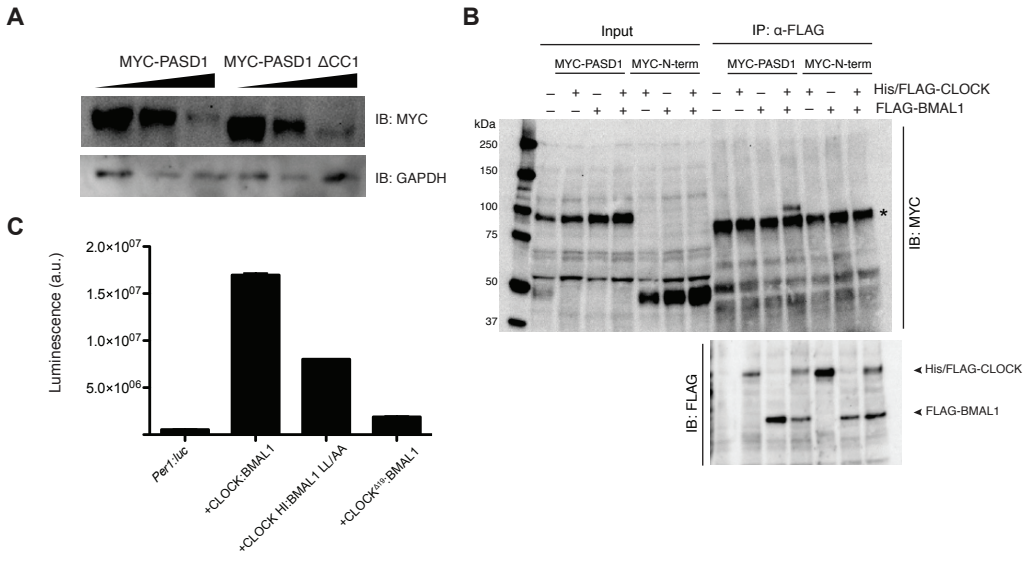

Supplementary Figure 4-3. Characterization of PASD1 and CLOCK:BMAL1 mutants.

(A) PASD1ΔCC1 shows similar expression levels compared to the full length protein when over-expressed. HEK293T cells were transiently transfected with equivalent amounts of plasmid and harvested under identical conditions. Protein levels were assessed by western blotting with endogenous GAPDH as a loading control. (B) Full length PASD1 interacts with CLOCK and/or BMAL1 when they are co-expressed, but the isolated PASD1 N-terminus cannot. HEK293T cells were transfected with the indicated plasmids and proteins were co-precipitated using FLAG affinity resin. The N-terminal construct (residues 1 – 311) contains the PAS-A domain of PASD1 and lacks the CC1 domain. Due to interference of the IgG (*) with the band for MYC-PASD1ΔCC1, the C-terminal construct was used to assess the effect of deletion of the CC1 domain on interaction with CLOCK and BMAL1 (see Fig. 3E). (C) CLOCK and BMAL1 mutants show decreased activity compared with wild-type CLOCK:BMAL1 complex but are active over the background of Per1:luc reporter. HEK293T cells were transfected with equivalent amounts of CLOCK and BMAL1 plasmids in the following combinations to yield activity over background: CLOCK:BMAL1, ~30-fold activation; CLOCK HI:BMAL1 LL/AA, ~12-fold activation; and CLOCKΔ19:BMAL1,~3-4-fold activation. Raw luminescence counts from one representative assay (in triplicate) are shown ± SD.

4.3.3 Regulation of CLOCK:BMAL1 by PASD1 CC1 and CLOCK Exon 19 are functionally linked

To probe how PASD1 impinges on transcriptional activation by CLOCK:BMAL1, we tested two transcription factor mutants that interfere discretely with two key regulatory domains on CLOCK:BMAL1: the BMAL1 TAD or CLOCK Exon 19. Both CLOCK:BMAL1 mutants had reduced activity relative to wild-type CLOCK:BMAL1, but overall activity of the heterodimer was sufficiently robust (~3-4 fold activation of the *Per1:luc* reporter over background) to probe regulation of the complexes (Supplementary Figure 4-3C). We first tested the CLOCK HI:BMAL1 LL/AA mutant, which interferes with sequestration of the BMAL1 TAD by CRY1. Although the CLOCK HI:BMAL1 LL/AA mutant abolished repression by CRY1, PASD1 still potently repressed transcriptional activation to suggest that PASD1 does not inhibit CLOCK:BMAL1 through sequestration of the BMAL1 TAD (Figure 4-3F). We then tested the ability of PASD1 to repress CLOCK$^{\Delta 19}$:BMAL1, which lacks the 51 amino acids encoded by Exon 19 (29, 38). CRY1 could still potently repress the residual transactivation potential in the CLOCK$^{\Delta 19}$:BMAL1 mutant (Figure 4-3G); however, PASD1 could no longer exhibited repression of CLOCK$^{\Delta 19}$:BMAL1 activity. We interpret these data to mean that PASD1 interferes with CLOCK:BMAL1 function in a manner that depends on the activating potential of Exon 19; once disrupted in the CLOCK$^{\Delta 19}$:BMAL1 mutant, PASD1 can no longer further repress the heterodimer.

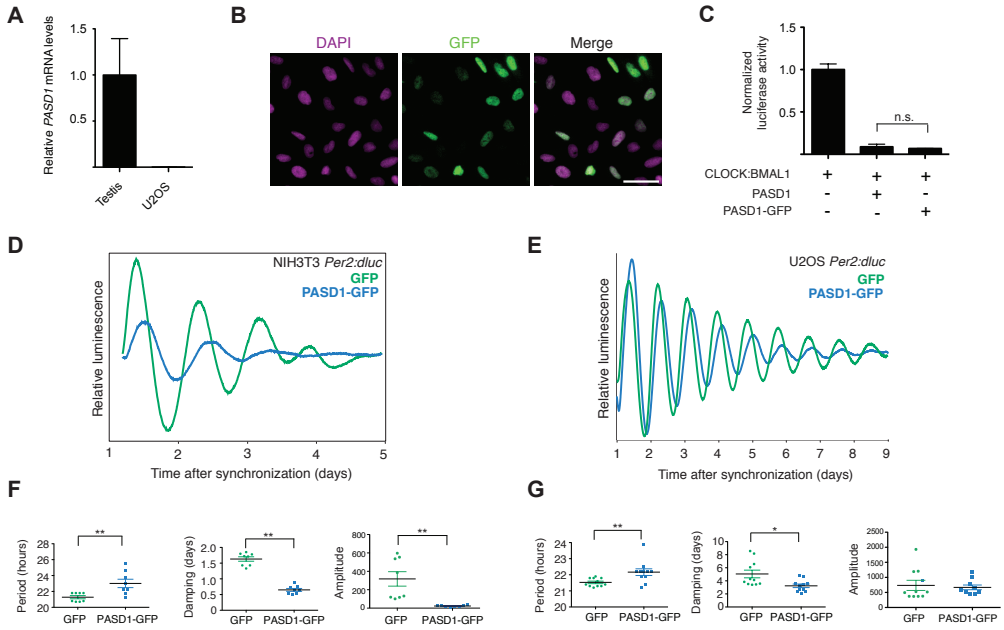

Figure 4-4 Overexpression of PASD1 lengthens period and increases damping of circadian cycling in cell culture.

(A) Comparison of PASD1 expression in human testis and U2OS cells by RT-qPCR. (B) Immunofluorescence of PASD1-GFP in a U2OS Per2:dluc cell line stably expressing PASD1-GFP. Scale bar, 20 μm. (C) Fusion of GFP to PASD1 does not affect repression of CLOCK:BMAL1. Significance was determined by Student's t-test: n.s., not significant. (D) Representative bioluminescence records from mouse NIH3T3 Per2:dluc cells expressing GFP or PASD1-GFP (n=8). (E) Representative bioluminescence records from human U2OS Per2:dluc cells expressing GFP or PASD1-GFP (n=11). (F) PASD1-GFP expression in NIH-3T3 Per2:dluc cells significantly lengthens period, increases damping rate and decreases amplitude. Period (hours) ± SEM: GFP 21.3 ± 0.2, PASD1-GFP 23.0 ± 0.53. Damping (days) ± SEM: GFP 1.29 ± 0.3, PASD1-GFP 0.65 ± 0.046. (G) PASD1-GFP expression in U2OS Per2:dluc cells significantly lengthens period and increases damping rate. Period (hours) ± SEM: GFP 21.55 ± 0.07, PASD1-GFP 22.2 ± 0.2. Damping (days) ± SEM: GFP 5.05 ± 0.6, PASD1-GFP 3.24 ± 0.27, n=11. Significance was determined by Student's t-test: *, $p < 0.05$; **, $p < 0.01$.

4.3.4 PASD1 suppresses circadian cycling

To determine the effect of PASD1 expression on intact molecular circadian oscillators, we examined circadian cycling in mouse NIH3T3 fibroblast cells, which completely lack the *PASD1* gene, and human U2OS osteosarcoma cells that cycle with high amplitude (51, 52) but do not express *PASD1* as determined by RT-qPCR (Figure 4-4A and Supplementary Figure 4-4A). We generated *Per2:dluc* reporter cell lines stably expressing PASD1-GFP or a GFP control after determining that GFP fusion does not alter PASD1 subcellular localization or attenuate PASD1 activity towards CLOCK:BMAL1 (Figures 4B-C and Supplementary Figure 4-4B). In both lines, expression of PASD1-GFP led to significant alterations in the molecular oscillator (Figure 4-4D-E) marked by an increase in the period (~1 h) and rate of damping (Figure 4-4F-G), which indicates defects in cell-autonomous clocks that lead to desynchronization of the population (53). In mouse NIH3T3 fibroblasts, we also noted a significant decrease in amplitude upon PASD1-GFP expression that was not as pronounced in U2OS cells, which could be attributable to the higher basal amplitude of cycling in the U2OS cell line. (Figure 4-4F-G). Collectively, these findings demonstrate that introduction of PASD1 into naïve cells attenuates the robustness of the molecular circadian oscillator.

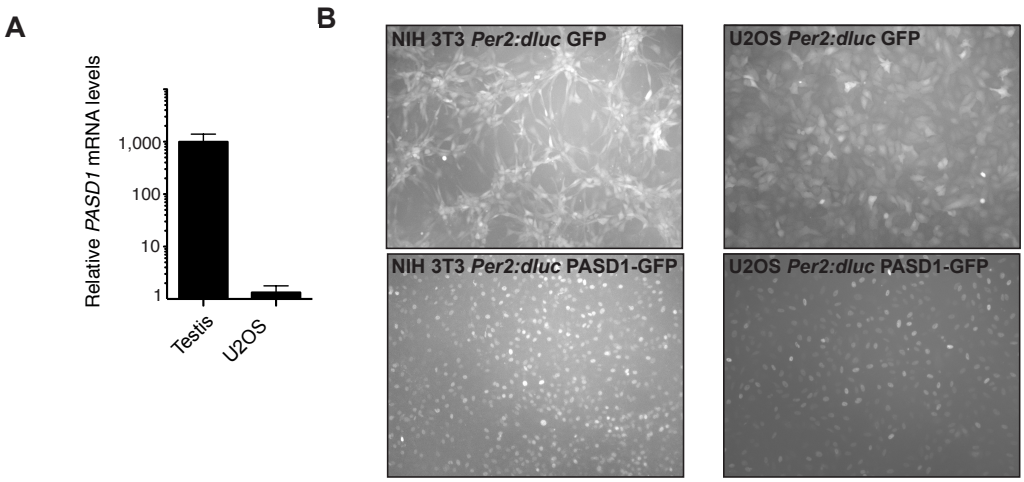

Supplementary Figure 4-4. Validation of reagents used in PASD1 overexpression studies.

(A) Comparison of PASD1 expression in human testis and U2OS cells by RT-qPCR. U2OS cells exhibit > 0.2% relative PASD1 mRNA abundance compared to expression in human testis, which is normalized to 1. Data are duplicated from Fig. 4A (linear y-axis) and shown in log10 format to illustrate the difference in PASD1 expression. (B) Representative images of GFP-positive cells taken immediately before bioluminescence recording of circadian rhythms. GFP-positive cells were sorted using fluorescence-activated flow cytometry and plated at 90-100% confluency 24 hours prior to recording.

4.3.5 Identification of PASD1-positive cancer cell lines

PASD1 is not expressed in cells of somatic origin unless it has been de-repressed due to malignant transformation (54). The circadian clock is frequently disrupted in cancer, allowing cells to escape its daily temporal control of regulated processes and facilitate tumor growth (5, 6, 55). To determine if upregulation of PASD1 influences the robustness of the circadian clock in

human cancer, we screened a panel of cancer cell lines by examining mRNA and protein expression of the two *PASD1* splice isoforms. TaqMan probes common to both splice isoforms (Exon 11-12) or specific for the longer *PASD1v2* isoform (Exon 14-15) reported similar levels of expression, indicating that the longer isoform is predominantly expressed in human cancer cells (Figure 4-5A) (43). Among cancer cell lines with the highest *PASD1* mRNA expression, we found that G-361 melanoma, NCI-H1299 non-small cell lung carcinoma, COR-L23 large cell lung carcinoma, and the BT-20 breast cancer line had *PASD1* transcript levels comparable to human testis (Figure 4-5A). Relative levels of PASD1 protein correlated with differences between mRNA transcripts when analyzed by western blotting and expression of the longer isoform was confirmed by use of isoform-specific antibodies (Figure 4-5B) (43). Immunohistochemical analysis of PASD1 expression in several cancer cell lines revealed cell-to-cell heterogeneity in nuclear PASD1 expression, particularly within SW480 colon cancer cells (Figure 4-5C). Heterogeneous expression of cancer biomarkers is often seen in tumors and can drastically affect the efficacy of cancer therapeutics (56). Moreover, in the context of circadian regulation, heterogeneous expression of PASD1 could lead to differences in period among individual cells that would serve to desynchronize cell-autonomous molecular oscillators to diminish overall clock function in the tumor microenvironment.

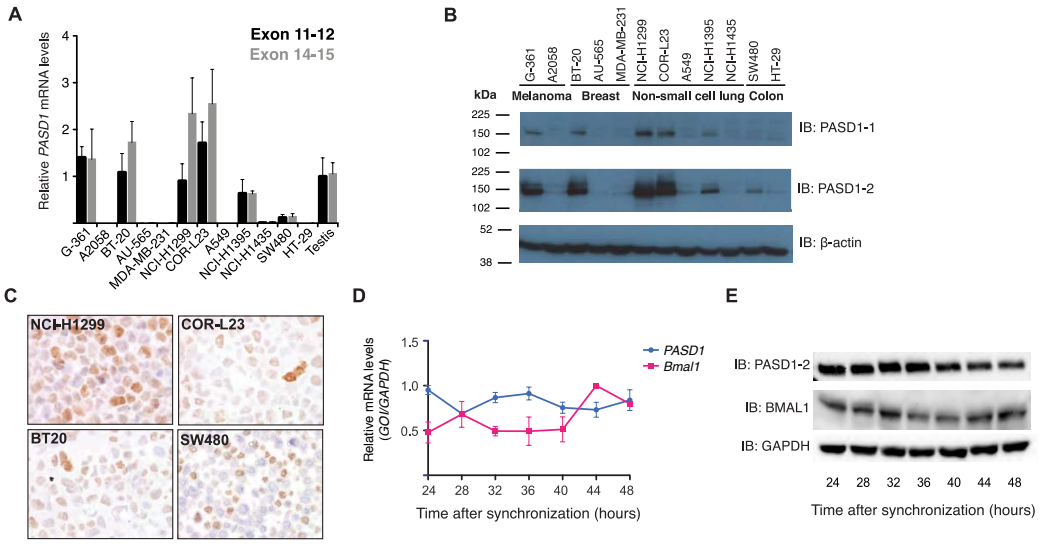

Figure 4-5. PASD1 mRNA and protein is expressed in a diverse array of human cancers.

(A) Examination of *PASD1* transcripts in a panel of cancer cell lines by RT-qPCR. Exon 11-12 TaqMan probe (Hs01098424_m1) recognizes both splice isoforms, while the Exon 14-15 (Hs00542871_m1) TaqMan probe recognizes only the long isoform. *PASD1* expression was normalized to TBP (TATA Box Binding Protein), 18S RNA and HPRT1 (Hypoxanthine phosphoribosyltransferase 1) and all samples are presented relative to *PASD1* expression in human testis, normalized to 1. Error bars indicate standard deviation from n=3 measurements. (B) Western blot analysis of PASD1 protein expression in the same cell lines as in panel A. The PASD1-1 monoclonal antibody recognizes an epitope between residues 195–474, common to both splice isoforms. The PASD1-2 monoclonal antibody recognizes an epitope between residues 640-773 that is specific to the longer isoform (43). (C) Immunohistochemistry of PASD1 positive cancer cell lines. Hematoxylin and eosin staining (blue), nuclei; PASD1 staining (brown). (D) RT-qPCR of *PASD1* and *Bmal1* in NCI-H1299 cells after circadian synchronization with 100 nM dexamethasone. Relative mRNA values are normalized to *GAPDH* and error bars represent the mean ± SEM of two independent experiments. (E) Western blot of PASD1 and BMAL1 protein expression in circadian synchronized NCI-H1299 cells. Data are representative of two independent experiments.

Other repressors of CLOCK:BMAL1 are transcriptionally regulated by the clock, giving rise to a circadian peak in mRNA abundance (28, 57–62). We examined *PASD1* and *Bmal1* mRNA and protein expression over a circadian period in NCI-H1299 cells after synchronization of cellular clocks by dexamethasone. We found that expression of *Bmal1* mRNA was rhythmic on the circadian timescale, but exhibited low amplitude in its oscillation (ANOVA, $p = 0.05$) (Figure 4-5D). *PASD1* mRNA expression was antiphasic to *Bmal1* with an even lower amplitude of oscillation that did not reach criteria for significance (ANOVA, $p = 0.12$). Protein levels of BMAL1 followed the same trend, with cyclical yet low amplitude circadian rhythms while PASD1 levels did not appear to cycle after synchronization (Figure 4-5E). Taken together, these data suggest that PASD1 may be a CLOCK:BMAL1 target; however, we were unable to detect a circadian oscillation of PASD1 mRNA or protein levels in NCI-H1299 cells.

4.3.6 Downregulation of PASD1 improves amplitude of cycling in human cancer cells

To assess the effect of endogenous PASD1 expression on circadian rhythms in human cancer cells, we chose to study the NCI-H1299 cell line (high expression) and the SW480 cell line (lower levels with more heterogeneous expression) by stably incorporating the *Per2:dluc* reporter gene (63). Co-immunoprecipitation experiments in NCI-H1299 *Per2:dluc* cells showed that a pool of endogenous PASD1 and BMAL1 interact (Figure 4-6A). Transfection of

the *Per2:dluc* lines with *PASD1* siRNA achieved knockdown of PASD1 in NCI-H1299 cells as assessed by RT-qPCR, although to a lesser degree in SW480 cells (Figure 4-6B). siRNA treatment of NCI-H1299 *Per2:dluc* cells reduced PASD1 protein levels (Figure 4-6C) and resulted in a significant increase in the amplitude of circadian cycling (Figure 4-6D-E). Fast Fourier Transform (FFT) power spectra of cycling data from NCI-H1299 *Per2:dluc* cells also demonstrated that knockdown of PASD1 improved amplitude (Figure 4-6F). This waveform analysis converts time domain cycling data into the frequency domain, illustrating both the period of the oscillation and its amplitude, demonstrated by the height of the strongest spectral peak that defines the circadian period. The amplitude of circadian cycling was also significantly improved upon PASD1 knockdown in SW480 *Per2:dluc* cells (Figure 4-6G-I). We detected a modest but non-significant trend towards a longer period in both lines with PASD1 knockdown (Supplementary Figure 4-5). The marked improvement of cycling amplitude in two distinct cancer cell lines upon knockdown of PASD1 demonstrates that it can suppress circadian clock function when upregulated in human cancer.

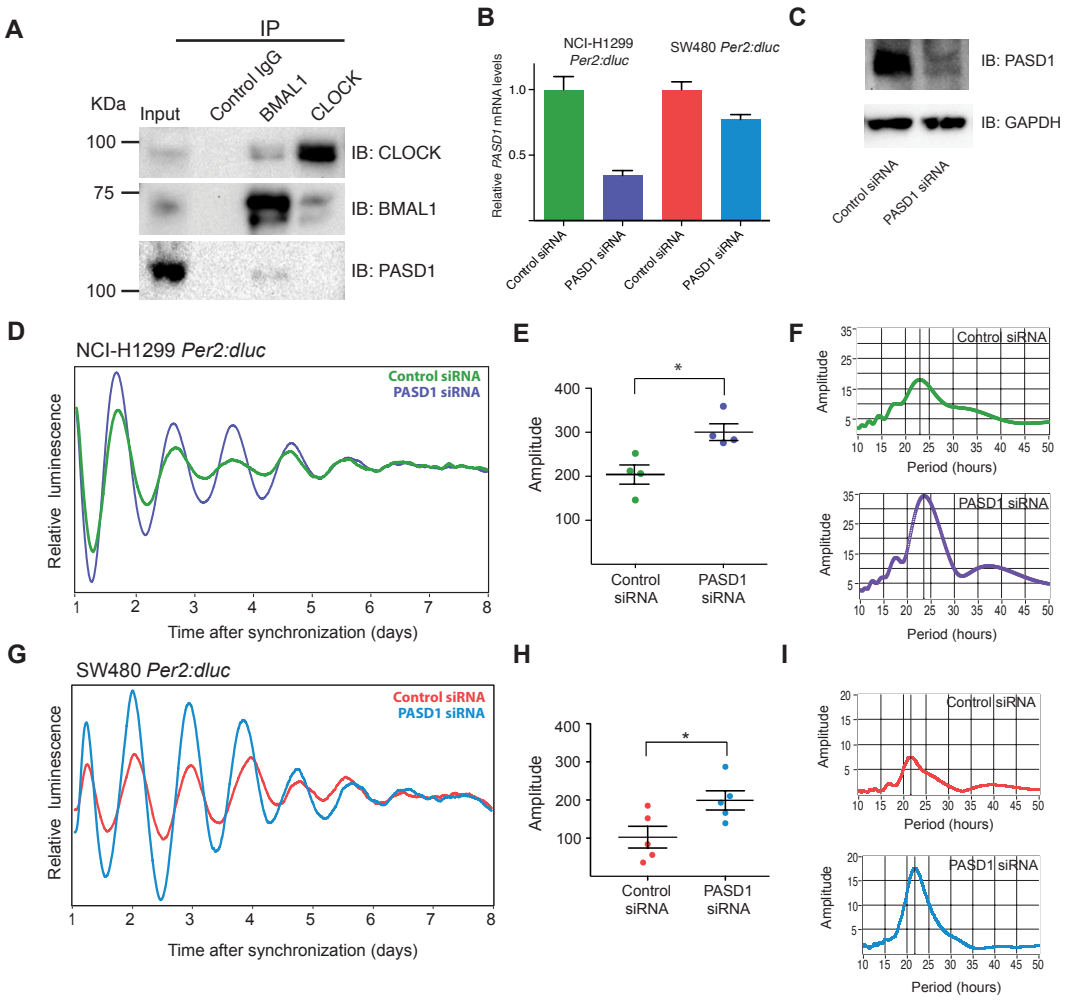

Figure 4-6. Reducing expression of PASD1 in cancer cells increases robustness of circadian rhythms

(A) Co-immunoprecipitation of endogenous CLOCK, BMAL1 and PASD1 from NCI-H1299 nuclear extract. (B) Reduction of *PASD1* mRNA in NCI-H1299 *Per2:dluc* and SW480 *Per2:dluc* cells after siRNA by RT-qPCR. (C) Knockdown of PASD1 protein in NCI-H1299 *Per2:dluc* cells with siRNA. Due to the lower level of heterogeneous expression of PASD1 in SW480 cells, protein levels were at the limit of detection by western blot using our polyclonal rPASD1 antibody; therefore, knockdown was assessed using RT-qPCR. (D) Representative bioluminescence records from NCI-H1299 *Per2:dluc* lung cancer cells transfected with control scramble or *PASD1* siRNA (n=4). (E) Mean amplitude values from independent experiments. Data are represented as mean ± SEM. Significance was assessed by Student's *t*-test, *, $p < 0.05$. (F) FFT analysis spectrum of cycling traces

shown in part D. G to I) Same as in panels D to F for SW480 *Per2:dluc* colon cancer cells. Student's *t*-test, *, $p < 0.05$. See also Supplementary Figure 4-5.

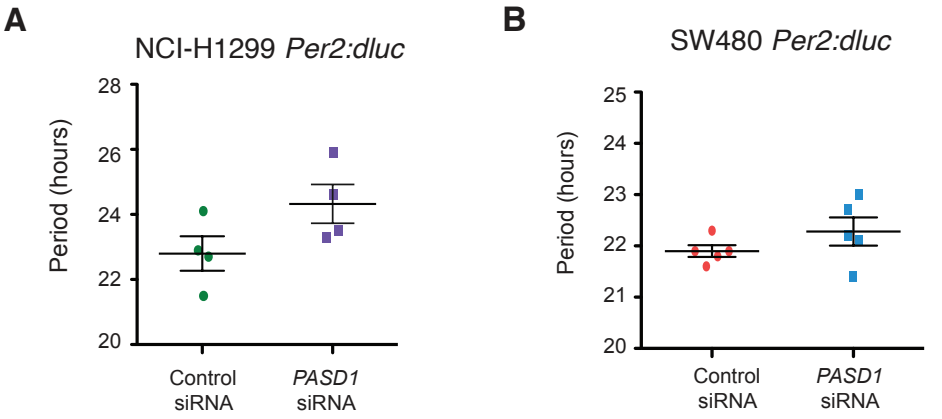

C

	Period (hours ± SD)	
NCI-H1299 *Per2:dluc*		
Control siRNA	22.80 ± 0.53	p = 0.1054
PASD1 siRNA	24.33 ± 0.59	
SW480 *Per2:dluc*		
Control siRNA	21.90 ± 0.12	p = 0.2371
PASD1 siRNA	22.28 ± 0.27	

Supplementary Figure 4-5. Knockdown of PASD1 in cancer cell lines shows a trend towards lengthened period.

(A) NCI-H1299 Per2:dluc and (B) SW480 Per2:dluc cells transfected with PASD1 siRNA show a trend towards lengthened period. Data represented 4 or 5 independent runs with mean ± SEM plotted. (C) Quantification of circadian periods in the two cell lines with statistical assessment. Statistical significance was assessed by Student's t-test (unpaired, two-tailed).

4.4 Discussion

Our findings establish that PASD1 is the bHLH-PAS paralog repressor for the circadian transcription factor CLOCK:BMAL1. As such, PASD1 fulfills a role analogous to the aryl hydrocarbon receptor repressor (AhRR) (16), inhibitory PAS protein (IPAS) (32), and neuronal PAS domain protein 1 (NPAS1) (33), each dedicated to repression of a specific bHLH-PAS signaling pathway. Several bHLH-PAS paralog repressors require their homologous PAS domains to interfere with the function of cognate transcription factors (16, 32), while others such as NPAS1 and SIM2 possess homologous PAS domains but utilize repressive domains in their C-termini (33, 40, 64). We discovered PASD1 by searching for PAS domain-containing homologs to CLOCK and BMAL1 in humans. However, our studies addressing the biochemical mechanism of PASD1 regulation highlighted an essential role for the C-terminal CC1 domain that bears homology to the essential regulatory region encoded by CLOCK Exon 19. The Id protein family also shares structural homology with CLOCK and BMAL1 in the helix-loop-helix DNA-binding domain that it uses to repress the complex (65, 66). However, by targeting a prevalent DNA-binding motif, these proteins also repress many transcriptional networks. Because PASD1 invokes sequence similarity with CLOCK to regulate CLOCK:BMAL1 activity, it appears to be more specific for the circadian pathway. We showed that PASD1 does not repress CLOCK:BMAL1 activity like cryptochromes, which sequester the BMAL1 transcriptional activation domain from coactivators

(unpublished data). Instead, PASD1 requires the activating potential of CLOCK Exon 19 to repress transcriptional activation by CLOCK:BMAL1. Collectively, these data suggest that PASD1 utilizes molecular mimicry of CLOCK Exon 19 to interfere with CLOCK:BMAL1 function.

CLOCK Exon 19 is essential for CLOCK:BMAL1 function and its deletion generates a dominant negative *Clock*$^{\Delta 19}$ mutant that suppresses circadian rhythms (29, 38). The 51 amino acids encoded by CLOCK Exon 19 are needed to interact with the coactivator histone methyltransferase MLL1 (27) and a vertebrate-specific repressor, CLOCK-Interacting Protein Circadian, CIPC (28). Even though MLL1 interacts with both CLOCK and BMAL1 by co-immunoprecipitation, it requires CLOCK Exon 19 to coordinate rhythmic changes in Histone H3 Lysine4 trimethylation (27). Unlike MLL1 and CIPC, we did not detect interaction of PASD1 with CLOCK; instead, our data show that PASD1 requires its CC1 domain to interfere with CLOCK:BMAL1 function that is mediated by Exon 19. The reciprocal relationship between PASD1 CC1 and CLOCK Exon 19 is further supported by similarities between PASD1 overexpression in 3T3 fibroblasts and heterozygous expression of the dominant negative *Clock*$^{\Delta 19}$ mutant, both of which exhibit decreased amplitude, long period and rapid damping (30). However, the exact mechanism by which PASD1 impinges on transcriptional activation by CLOCK:BMAL1 remains to be determined.

The limited distribution of PASD1 across tissues is analogous to other bHLH-PAS repressors that are expressed selectively to control developmental or tissue-specific programs of transcriptional activation (32, 34, 35, 67). One powerful example of this is inhibition of the hypoxia inducible factor, HIF (HIF-1α:ARNT), in the hypoxic cornea by its paralog repressor IPAS, which prevents neovascularization in the cornea that would interfere with vision (32). By virtue of its limited tissue distribution, PASD1 is poised to suppress circadian rhythms in the germline and, as a consequence of its demethylation and upregulation, in somatic cancers (43, 45). Notably, mouse and hamster testis do not exhibit molecular circadian rhythms (57, 68, 69). It has yet to be demonstrated that testis from other mammals, including humans, do not have circadian rhythms; however, based on the data presented here, we speculate that high levels of PASD1 in human testis could lead to suppression of circadian rhythms in the germline (43). Connections between the lack of circadian cycling in undifferentiated embryonic stem cells and the germline are just coming to light (70–72), making PASD1 an interesting link that could be explored further.

To date, cancer/testis antigens have largely been explored as targets for cancer immunotherapy (44–46). It is still unclear whether they simply serve as cancer biomarkers or whether their upregulation in somatic cancer has consequences for tumor progression by promoting return to a germ-like state (73). Recent studies show that some cancer/testis antigens possess activities consistent with the latter hypothesis, from promoting destabilization of tumor

suppressors to regulating genomic stability (74, 75). Here we describe a role for a cancer/testis antigen in suppression of the circadian clock, showing that PASD1 can attenuate clock function even when heterogeneously expressed in cancer cells. Circadian disruption has been connected to increased incidence of diabetes, cardiovascular disease, and cancer (2, 3, 5) but there is a growing appreciation for reciprocal regulation of circadian rhythms by disease or altered metabolic states. In particular, consumption of a high fat diet alters the metabolic state to suppress CLOCK:BMAL1-driven transcriptional activation and dampen circadian amplitudes, allowing for the rewiring of vast transcriptional programs (76, 77). These studies demonstrate the importance of maintaining robust circadian amplitudes to promote proper temporal regulation of physiology. Our discovery of PASD1 as a circadian bHLH-PAS paralog repressor that is only expressed in somatic tissues after oncogenic transformation suggests that it may represent a molecular link from oncogenesis to circadian disruption.

4.5 Materials and Methods

4.5.1 Immunofluorescence

Cells were fixed with 4% paraformaldehyde for 10 minutes, then permeabilized and blocked in phosphate buffered saline (PBS) containing 1% horse serum and 0.05% Triton X-100 for 15 minutes. Primary incubation was carried out for 1 hour at room temperature (RT) in blocking solution with chicken anti-GFP (1:1,500; Aves labs) or mouse anti-MYC (1:1,000; Abcam). Cells

were washed 3x with PBS, then incubated with secondary Alexa Fluor conjugated antibodies (1:2,000; Molecular Probes) and DAPI (Life Technologies) for 30 minutes. Slides were mounted in Fluoromount-G (Southern Biotech) and analyzed on a Keyence BZ-9000 Fluorescence Microscope.

4.5.2 Antibodies

Polyclonal antibodies were generated against human PASD1 (rPASD1) (epitope: DQMRSAEQTRLMPAEQRDS, residues 751 – 770) and human BMAL1 (78) (epitope: LEADAGLGGPVDFSDLPWPL, residues 607-626) by immunization of KLH-conjugated peptides in rabbits using standard protocols (Pierce Biotechnology). Serum was affinity purified using the SulfoLink Immobiliation Kit using the manufacturer's instructions (Thermo) after conjugation of the antigenic peptide to the immobile phase. Purified antibodies were dialyzed into 0.15M glycine, 50mM Tris-HCl, pH 7.0 with 50% glycerol and aliquoted for storage at -80°C. Hybridoma supernatants containing anti-PASD1 monoclonal antibodies (PASD1-1 and PASD1-2) were as previously described (43).

4.5.3 Co-immunoprecipitations

HEK293T cells (ATCC) were grown in DMEM supplemented with 10% fetal bovine serum. Cells were transfected using the calcium phosphate method with plasmids expressing His_6FLAG-CLOCK (pSG5-CLOCK), FLAG-BMAL1 (pSG5-BMAL1) and His_6MYC-tagged truncations of pCDNA4B-PASD1

as follows: PASD1 (aa 1-638), C-term (aa 312-638), C-termΔCC1 (aa 312-638), N-term (aa 1-311) as indicated. Cells were seeded into 60 mm dishes (750,000 cells) 16 hours prior to transfection. Approximately 24 hours post-transfection, cells were incubated on ice for 10 min. in PASD1 lysis buffer (20 mM HEPES-KOH pH 7.5, 100 mM NaCl, 1 mM EDTA, 1% Triton X-100, 5% glycerol), then sonicated briefly (~2 sec) on low power to extract proteins from chromatin. Extracts were clarified by centrifugation at 13.2K rpm for 10 min. at 4°C. 25 µL of clarified extract was removed for input sample. The remaining extract was added to 300 µL lysis buffer containing 15 µl anti-Flag M2 affinity resin (Sigma). Tubes were rotated end over end for 4 hours, and resin was washed three times with 400 µL lysis buffer. Proteins were eluted from resin by addition of 30 µL 2X SDS Laemmli buffer containing 1% β-mercaptoethanol and boiled for 4 minutes. Proteins were resolved by standard SDS-PAGE (7.5% gel, BioRad) and transferred to 0.45 µm nitrocellulose membrane (BioRad). Membranes were blocked with 5% (w/v) non-fat milk in Tris-buffered saline with Tween-20 (TBST; 20 mM Tris pH 7.5, 150 mM NaCl, 0.1% (v/v) Tween-20) and probed with anti-FLAG (1:2,000; Sigma-Aldrich) or anti-MYC (1:2,500; 9E10 ascites fluid, University of Iowa Developmental Studies Hybridoma Bank, DSHB). HRP-conjugated secondary antibodies were used at 1:10,000 (Santa Cruz Biotechnology) in TBST. Western signal was detected using Clarity ECL reagent (Bio-Rad) and visualized on a ChemiDoc XRS+ imager (Bio-Rad).

For endogenous co-immunoprecipitations from nuclear extract, approximately 1 x 10^8 U2OS PASD1-GFP or NCI-H1299 cells were lysed in hypotonic lysis buffer (10 mM HEPES-KOH pH 7.5, 10 mM KCl, 1.5 mM $MgCl_2$, 340 mM sucrose, 10% glycerol, 0.1% Triton X-100) containing 1x protease inhibitor cocktail (Roche). Nuclei were pelleted by centrifugation at 4K rpm for 5 min at 4°C, washed once with hypotonic lysis buffer, then resuspended in PASD1 lysis buffer (20 mM HEPES-KOH [7.5], 100 mM NaCl, 1 mM EDTA, 1% Triton X-100, 5% glycerol) containing 1x EDTA-free protease inhibitor cocktail (Roche) and 1 mM PMSF. Lysates were incubated on ice for 10 min, sonicated briefly on low power, then centrifuged at 13.2K rpm for 10 min at 4°C. Cell lysates were incubated with 4 µg of rabbit normal IgG (Santa Cruz Biotechnology), CLOCK (H-276; Santa Cruz Biotechnology), BMAL1 or rPASD1 antibody for 2 hours at 4°C, followed by incubation with 15 µL protein A/G agarose (Pierce) overnight at 4°C. IPs were washed three times with PASD1 lysis buffer containing 0.05% Triton X-100 and once with lysis buffer without Triton X-100. Samples were boiled in SDS sample buffer containing 5% β-mercaptoethanol and 50 mM DTT. Proteins were resolved by standard SDS-PAGE (7.5% gel, BioRad) and transferred to 0.45 µm nitrocellulose membrane (BioRad). Membranes were blocked with 5% non-fat milk/TBST and probed with anti-CLOCK (1:250; S-19, SCBT), anti-BMAL1 (1:250; B-1, SCBT), or anti-PASD1 (1:100; PASD1-2) antibodies in 2.5% non-fat milk/TBST. HRP-

conjugated secondary antibodies were used at 1:10,000 (SCBT) in 2.5% non-fat milk/TBST.

4.5.4 Transient transfection and reporter assays

For *Per1*:*luc* reporter gene assays, plasmids were transfected in duplicate into HEK293T cells in a 48-well plate using LT-1 transfection reagent (Mirus) with the indicated plasmids: 5 ng pGL3 *Per1:luc* reporter, 100 ng each pSG5-BMAL1 and pSG5-CLOCK. Full-length cDNA for human PASD1 (accession # BC040301.1; Open Biosystems) was validated by complete sequencing. Amounts of pcDNA4B- His_6MYC-FLAG-CRY1 and pcDNA4B His_6MYC-PASD1 used were as follows: 1, 5 and 50 ng of plasmid were used in the titration of CRY1 and PASD1v2, and 50, 100 and 200 ng of plasmid were used in the titration of PASD1 (aa 1-638) and PASD1ΔCC1 (aa 1-638 with deletion of aa 315-465); in all cases, empty pcDNA4B vector was used to normalize total plasmid to 800 ng/well. For full-length PASD1 (aa1-773) and PASD1 C-term (312-773), 10 or 100 ng were transfected for each construct. Cells were harvested 30 hours after transfection using Passive Lysis Buffer (NEB) and luciferase activity assayed with Bright-Glo luciferin reagent (Promega) on a Perkin Elmer EnVision plate reader. Each reporter assay was repeated at least three independent times.

4.5.5 Lentiviral constructs and production

NIH3T3, U2OS, NCI-H1299 and SW480 cells (ATCC) were first infected with pLV7-Bsd-P(Per2)-dLuc reporter (a kind gift from Andrew Liu, University

of Memphis) followed by blasticidin selection to generate stable reporter cell lines. For overexpression studies in U2OS and NIH3T3 *Per2:dLuc* cells, PASD1-EGFP (PASD1, aa 1-773) and EGFP constructs were cloned into the pCDH-neo-514B-1 lentiviral vector (Systems Biosciences). Third-generation lentiviruses were generated by transient co-transfection of HEK293T cells with a four-plasmid combination as follows: one 150 mm dish containing 1.0 x 10^7 293T cells was transfected using the calcium phosphate method with 40 µg lentiviral vector, 20 µg pMDLg/pRRE (Addgene, #12251), 10 µg pRSV-Rev (Addgene #12253) and 12 µg pMD2.G (Addgene, #12259). Supernatants were collected 48 hours after transfection and lentiviral particles were concentrated using PEG-IT (Systems Biosciences) according to the manufacturer's protocol.

4.5.6 Lentiviral transduction

NIH3T3 and U2OS cells were grown to ~60 - 70% confluency in 60 mm dishes and infected with EGFP or PASD1-EGFP lentiviral particles to obtain a multiplicity of infection (MOI) of 1 using 8 µg/mL polybrene (Santa Cruz Biotechnology). When cultures reached confluency, cells were trypsinized, expanded and subjected to 400 µg/mL G418. After approximately one week of antibiotic selection (determined by the kill curve of mock-infected cells), cells were sorted for GFP positive cells by FACS using the FITC channel (BD FACSAria II Cell Sorter) to obtain a pure transgene positive population. Immediately after sorting, cells were plated for bioluminescence recording.

4.5.7 siRNA-mediated PASD1 knockdown

NCI-H1299 *Per2:dluc* and SW480 *Per2:dluc* cells were grown to ~70% confluency in 35 or 60 mm dishes. Cells were transfected with siRNA duplexes at 100nM final concentration using Lipofectamine 2000 according to the manufacturer's protocol. After 72 hours of incubation with siRNA, mRNA was isolated from 60 mm dishes and subject to RT-qPCR or 35 mm dishes were prepared for bioluminescence recording. To visualize PASD1 protein knockdown by western blot, 1.5 x 10^6 NCI-H1299 *Per2:dluc* cells were transfected with siRNA as described above and the cells were lysed in 150 µL PASD1 lysis buffer after 72 hours incubation time as described above. 50 µg total protein was resolved by standard SDS-PAGE (7.5% gel, BioRad) and transferred to 0.45 µm nitrocellulose membrane (BioRad). Membranes were blocked with 5% non-fat milk/TBST and probed with anti-rPASD1 (1:500) in 2.5% (w/v) non-fat milk/TBST. HRP-conjugated secondary antibodies were used at 1:10,000 (SCBT) in 2.5% (w/v) non-fat milk/TBST.

Table 4-1 siRNA sequences

siRNA sequences	5' – 3'
Scramble control	GAAGCCCATTTAGATACCTCATGAT
PASD1 S1	TCAACCAAGTGACGCTACAGTTATT
PASD1 S2	TCCTGTGGTCTTTAGTGGCTTGTTT

*100nM of Scramble control and 50nM of PASD1 S1 with 50nM PASD1 S2

4.5.8 Bioluminescence recording and data analysis

Cell lines were generated as described above and were grown to 90 – 100% confluency under each condition in 35 mm dishes. After reaching appropriate confluency, cell culture media was replaced with HEPES-buffered phenol-free DMEM media containing 100 nM dexamethasone and 100 μM D-luciferin. Dishes were covered with 40 mm glass coverslips (Fisher Scientific) and sealed with vacuum grease to prevent evaporation. Emission of bioluminescence from reporter cells was monitored at 37°C without added CO_2 using a LumiCycle luminometer (Actimetrics). Dominant circadian period, amplitude and damping were extracted using the accompanying LumiCycle software and fit using the dampened sinusoidal waveform. In all bioluminescence traces, the data shown are representative from greater than three independent experiments (on average, n = 8-11).

4.5.9 Reverse transcription and qPCR

To assess *PASD1* mRNA knockdown after siRNA treatment in NCI-H1299 *Per2:dluc* and SW480 *Per2:dluc, t*otal RNA was isolated from cells using TRIzol reagent according to the manufacturer's instructions (Life Technologies) with the following modifications: after precipitation with isopropanol, the pellet was resuspended in 360 μL SDS extraction buffer (20 mM Tris-HCl pH 7.5, 1 mM EDTA, 0.5% (w/v) SDS). After resuspending the pellet, 0.1 volume of 3 M NaOAc (pH 5.3) and 200 μL phenol:chloroform:isoamyl alcohol were added and centrifuged at 12,000g for

15 min. at 4°C in a phase lock tube (5 Prime). RNA was then washed with 75% ethanol and resuspended in RNAse free water. RNA was treated with TURBO DNA-free kit (Life Technologies). For analysis of transcripts, 1 µg total RNA was reverse transcribed using the iScript kit (BioRad). cDNA reactions were diluted 1:10 and 4 µL of cDNA dilution were used for qPCR (20 µL reaction volume). qPCR reactions were performed using iTaq SYBR Green supermix (BioRad) in a 96-well plate format on a BioRad CFX Connect instrument. Transcript levels were normalized to human *ACTB and GAPDH*. hACTB: 250nM, 250 bp amplicon; hPASD1: 250nM, 238 bp amplicon; hBMAL1: 250nM, 187bp amplicon; hGAPDH: 250nM, 140 bp amplicon.

Table 4-2. Oligonucleotides for qPCR

SYBR	5' – 3'
Human beta actin (hACTB) FOR	CATGTACGTTGCTATCCAGGC
Human beta actin (hACTB) REV	CTCCTTAATGTCACGCACGAT
Human PASD1 FOR	TCCAGAGAGCAGGCTGAACAA
Human PASD1 REV	AAGCCGGATGTAATCCTGTG
Human BMAL1 FOR	CATTAAGAGGTGCCACCAATCC
Human BMAL1 REV	TCATTCTGGCTGTAGTTGAGGA
Human GAPDH FOR	CATCAATGGAAATCCCATCA
Human GAPDH REV	TTCTCCATGGTGGTGAAGAC

Taqman	
PASD1 Exon 11 – 12 region	Hs01098424_m1
PASD1 Exon 14-15	Hs00542871_m1

For RT-qPCR performed on the panel of cancer cell lines, total RNA was extracted using QIAgen's RNeasy Mini kit. For analysis of transcripts, 500 ng of total RNA was used for cDNA synthesis with 100 ng random primers (Promega) and 100U Superscript III (Invitrogen) in a 20 µL reaction. cDNAs were diluted 1:5 and 4 µL of the diluted cDNAs were used for qPCR (20 µL reaction volume). qPCR was performed using 2 TaqMan assays for PASD1 and EXPRESS qPCR Supermix (Invitrogen) on Chromo4 Real-Time Detector (Biorad). Expression was jointly normalized to TBP (TATA Box Binding Protein), 18S RNA and HPRT1 (Hypoxanthine phosphoribosyltransferase 1) and presented relative to expression in RVH-421 cells. Human testis total RNA samples were purchased from: Takara-Clontech (Saint-Germain-en-Laye, France), Ambion (via Invitrogen; Paisley, UK) and Agilent (Stockport UK).

4.5.10 Immunohistochemistry

Formalin-fixed paraffin-embedded cell pellets were prepared by fixing cells in formalin for 24 hours then processing and embedding in paraffin according to standard histological procedures. 4 µm sections were dewaxed, rehydrated and then subjected to pressure cooker antigen retrieval in 50 mM

Tris pH 9, 2 mM EDTA for 2 minutes and then incubated with the PASD1-1 monoclonal antibody, or negative control antibody, at a dilution of 1:60 for 2 hours at room temperature. Labeling was detected using the Novocastra Novolink™ Polymer Detection System (Leica Biosystems, Newcastle, UK).

4.5.11 Western blotting

For western blotting of the panel of cancer cell lines, lysates were prepared using Mammalian Protein Extraction reagent containing Universal Nuclease (Pierce). 30 µg whole cell lysates were resolved on 7.5% acrylamide gel and transferred to Protran nitrocellulose membrane (GE Healthcare). Membranes were blocked in 5% (w/v) low fat milk in 1X PBS for 1 hour at RT, and were then incubated with primary antibodies overnight at 4°C diluted in 5% (w/v) low fat milk in PBS at the following concentrations: 1:10 PASD1-1; 1:10 PASD1-2, or 1:20,000 anti-β-Actin (Sigma, clone AC-15). IgG-HRP secondary antibodies (Dako) were diluted 1:5,000 in 5% low-fat milk/PBS and visualized with ECL reagent (GE Healthcare).

4.6 References

1. Zhang R, Lahens NF, Ballance HI, Hughes ME, Hogenesch JB (2014) A circadian gene expression atlas in mammals: Implications for biology and medicine. Proc Natl Acad Sci 111(45):16219–16224.
2. Marcheva B, et al. (2010) Disruption of the clock components CLOCK and BMAL1 leads to hypoinsulinaemia and diabetes. Nature 466:627–631.
3. Jeyaraj D, et al. (2012) Circadian rhythms govern cardiac repolarization and arrhythmogenesis. Nature 483:96–99.

4. Kondratov R V, Kondratova AA, Gorbacheva VY, Vykhovanets O V, Antoch MP (2006) Early aging and age-related pathologies in mice deficient in BMAL1, the core componentof the circadian clock. Genes Dev 20:1868–1873.
5. Filipski E, Lévi F (2009) Circadian disruption in experimental cancer processes. Integr Cancer Ther 8:298–302.
6. Takahashi JS, Hong H-K, Ko CH, McDearmon EL (2008) The genetics of mammalian circadian order and disorder: implications for physiology and disease. Nat Rev Genet 9:764–775.
7. Koike N, et al. (2012) Transcriptional Architecture and Chromatin Landscape of the Core Circadian Clock in Mammals. Science (80-) 338:349–354.
8. Gustafson CL, Partch CL (2014) Emerging models for the molecular basis of mammalian circadian timing. Biochemistry. doi:10.1021/bi500731f.
9. Lee C, Etchegaray JP, Cagampang FR, Loudon AS, Reppert SM (2001) Posttranslational mechanisms regulate the mammalian circadian clock. Cell 107:855–867.
10. Nagoshi E, et al. (2004) Circadian gene expression in individual fibroblasts: Cell-autonomous and self-sustained oscillators pass time to daughter cells. Cell 119:693–705.
11. Yoo S-H, et al. (2004) PERIOD2::LUCIFERASE real-time reporting of circadian dynamics reveals persistent circadian oscillations in mouse peripheral tissues. Proc Natl Acad Sci U S A 101:5339–5346.
12. Welsh DK, Yoo SH, Liu AC, Takahashi JS, Kay SA (2004) Bioluminescence imaging of individual fibroblasts reveals persistent, independently phased circadian rhythms of clock gene expression. Curr Biol 14:2289–2295.
13. Panda S, et al. (2002) Coordinated transcription of key pathways in the mouse by the circadian clock. Cell 109:307–320.

14. Storch K-F, et al. (2002) Extensive and divergent circadian gene expression in liver and heart. Nature 417:78–83.
15. Gu YZ, Moran SM, Hogenesch JB, Wartman L, Bradfield CA (1998) Molecular characterization and chromosomal localization of a third alpha-class hypoxia inducible factor subunit, HIF3alpha. Gene Expr 7:205–213.
16. Mimura J, Ema M, Sogawa K, Fujii-Kuriyama Y (1999) Identification of a novel mechanism of regulation of Ah (dioxin) receptor function. Genes Dev 13:20–25.
17. Ema M, et al. (1996) Two new members of the murine Sim gene family are transcriptional repressors and show different expression patterns during mouse embryogenesis. Mol Cell Biol 16:5865–5875.
18. Crews ST (1998) Control of cell lineage-specific development and transcription by bHLH- PAS proteins. Genes Dev 12:607–620.
19. Huang N, et al. (2012) Crystal Structure of the Heterodimeric CLOCK:BMAL1 Transcriptional Activator Complex. Science (80-) 337:189–194.
20. Wang Z, Wu Y, Li L, Su X-D (2013) Intermolecular recognition revealed by the complex structure of human CLOCK-BMAL1 basic helix-loop-helix domains with E-box DNA. Cell Res 23:213–24.
21. Scheuermann TH, et al. (2009) Artificial ligand binding within the HIF2alpha PAS-B domain of the HIF2 transcription factor. Proc Natl Acad Sci U S A 106:450–455.
22. Freedman SJ, et al. (2002) Structural basis for recruitment of CBP/p300 by hypoxia-inducible factor-1 alpha. Proc Natl Acad Sci U S A 99:5367–5372.
23. Kobayashi A, Numayama-Tsuruta K, Sogawa K, Fujii-Kuriyama Y (1997) CBP/p300 functions as a possible transcriptional coactivator of Ah receptor nuclear translocator (Arnt). J Biochem 122:703–710.
24. Takahata S, et al. (2000) Transactivation mechanisms of mouse clock transcription factors, mClock and mArnt3. Genes to Cells 5:739–747.

25. Kiyohara YB, et al. (2006) The BMAL1 C terminus regulates the circadian transcription feedback loop. Proc Natl Acad Sci U S A 103:10074–10079.

26. Czarna A, et al. (2011) Quantitative analyses of cryptochrome-mBMAL1 interactions: mechanistic insights into the transcriptional regulation of the mammalian circadian clock. J Biol Chem 286:22414–22425.

27. Katada S, Sassone-Corsi P (2010) The histone methyltransferase MLL1 permits the oscillation of circadian gene expression. Nat Struct Mol Biol 17:1414–1421.

28. Zhao W-N, et al. (2007) CIPC is a mammalian circadian clock protein without invertebrate homologues. Nat Cell Biol 9:268–275.

29. Gekakis N, et al. (1998) Role of the CLOCK protein in the mammalian circadian mechanism. Science 280:1564–1569.

30. Vitaterna MH, et al. (2006) The mouse Clock mutation reduces circadian pacemaker amplitude and enhances efficacy of resetting stimuli and phase-response curve amplitude. Proc Natl Acad Sci U S A 103:9327–9332.

31. Evans BR, et al. (2008) Repression of aryl hydrocarbon receptor (AHR) signaling by AHR repressor: role of DNA binding and competition for AHR nuclear translocator. Mol Pharmacol 73:387–398.

32. Makino Y, et al. (2001) Inhibitory PAS domain protein is a negative regulator of hypoxia-inducible gene expression. Nature 414:550–554.

33. Teh CHL, et al. (2006) Neuronal PAS domain protein 1 is a transcriptional repressor and requires arylhydrocarbon nuclear translocator for its nuclear localization. J Biol Chem 281:34617–34629.

34. Yamamoto J, et al. (2004) Characteristic expression of aryl hydrocarbon receptor repressor gene in human tissues: organ-specific distribution and variable induction patterns in mononuclear cells. Life Sci 74:1039–1049.

35. Fan CM, et al. (1996) Expression patterns of two murine homologs of Drosophila single-minded suggest possible roles in embryonic patterning and in the pathogenesis of Down syndrome. Mol Cell Neurosci 7:1–16.
36. Schultz J, Milpetz F, Bork P, Ponting CP (1998) SMART, a simple modular architecture research tool: identification of signaling domains. Proc Natl Acad Sci U S A 95:5857–5864.
37. Letunic I, Doerks T, Bork P (2014) SMART: recent updates, new developments and status in 2015. Nucleic Acids Res . doi:10.1093/nar/gku949.
38. King DP, et al. (1997) Positional cloning of the mouse circadian clock gene. Cell 89:641–653.
39. Liggins AP, Brown PJ, Asker K, Pulford K, Banham AH (2004) A novel diffuse large B-cell lymphoma-associated cancer testis antigen encoding a PAS domain protein. Br J Cancer 91:141–149.
40. Moffett P, Reece M, Pelletier J (1997) The murine Sim-2 gene product inhibits transcription by active repression and functional interference. Mol Cell Biol 17:4933–4947.
41. Mueller JL, et al. (2013) Independent specialization of the human and mouse X chromosomes for the male germ line. Nat Genet 45:1083–7.
42. Djureinovic D, et al. (2014) The human testis-specific proteome defined by transcriptomics and antibody-based profiling. Mol Hum Reprod 20(6):476–488.
43. Cooper CDO, et al. (2006) PASD1, a DLBCL-associated cancer testis antigen and candidate for lymphoma immunotherapy. Leukemia 20(12):2172–2174.
44. Ait-Tahar K, et al. (2009) Cytolytic T-cell response to the PASD1 cancer testis antigen in patients with diffuse large B-cell lymphoma. Br J Haematol 146:396–407.
45. Whitehurst AW (2014) Cause and consequence of cancer/testis antigen activation in cancer. Annu Rev Pharmacol Toxicol 54:251–72.

46. Joseph-Pietras D, et al. (2010) DNA vaccines to target the cancer testis antigen PASD1 in human multiple myeloma. Leuk Off J Leuk Soc Am Leuk Res Fund, UK 24:1951–1959.

47. Liggins AP, Lim SH, Soilleux EJ, Pulford K, Banham AH (2010) A panel of cancer-testis genes exhibiting broad-spectrum expression in haematological malignancies. Cancer Immun a J Acad Cancer Immunol 10:8.

48. Padeken J, Heun P (2014) Nucleolus and nuclear periphery: Velcro for heterochromatin. Curr Opin Cell Biol 28:54–60.

49. Kondratov R V., et al. (2003) BMAL1-dependent circadian oscillation of nuclear CLOCK: Posttranslational events induced by dimerization of transcriptional activators of the mammalian clock system. Genes Dev 17:1921–1932.

50. Kwon I, et al. (2006) BMAL1 shuttling controls transactivation and degradation of the CLOCK/BMAL1 heterodimer. Mol Cell Biol 26:7318–7330.

51. Hirota T, et al. (2008) A chemical biology approach reveals period shortening of the mammalian circadian clock by specific inhibition of GSK-3ß. PNAS 105:20746–20751.

52. Vollmers C, Panda S, DiTacchio L (2008) A high-throughput assay for siRNA-based circadian screens in human U20S cells. PLoS One 3. doi:10.1371/journal.pone.0003457.

53. Izumo M, Sato TR, Straume M, Johnson CH (2006) Quantitative Analyses of Circadian Gene Expression in Mammalian Cell Cultures. PLoS Comput Biol 2(10):e136.

54. Kim R, Kulkarni P, Hannenhalli S (2013) Derepression of Cancer/testis antigens in cancer is associated with distinct patterns of DNA hypomethylation. BMC Cancer 13:144.

55. Sahar S, Sassone-Corsi P (2009) Metabolism and cancer: the circadian clock connection. Nat Rev Cancer 9:886–896.

56. Marusyk A, Almendro V, Polyak K (2012) Intra-tumour heterogeneity: a looking glass for cancer? Nat Rev Cancer 12:323–334.
57. Miyamoto Y, Sancar A (1999) Circadian regulation of cryptochrome genes in the mouse. Mol Brain Res 71:238–243.
58. Albrecht U, Sun ZS, Eichele G, Lee CC (1997) A differential response of two putative mammalian circadian regulators, mper1 and mper2, to light. Cell 91:1055–1064.
59. Shearman LP, Zylka MJ, Weaver DR, Kolakowski LF, Reppert SM (1997) Two period homologs: Circadian expression and photic regulation in the suprachiasmatic nuclei. Neuron 19:1261–1269.
60. Honma S, et al. (2002) Dec1 and Dec2 are regulators of the mammalian molecular clock. Nature 419:841–844.
61. Annayev Y, et al. (2014) Gene model 129 (Gm129) encodes a novel transcriptional repressor that modulates circadian gene expression. J Biol Chem 289:5013–24.
62. Anafi RC, et al. (2014) Machine Learning Helps Identify CHRONO as a Circadian Clock Component. PLoS Biol 12. doi:10.1371/journal.pbio.1001840.
63. Zhang EE, et al. (2009) A Genome-wide RNAi Screen for Modifiers of the Circadian Clock in Human Cells. Cell 139:199–210.
64. Moffett P, Pelletier J (2000) Different transcriptional properties of mSim-1 and mSim-2. FEBS Lett 466:80–86.
65. Ward SM, Fernando SJ, Hou TY, Duffield GE (2010) The transcriptional repressor ID2 can interact with the canonical clock components CLOCK and BMAL1 and mediate inhibitory effects on mPer1 expression. J Biol Chem 285:38987–39000.
66. Duffield GE, et al. (2009) A Role for Id2 in Regulating Photic Entrainment of the Mammalian Circadian System. Curr Biol 19:297–304.
67. Michael AK, Partch CL (2013) bHLH-PAS proteins: functional specification through modular domain architecture.Michael AK, Partch CL.

bHLH-PAS proteins: functional specification through modular domain architecture. OA Biochem 1(2):16.

68. Morse D, Cermakian N, Brancorsini S, Parvinen M, Sassone-Corsi P (2003) No circadian rhythms in testis: Period1 expression is clock independent and developmentally regulated in the mouse. Mol Endocrinol 17:141–151.

69. Alvarez JD, Sehgal A (2005) The thymus is similar to the testis in its pattern of circadian clock gene expression. J Biol Rhythms 20:111–121.

70. Umemura Y, et al. (2014) Transcriptional program of Kpna2/Importin-α2 regulates cellular differentiation-coupled circadian clock development in mammalian cells. Proc Natl Acad Sci . doi:10.1073/pnas.1419272111.

71. Yagita K, et al. (2010) Development of the circadian oscillator during differentiation of mouse embryonic stem cells in vitro. Proc Natl Acad Sci U S A 107:3846–3851.

72. Paulose JK, Rucker EB, Cassone VM (2012) Toward the Beginning of Time: Circadian Rhythms in Metabolism Precede Rhythms in Clock Gene Expression in Mouse Embryonic Stem Cells. PLoS One 7. doi:10.1371/journal.pone.0049555.

73. Simpson AJG, Caballero OL, Jungbluth A, Chen Y-T, Old LJ (2005) Cancer/testis antigens, gametogenesis and cancer. Nat Rev Cancer 5:615–625.

74. Doyle JM, Gao J, Wang J, Yang M, Potts PR (2010) MAGE-RING protein complexes comprise a family of E3 ubiquitin ligases. Mol Cell 39:963–974.

75. Cappell KM, et al. (2012) Multiple Cancer Testis Antigens Function To Support Tumor Cell Mitotic Fidelity. Mol Cell Biol 32:4131–4140.

76. Hatori M, et al. (2012) Time-restricted feeding without reducing caloric intake prevents metabolic diseases in mice fed a high-fat diet. Cell Metab 15:848–860.

77. Eckel-Mahan KL, et al. (2013) Reprogramming of the circadian clock by nutritional challenge. Cell 155:1464–1478.

78. Rey G, et al. (2011) Genome-wide and phase-specific DNA-binding rhythms of BMAL1 control circadian output functions in mouse liver. PLoS Biol 9. doi:10.1371/journal.pbio.1000595.

79. Doi M, Hirayama J, Sassone-Corsi P (2006) Circadian Regulator CLOCK Is a Histone Acetyltransferase. Cell 125:497–508.

80. Dioum EM, et al. (2009) Regulation of hypoxia-inducible factor 2alpha signaling by the stress-responsive deacetylase sirtuin 1. Science 324:1289–1293.

5 CHAPTER 5 — BIOCHEMICAL PROPERTIES OF CRY1 AND CRY2 CONTRIBUTE TO THEIR DISTINCT AND SHARED ROLES IN THE MAMMALIAN CLOCK

5.1 Introduction

Cryptochromes are the driving force in the negative feedback loop of the mammalian circadian clock (1, 2). Together, and independently of PER proteins, they rhythmically inhibit the transcriptional activity of CLOCK:BMAL1 to produce daily rhythms in gene expression. Genome-wide studies reveal that CLOCK:BMAL1 is found at a multitude of E-box elements throughout the genome and sits at the core of the circadian regulatory network that controls the expression of nearly 40% of genes throughout the body (3, 4). As a major regulator of transcription, disruption of precise control of CLOCK:BMAL1 activity is associated with disease (5). To protect this widespread molecular clockwork from genetic disturbance, most of the central circadian clock genes exist as paralog pairs (PER1 and PER2, CRY1 and CRY2, CLOCK and NPAS2, BMAL1 and BMAL2) (6–8). It is believed that this redundancy acts as a compensatory mechanism to provide robustness of the clock in response to environmental and genetic insults (e.g. DNA damage, genetic mutations, etc.). However, these paralogs are not necessarily entirely functionally redundant. For example, *Bmal1* is the only single gene knockout that renders the animal arrhythmic, and its function cannot be replaced by its paralog, *Bmal2* (9–11). Similarly, it appears that *Npas2* and *Clock* have functionally distinct roles in

peripheral tissues and the superchiasmatic nucleus (SCN), as *Npas2* is unable to replace *Clock* function in the peripheral tissues to maintain rhythms, but can compensate for *Clock* in the networked tissue of the SCN (12). These findings suggest that distinct and subtle characteristics of these circadian homologs confer their differential ability to preserve rhythmicity, and this also depends on the tissue.

Since their identification as critical circadian components almost 20 years ago, many studies have collectively revealed how CRYs contribute to circadian timekeeping through multifaceted mechanisms (13). Recent ChIP-Seq data suggest that there are distinct repressive complexes that occur throughout the night (4). Early in the evening, there is an 'early' repressive complex where both CRY proteins (primarily CRY2), PERs and other chromatin modifying complexes are found at CLOCK:BMAL1 sites (14, 15). Later in the evening, unique elements in the *Cry1* promoter regulate its delayed expression compared to CRY2 (16), and only CRY1 is found at CLOCK:BMAL1 in the 'late' repressive complex. This 'late' complex provides an additional delay in the repressive phase and maintains the transcription factor repressed, yet poised to begin activating genes in the early morning. It has been shown by our lab and others, that CRY1 inhibits CLOCK:BMAL1 through multivalent interactions with this core transcription factor (11, 17, 18). The coiled-coil (CC) helix of CRY1 binds the transactivation domain (TAD) of BMAL1 to sequester it from coactivators such as CBP/p300. CRY1 also interacts directly with the PAS-B

domain of CLOCK using an evolutionarily conserved pocket to stably dock the repressor onto the transcription factor (18). Mutations at both CLOCK PAS-B and the BMAL1 TAD are required to nearly eliminate the ability of CRY1 to inhibit CLOCK:BMAL1 activity (19, 20). It appears that this dual-mode of interaction is how CRY1 is able to strongly inhibit CLOCK:BMAL1 independently of PER in the 'late' complex.

Since their initial discovery, the distinct and shared roles of *Cry1* and *Cry2* in the cell have been unclear. In support of their critical role in circadian rhythms, *Cry1* –/–;*Cry2* –/– mice are completely arrhythmic (2). However,

Cry1 –/– mice have ~1 hour short period phenotype, while *Cry2* –/– mice show an opposing ~1 hour long period phenotype (1, 7). The question emerged from these initial findings – if these proteins are paralogs and fulfilling redundant roles, why does knocking them out produce opposing phenotypes?

Notably, *Cry1* and *Cry2* play distinct roles in generating and maintaining cell-autonomous circadian rhythms. Notably, dissociated individual SCN neurons derived from *Cry1* –/– mice are arrhythmic, whereas neurons from

Cry2 –/– mice show persistent rhythms with longer periods than wild type cells (21). Similarly, peripheral tissue explants and individual cells from *Cry1* –/– mice are arrhythmic, supporting a more dominant role of CRY1 in the molecular clockwork than CRY2 (21, 22). Indeed, reconstitution of *Cry1* into

Cry1 –/–;*Cry2* –/– MEFS can restore rhythms, while upon reintroducing *Cry2*, the cells remain arrhythmic. Taking advantage of these intrinsic properties of CRYs ability to generation oscillation, Andrew Liu and colleagues performed genetic complementation studies using *Cry1* –/–;*Cry2* –/– MEFs (23). They reintroduced CRY1 or CRY2 protein expression under the native *Cry1* promoter to uncouple the influence of transcriptional regulation on CRYs ability to reconstitute rhythms. Using this chimeric approach, and swapping amino acid sequences between CRY1 and CRY2, they identified a region within the PHR domain of the CRYs that confers the ability of CRY2 to reconstitute rhythms. This suggested for the first time that the difference between the mammalian CRYs is encoded in the protein sequence, and not driven by transcriptional control or relative protein abundance.

Previously, we identified that CRY1 uses its CC helix to bind the BMAL1 TAD with modest affinity and uses its secondary pocket to bind the PAS-B domain of CLOCK to form a stable ternary complex (18, 20). Leveraging these mechanistic findings for CRY1, here we sought to investigate how CRY1 interacts with the CLOCK:BMAL1 heterodimer. We found that CRY2 interacts with the TAD of BMAL1 with an affinity similar to CRY1. However, CRY2 does not bind CLOCK PAS-B or the larger CLOCK:BMAL1 PAS-AB core by size exclusion, suggesting it has a much lower affinity for the CLOCK:BMAL1 PAS-AB core compared to CRY1. CRY2 is found in the ‘early repressive complex’ together with PER2 (4). The PER2 CBD binds at the CC helix of CRY2, the

same site that binds the BMAL1 TAD (24). Does the interaction of CRYs with the PER2 CBD influence their ability to bind the BMAL1 TAD? To address the influence of PER2 on the interaction of CRY2 with CLOCK:BMAL1 we asked if CRY2 can bind the BMAL1 TAD in the presence of PER2 CBD to form a ternary complex. Indeed, a CRY2:PER2:BMAL1 TAD complex can be isolated, suggesting these proteins all bind synergistically at this interface. These data together suggest that CRY2, together with PER2, primarily uses the TAD of BMAL1, not docking on CLOCK PAS-B, to inhibit CLOCK:BMAL1 activity in a fundamentally different manner than CRY1.

5.2 Results

5.2.1 CRY1 and CRY2 bind the BMAL1 TAD with similar affinity

We previously showed that the PHR domain of CRY1 (residues 1-491) binds the BMAL1 TAD with a K_d of ~1 μM. The CC helix of CRYs is sufficient to bind the BMAL1 TAD and appears to be the primary docking site (17, 20). We tested whether CRY2 PHR also binds the BMAL1 TAD. Using a fluorescence polarization assay, we labeled the minimal region of the BMAL1 TAD (residues 594–626) with a TAMRA fluorophore and titrated increasing amounts of CRY1 PHR (as previously described) or CRY2 PHR. We found that CRY2 binds the BMAL1 TAD with a similar affinity (K_d = 1.14 ± 0.67 μM) to CRY1 (K_d = 0.99 ± 0.27 μM), suggesting it too acts to sequester the TAD from co-activators as part of its repressive mechanism (Figure 5-1).

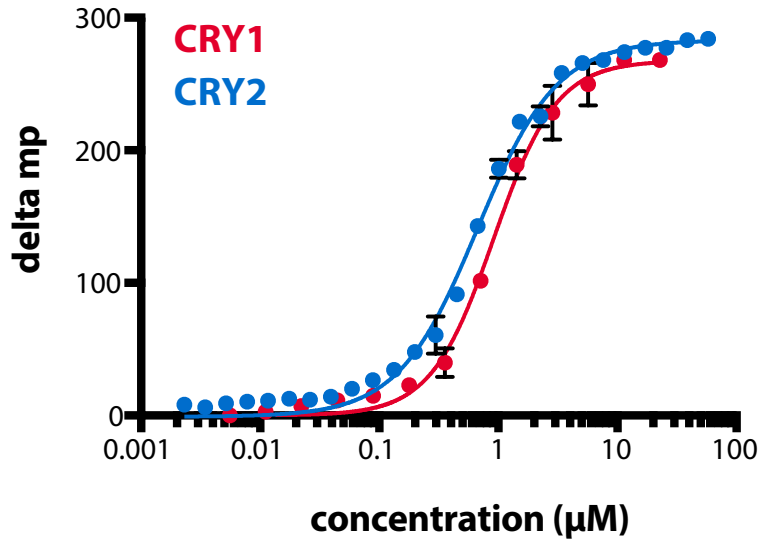

Figure 5-1. CRY1 and CRY2 bind the minimal BMAL1 TAD.

CRY1 PHR (red) or CRY2 PHR (blue) was titrated into a TAMRA labeled BMAL1 TAD (residues 594 – 626) and the change in fluorescence polarization was measured. CRY1 K_d = 0.99 ± 0.27 μM (25), CRY2 K_d = 1.14 ± 0.67 μM. The plots shown are representative of three independent experiments. Error bars represent s.e.m. for technical replicates within an individual assay.

5.2.2 CRY2 does not form a stable complex with CLOCK:BMAL1 PAS-AB core

Previous work showed that CRY1 binds to CLOCK through the PAS-B domain, and mutation of a single residue (W362A) was sufficient to disrupt the interaction *in vitro* and in cells (18, 20, 26). Therefore, CRY1 binding to CLOCK:BMAL1 appears to be predicated on docking onto the PAS-B domain; what about CRY2? We tested if CRY2 PHR directly interacts with CLOCK PAS-

B. Incubation of CRY1 PHR with CLOCK PAS-B resulted in a 1:1 molar stoichiometric complex by size exclusion analysis (18). Under identical conditions, CRY2 did not interact with CLOCK PAS-B. (Figure 5-2A). Speculating that CRY2 might use a distinct mode of interaction with the PAS-AB core, outside of CLOCK PAS-B, we mixed CRY2 with the CLOCK:BMAL1 PAS-AB heterodimer (1:1 molar ratio) and also saw no evidence of interaction, as there was no shift in peak migration (Figure 5-2B). These data suggest that CRY2 PHR has a much weaker affinity for CLOCK PAS-B and the entire CLOCK:BMAL1 PAS-AB core compared to CRY1. There might be weak interactions between CRY2 PHR and the PAS-AB core. However, they are below the detection limit for this assay.

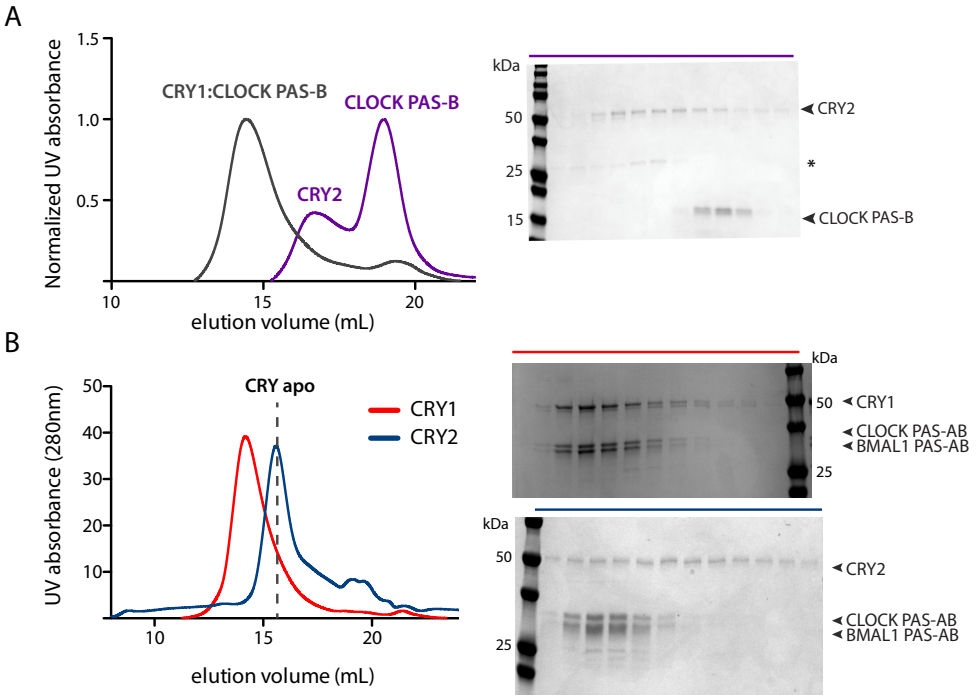

Figure 5-2. CRY2 does not interact stably with CLOCK PAS-B or the CLOCK:BMAL1 PAS-AB dimer.

(A) Size exclusion chromatography (SEC) analysis of complex formation with CRY1 PHR (gray) or CRY2 PHR (purple) mixed with the isolated CLOCK PAS-B. Proteins were mixed and incubated at 4°C overnight and then injected on a Superdex 200 10/300 GL column. The peak fraction of CRY2 PHR with CLOCK PAS-B was analyzed by SDS-PAGE and stained by Coomassie dye. Asterisk indicates slight His-TEV contamination. UV traces were normalized by setting the largest A_{280} peak within each trace to 1. (B) SEC analysis of CRY1 PHR with the CLOCK:BMAL1 PAS-AB dimer (red) and CRY2 PHR with the CLOCK:BMAL PAS-AB dimer (blue). Corresponding peak fractions are shown in the SDS-PAGE gel (right).

5.2.3 PER2 CRY-binding domain shows independent modes of interaction with CRY

Inspection of the CRY1/2:PER2 CBD structures reveals that the PER2 CBD transverses much of the PHR domain in both CRYs (27, 24). Within the PER2 C-terminus, three α-helices wrap around the CRY CC helix. This interaction is stabilized by a molecule of zinc that is coordinated by cysteines contributed by both PER and CRY. This ‘molecular clasp’ type of stabilization mediates the protein-protein interaction and provides a mechanism to sense the oxidative state of the cell (Figure 5-4).

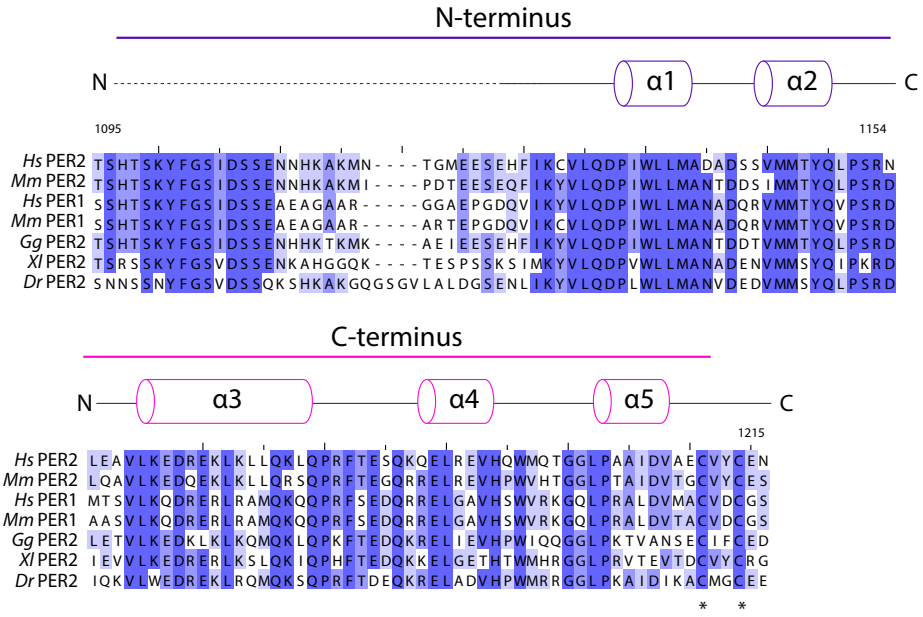

Figure 5-3. Domain schematic and alignment of PER2 Cry-binding domain across vertebrates.

The dashed line indicates disordered regions that do not show density in the x-ray crystal structure (PDB:4U8H). Secondary structure is indicated above the sequence alignment (barrels, α-helices). *Hs, homo sapiens; Mm, mus musculus; Gg, Gallus gallus; Xl, Xenopus laevis; Dr, Danio rerio*. Asterisks (*) indicate cysteines involved in zinc binding.

The N-terminus of PER2 CBD wraps adjacent to the secondary pocket of CRY1. There is a short highly-conserved helix within this region that makes significant contacts with CRY, while most amino acids within this region that were subject to crystallization do not show density and are presumed to be flexible (Figure 5-3). We aimed to investigate if these two structurally and potentially functionally bimodal regions of PER2 interact with CRYs independently of each other. Both the N-terminus (light purple, residues 1095-

1154) and C-terminus (pink, residues 1154-1215) (Figure 5-3) individually co-migrate with CRY2 by size exclusion chromatography, suggesting that they each make significant contacts with CRYs (Figure 5-4B and C). Previous studies identified point mutations in the PER2 CBD C-terminus that reduced binding of the PER2 CBD to CRYs, pointing to this region as a critical stabilizing interface (24, 28). Despite the minimal contacts of the N-terminal region of the PER2 CBD with CRYs, and the attenuated effect of mutations in this region on CRY1 binding *in vitro* and *in vivo* (24, 28), α-helices 1 and 2 appear to drive stable association and dock this motif onto CRYs, while the unstructured extension may be regulatory in protein-protein interactions.

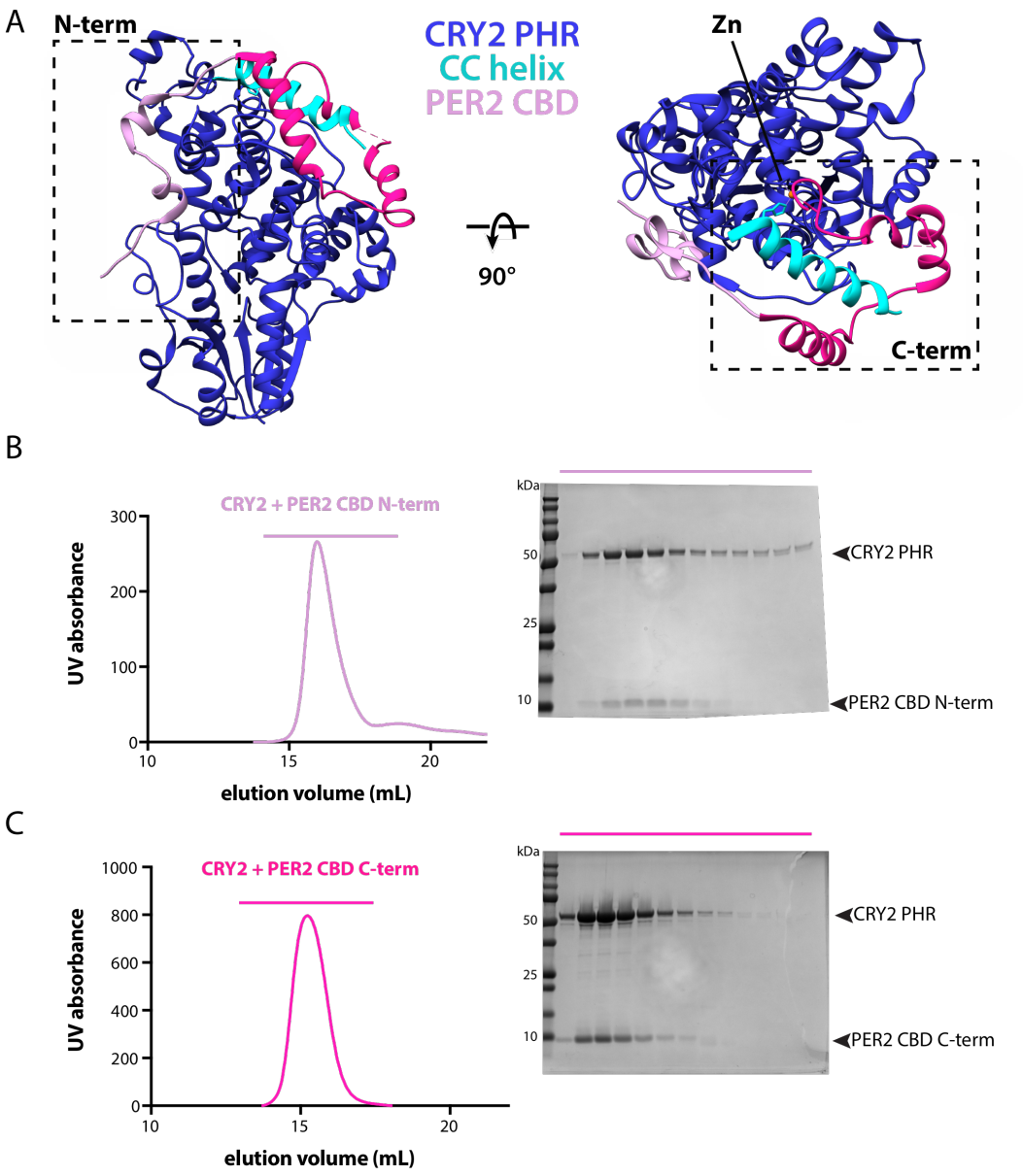

Figure 5-4. PER2 CRY-binding domain makes multiple stable contacts with the CRY PHR.

(A) CRY2:PER2 CBD structure (PDB: 4U8H), indicating the regions of the PER2 CBD used in the binding assays. The zinc ion is coordinated by the C-terminal region of PER2 CBD and CRY2 PHR. The N-terminus is colored in light purple (residues 1095-1154) and the C-terminus in pink (1154-1215). Residues 1095 – 1130 within the N-terminus were present in the crystallization construct but did not show significant density for assignment.

(B) Size exclusion analysis of the PER2 CBD N-terminus alone with the CRY2 PHR. Proteins were incubated for ~30 min. run on a Superdex 200 10/300 GL column. Peak fractions were analyzed by SDS-PAGE. (C) Size exclusion analysis of the C-terminus alone with CRY2 PHR performed as described above.

Because the N-terminal region of PER2 CBD is adjacent to the secondary pocket that CRY1 uses to bind CLOCK PAS-B, we hypothesized that PER2 could act as a scaffold and bridge the interaction interface to bind CLOCK PAS-B. However, this appears to not be the case, as we do not see an interaction of CLOCK PAS-B with a CRY1:PER2 complex by size exclusion (Figure 5-5). It will be interesting to determine if the PER2 CBD makes any contacts with the CLOCK:BMAL1 PAS domains in the context of the full-length proteins, possibly stabilizing a quaternary complex of these core clock proteins in the ‘early’ repressive phase of repression.

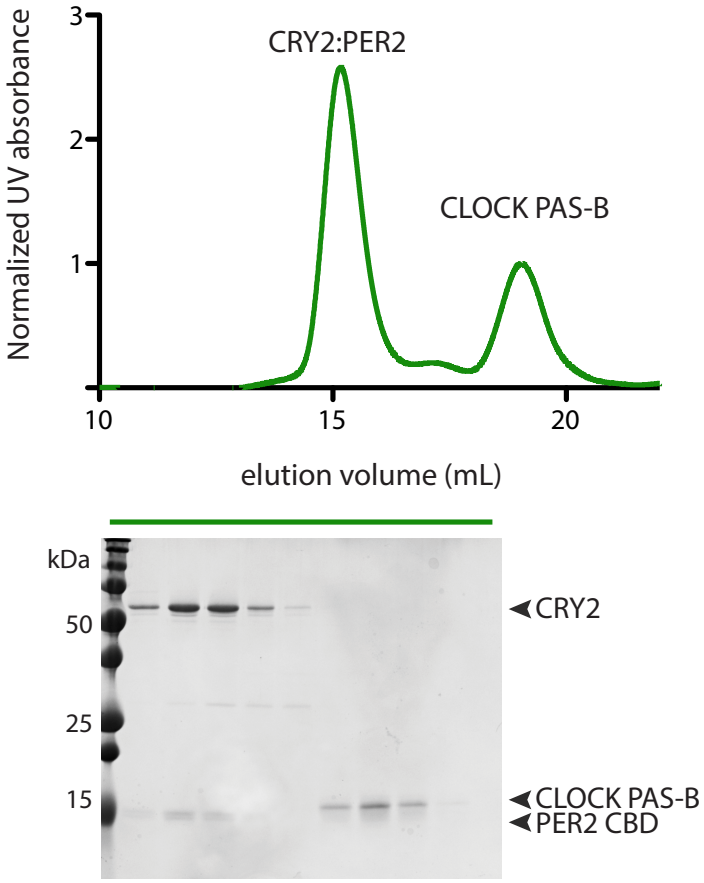

Figure 5-5. PER2 CBD does not induce a CRY2-CLOCK PAS-B interaction.

Size exclusion chromatography (SEC) analysis of complex formation with CRY2:PER2 and CLOCK PAS-B. Proteins were incubated overnight then injected on a Superdex 200 10/300 GL column. The peak fractions of were analyzed by SDS-PAGE and stained by Coomassie dye. A stable CRY2:PER2 complex forms (first eluting peak, 14.8mL) and CLOCK PAS-B elutes later in the column at ~18.1 mL.

5.2.4 CRY2:PER2 complexes bind the BMAL1 TAD synergistically

As shown in Figure 5-4, the C-terminus of PER2 CBD sandwiches the entire CRY CC helix, the same region of CRY1 that binds the BMAL1 TAD. This evokes the question, does PER2 binding prevent BMAL1 TAD binding, or do they form a ternary complex? To test this, we performed a fluorescence polarization (FP) assay using the fluorescently labeled BMAL1 TAD, and titrated increasing amounts of a CRY1:PER2 or CRY2:PER2 complex. Indeed, both CRY1:PER2 and CRY2:PER2 complexes bound the BMAL1 TAD with a similar affinity as CRYs alone (~1 μM, Figure 5-6). The PER2 CBD did not bind the BMAL1 TAD alone, shown by no change in fluorescence polarization of the BMAL1 TAD even at high concentrations of the PER2 CBD. Taken together, these data suggest the BMAL1 TAD recognizes an exposed interface on the CRY1 CC helix or a shared CRY:PER2 interface (Figure 5-6B) . Interestingly, CRY2 has a modestly higher affinity for the BMAL1 TAD when bound by PER2 compared to CRY1.

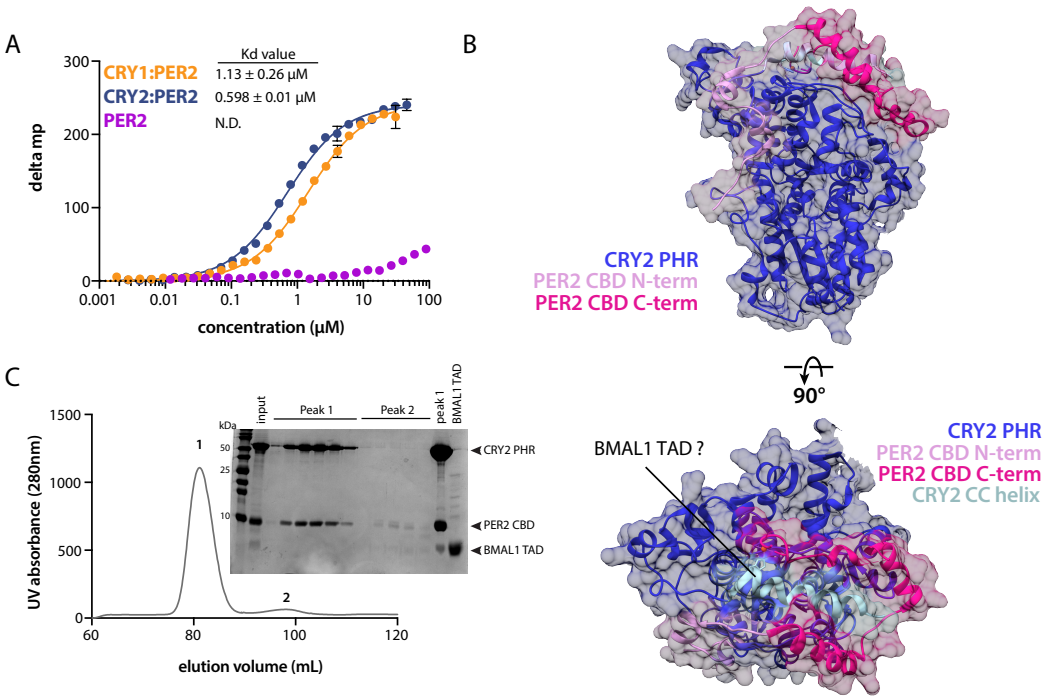

Figure 5-6. PER2 CBD and BMAL1 TAD can both bind to the CRY CC simultaneously.

(A) Fluorescence polarization assay of the TAMRA labeled BMAL1 TAD (residues 594-626) titrated with preformed CRY1:PER2, CRY2:PER2 complexes or PER2 CBD alone. CRY1 PHR or CRY2 PHR was mixed in a 1:1 molar ratio with PER2 CBD with a molar equivalent of zinc sulfate, and the complexes were isolated by size exclusion chromatography. Pure complexes were concentrated and used in the FP assay. The plots shown are representative of three independent experiments. Error bars represent technical replicates within an individual assay. (B) Size exclusion chromatography of CRY2 PHR mixed with 1.5 excess PER2 CBD C-term (residues 1154-1215) and 1.5 excess BMAL1 TAD, the same unlabeled construct used in the FP assay in panel A. A molar excess of zinc sulfate was included in the binding buffer. The sample was run on a 16/60 Superdex 200 GL column. Peak fractions were run on SDS-PAGE. Due to weak staining and reactivity by Coomassie staining of the BMAL1 TAD, peak 1 was concentrated to ~5 mg/mL and included on the gel.

To confirm that what we see in the FP assay is indeed the assembly of a ternary CRY:PER:BMAL1 complex, we performed size exclusion analysis to verify all three proteins are found in a complex together. Mixing the PHR domain of CRY2, the C-terminus of PER2 CBD and the minimal BMAL1 TAD, we saw that all three proteins bound in a stoichiometric complex (Figure 5-6C). This describes a direct and coordinated interaction of a CRY:PER complex with CLOCK:BMAL1. These findings also support the presence of a CRY:PER:CLOCK:BMAL1 complex early in the repressive phase, and provides insight into how the PER2 CBD may play an active role in the assembly and disassembly of these complexes during this delay in the feedback mechanism to generate cell-autonomous circadian rhythms.

5.3 Discussion

Here we describe a biochemical difference between CRY1 and CRY2 within the core clock mechanism. CRY2 is found principally in the early repressive complex and our studies reveal that it associates with CLOCK:BMAL1 in a fundamentally different manner than CRY1. Since CRY2 appears to lack the strong interaction with CLOCK that CRY1 possesses, we propose this explains in part why CRY2 is a weaker repressor in the circadian clockwork and its deletion shows a weaker phenotype in animals, where

Cry1 +/–;*Cry2* –/– mice show more persistent rhythms than

Cry1 –/–;*Cry2* +/– mice (29). This also suggests that CRY1 knockout renders cells arrhythmic, in part because CRY2 cannot compensate for the strong interaction of CRY1 at CLOCK PAS-B, precluding formation of the 'late repressive complex'. Indeed, CRY1 may be able to functionally compensate in *Cry2* –/– cells as both CRYs have a similar affinity to the BMAL1 TAD and presumably biochemically, CRY1 could occupy both the early and late repressive complexes. While biochemically CRY1 may compensate for CRY2 in Cry2 –/– cells, the *Cry1* promoter contains unique elements that control its late expression profile (16). It will be interesting to investigate the contribution of this delayed CRY1 protein abundance on the assembly of the repressive complexes. These data also suggest that PER2 might be a necessary accessory protein for CRY2 to repress early in the evening. It might also partly explain why CRY2 is found together with PER proteins and CRY1 is found at CLOCK:BMAL1 sites independently of PER.

While it is still yet to be determined how even the most minimal CRY binding region of PER2 modulates CRYs interaction with other proteins, including CLOCK:BMAL1, we describe here that PER2 binding to CRY is compatible with BMAL1 TAD binding. This result may not be surprising, as CRY and PER proteins enter the nucleus bound to one another and encounter the CLOCK:BMAL1 complex (30). However, numerous mutually exclusive interactions within the clockwork have been described that compete for binding to regions of CRY, e.g. PER2 CBD competes with FBXL3, a ubiquitin ligase,

and prevents CRY ubiquitination and degradation (27, 24, 31). Furthermore, this describes an interface where CRY and PER proteins together directly bind to the CLOCK:BMAL1 heterodimer.

Inspection of the sequence differences within the PHR of the CRY proteins does not reveal much about their observed functional differences, as CRY1 and CRY2 proteins share a high degree of sequence similarity (~80% identity) within the PHR domain. The two CRY proteins are most divergent in sequence within their C-termini; however, the tails appear to contribute to amplitude and period, not the ability to restore rhythmicity to cells (23). It will be interesting to further investigate how the CRY C-terminal tails also contribute to the assembly of these repressive complexes and regulate the interaction of CRYs with CLOCK:BMAL1. Recent studies found a genetic mutation in humans that results in deletion of a single exon within the CRY1 C-terminal tail that increases CRY1 interaction with CLOCK:BMAL1 (32). This hereditary mutation is dominant and remarkably prevalent in the human population (1 out of 75 people) and results in delayed sleep phase disorder (DSPD). These findings demonstrate that changes in CRY1 affinity for CLOCK:BMAL1 have powerful consequences on clock timing in humans.

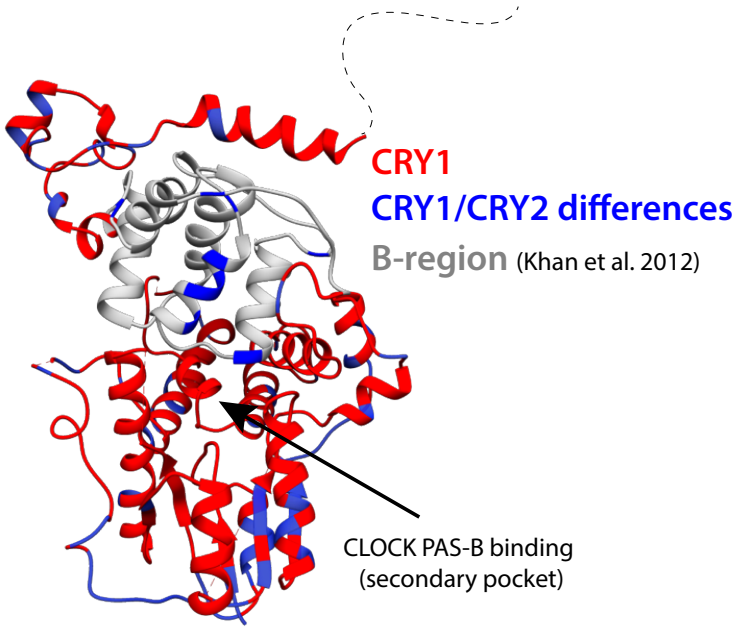

Figure 5-7. Functionally differentiating region of CRY1 and CRY2.

CRY1 PHR structure (PDB:5T5X) is shown in red. Amino acid differences between CRY1 and CRY2 are highlighted in blue. The B-region identified by Andrew Liu and colleagues is indicated in gray, near the CLOCK PAS-B binding pocket (23).

The previously identified cryptochrome differentiating region that renders CRY2 CRY1-like in its ability to restore circadian rhythms, maps to a region near the secondary pocket on both CRY structures (Figure 5-7)(23). While there are only a handful of amino acids that differ between the two proteins within that region, it appears that these residues are critical to the topology of the pocket and define the interaction with CLOCK PAS-B. Moving towards atomic resolution structure of these larger circadian repressive complexes shows promise to reveal how these complexes assemble and the

biochemical basis for the precisely delayed repression phase that is critical for circadian oscillation.

5.4 Materials and Methods

5.4.1 Recombinant protein expression and purification.

Using the baculovirus expression system (Invitrogen) His_6-tagged mouse CRY2 PHR (residues 1-512) was expressed in Sf9 suspension insect cells (Expression Systems). CLOCK PAS-B (residues 261–395), and PER2 CBD (residues 1095-1215) were expressed in *E. coli* Rosetta2 (DE3) cells as a fusion to the solubilizing tags His_6-NusA and glutathione S transferase (GST), respectively.

For His_6-tagged mouse CRY2 PHR Sf9 suspension cells were infected with a P3 virus at 1.5 x 10^6 cells/mL and grown for 72 hours. Following brief centrifugation at 4K rpm, cells were resuspended in 50 mM Tris pH 8.0, 200 mM NaCl, 20 mM imidazole, 10% glycerol, 0.2% triton x-100, 0.1% NP40, 0.4% Tween-20, 5 mM β-mercaptoethanol and EDTA-free protease inhibitors (Pierce). Cells were lysed using a microfluidizer followed by brief sonication for 15 sec. on/30 sec. off for 3 pulses at 40% amplitude. Lysate was clarified at 20K rpm, 4°C for 1 hour. The protein was then isolated by Ni^{2+}-nitrilotriacetic acid affinity chromatography (QIAGEN) followed by ion exchange and size-exclusion chromatography. The protein was isolated by Ni^{2+}-nitrilotriacetic acid affinity chromatography (QIAGEN). The eluted protein was further purified by

ion exchange and size-exclusion chromatography into 20 mM HEPES (pH 7.5), 125 mM NaCl, 10% glycerol and 2 mM TCEP.

PER2 CBD was expressed in *E. coli* SoluBL21 cells as a fusion to the solubilizing tag Glutathione S-Transferase (GST). Protein expression was induced with 0.5 mM IPTG at an OD_{600} of 0.8, and grown for an additional 16 h at 18 °C. Soluble protein was purified by GST affinity chromatography (GE Healthcare), followed by cleavage of the tag with GST-TEV protease overnight at 4°C. Subsequent GST affinity chromatography was performed to remove the protease and cleaved tag. The protein was further purified by size-exclusion chromatography as described above.

CLOCK PAS-B, CLOCK PAS-AB and BMAL1 PASAB constructs were expressed and purified as described in previous Chapter 3.

5.4.2 Analytical size-exclusion chromatography.

For analysis of complex formation by size-exclusion chromatography (SEC), purified proteins were injected on a Superdex 200 10/300 GL analytical column or Superdex 200 16/60 GL in 20 mM HEPES pH 7.5, 125 mM NaCl, 5% glycerol and 2 mM TCEP. Proteins were incubated briefly (~30 min). or overnight and analyzed by SEC. All size-exclusion columns were calibrated with a low-molecular-weight gel filtration standards kit (GE Healthcare Life Sciences). The content of each peak was evaluated by SDS-PAGE and Coomassie staining.

5.4.3 Fluorescence anisotropy.

The BMAL1 short TAD WT probes were purchased from Bio-Synthesis with a 5,6-TAMRA fluorescent probe covalently attached to the N terminus. Equilibrium binding assays with CRY1 PHR, CRY2 PHR and PER2 CBD were performed in FP buffer: 50 mM Bis-Tris Propane pH 7.5, 100 mM NaCl, 2 mM TCEP and 0.05% (vol/vol) Tween-20. CRY1/2:PER2 CBD complexes were preformed and run on a Superdex 200 10/300 GL into FP buffer with ~100μM zinc sulfate. Concentrated stocks of BMAL1 TAD probes were stored between 15-200 μM at −70°C and diluted into assay buffer to 50 nM alone and in the presence of increasing concentrations of test proteins. Plates were incubated at room temperature for 10-20 min prior to analysis. Binding was monitored by changes in fluorescence polarization with an EnVision 2103 multilabel plate reader (Perkin Elmer) with excitation at 531 nm and emission at 595 nm. The equilibrium binding dissociation constant (K_D) were calculated by fitting the dose-dependent change in millipolarization (Δmp) to a one-site specific binding model in Prism 6.0 (GraphPad), with averaged Δmp values from duplicate or triplicate assays. Data shown are from a representative experiment (n = 2 replicates) of three independent assays.

5.5 References

1. van der Horst GT, et al. (1999) Mammalian Cry1 and Cry2 are essential for maintenance of circadian rhythms. *Nature* 398(6728):627–30.
2. Kume K, et al. (1999) mCRY1 and mCRY2 are essential components of the negative limb of the circadian clock feedback loop. *Cell* 98(2):193–

205.

3. Zhang R, Lahens NF, Ballance HI, Hughes ME, Hogenesch JB (2014) A circadian gene expression atlas in mammals: Implications for biology and medicine. *Proc Natl Acad Sci* 111(45):16219–16224.
4. Koike N, et al. (2012) Transcriptional Architecture and Chromatin Landscape of the Core Circadian Clock in Mammals. *Science (80-)* 338:349–354.
5. Takahashi JS, Hong H-K, Ko CH, McDearmon EL (2008) The genetics of mammalian circadian order and disorder: implications for physiology and disease. *Nat Rev Genet* 9:764–775.
6. Shearman LP, Zylka MJ, Weaver DR, Kolakowski LF, Reppert SM (1997) Two period homologs: Circadian expression and photic regulation in the suprachiasmatic nuclei. *Neuron* 19:1261–1269.
7. Vitaterna MH, et al. (1999) Differential regulation of mammalian Period genes and circadian rhythmicity by cryptochromes 1 and 2. *Proc Natl Acad Sci* 96(21):12114–12119.
8. Reick M, Garcia JA, Dudley C, McKnight SL (2001) NPAS2: An analog of clock operative in the mammalian forebrain. *Science (80-)* 293(5529):506–509.
9. Bunger MK, et al. (2000) Mop3 is an essential component of the master circadian pacemaker in mammals. *Cell* 103(7):1009–1017.
10. Shi S, et al. (2010) Circadian Clock Gene Bmal1 Is Not Essential; Functional Replacement with its Paralog, Bmal2. *Curr Biol* 20(4):316–321.
11. Xu H, et al. (2015) Cryptochrome 1 regulates the circadian clock through dynamic interactions with the BMAL1 C terminus. *Nat Struct Mol Biol* 22(6):476–484.
12. Debruyne JP, Weaver DR, Reppert SM (2007) CLOCK and NPAS2 have overlapping roles in the suprachiasmatic circadian clock. *Nat Neurosci*

10(5):543–545.

13. Michael AK, Fribourgh JL, Van Gelder RN, Partch CL (2017) Animal Cryptochromes: Divergent Roles in Light Perception, Circadian Timekeeping and Beyond. *Photochem Photobiol* 93(1):128–140.
14. Brown SA, et al. (2005) PERIOD1-associated proteins modulate the negative limb of the mammalian circadian oscillator. *Science* 308(5722):693–6.
15. Duong HA, Weitz CJ (2014) Temporal orchestration of repressive chromatin modifiers by circadian clock Period complexes. *Nat Struct Mol Biol* 21(2):126–132.
16. Ukai-Tadenuma M, et al. (2011) Delay in feedback repression by cryptochrome 1 Is required for circadian clock function. *Cell* 144(2):268–281.
17. Czarna A, et al. (2011) Quantitative analyses of cryptochrome-mBMAL1 interactions: mechanistic insights into the transcriptional regulation of the mammalian circadian clock. *J Biol Chem* 286:22414–22425.
18. Michael AK, et al. (2017) Formation of a repressive complex in the mammalian circadian clock is mediated by the secondary pocket of CRY1. *Proc Natl Acad Sci* . doi:10.1073/pnas.1615310114.
19. Sato TK, et al. (2006) Feedback repression is required for mammalian circadian clock function. *Nat Genet* 38(3):312–319.
20. Xu H, et al. (2015) Cryptochrome 1 regulates the circadian clock through dynamic interactions with the BMAL1 C terminus. *Nat Struct Mol Biol* 22(6):476–84.
21. Liu AC, et al. (2007) Intercellular Coupling Confers Robustness against Mutations in the SCN Circadian Clock Network. *Cell* 129(3):605–616.
22. Yagita K, Tamanini F, van Der Horst GT, Okamura H (2001) Molecular mechanisms of the biological clock in cultured fibroblasts. *Science* 292(5515):278–281.

23. Khan SK, et al. (2012) Identification of a novel cryptochrome differentiating domain required for feedback repression in circadian clock function. *J Biol Chem* 287(31):25917–25926.
24. Nangle SN, et al. (2014) Molecular assembly of the period-cryptochrome circadian transcriptional repressor complex. *Elife* 3(August2014):1–14.
25. Gustafson CL, et al. A Slow Conformational Switch in the BMAL1 Transactivation Domain Modulates Circadian Rhythms. *Mol Cell*. doi:https://doi.org/10.1016/j.molcel.2017.04.011.
26. Zhao W-N, et al. (2007) CIPC is a mammalian circadian clock protein without invertebrate homologues. *Nat Cell Biol* 9(3):268–275.
27. Schmalen I, et al. (2014) Interaction of circadian clock proteins CRY1 and PER2 is modulated by zinc binding and disulfide bond formation. *Cell* 157(5):1203–1215.
28. Czarna A, et al. (2013) XStructures of drosophila cryptochrome and mouse cryptochrome1 provide insight into circadian function. *Cell* 153(6). doi:10.1016/j.cell.2013.05.011.
29. Horst GTJ van der, et al. (1999) Mammalian Cry1 and Cry2 are essential for maintenance of circadian rhythms. *Nature* 398(6728):627–630.
30. Lee C, Etchegaray J-P, Cagampang FRA, Loudon ASI, Reppert SM (2001) Posttranslational Mechanisms Regulate the Mammalian Circadian Clock. *Cell* 107:855–867.
31. Xing W, et al. (2013) SCF(FBXL3) ubiquitin ligase targets cryptochromes at their cofactor pocket. *Nature* 496(7443):64–8.
32. Patke A, et al. (2017) Mutation of the Human Circadian Clock Gene CRY1 in Familial Delayed Sleep Phase Disorder. *Cell* 169(2):203–215.e13.

6 CHAPTER 6 — MOLECULAR ASSEMBLY OF CIRCADIAN REPRESSIVE COMPLEXES

6.1 Introduction

6.1.1 An oscillator requires a periodic fluctuation between two states

For decades, the transcription/translation feedback loop has been accepted as the canonical model of circadian rhythms (1, 2). This model provides a periodic fluctuation between a transcriptionally active state where CLOCK:BMAL1, together with CBP/p300, recruits RNA polymerase II to activate transcription, and a 'repressed' state where CLOCK:BMAL1 activity is inhibited by PER and CRY proteins (2). During the active state, CLOCK:BMAL1 stimulates the expression of numerous genes, including its own repressors, *Per* and *Cry*, which are translated in the cytoplasm (3–6) (Figure 6-1).

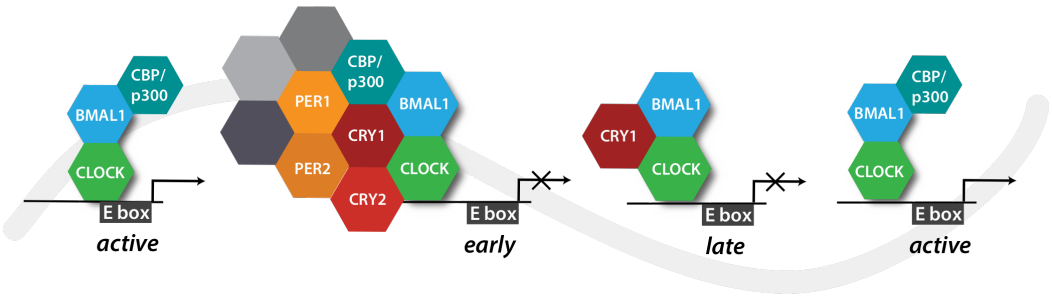

Figure 6-1. Schematic of nuclear circadian repressive complexes.

CLOCK:BMAL1 is activated by CBP/p300 during ~CT4 – CT16 (daytime). During the evening, CT16 – CT4, repressive complexes are found at CLOCK:BMAL1 sites. Gray hexagons indicate PER-associated chromatin modifiers whose identity is yet to be fully elucidated (7).

To establish the necessary delay in repression of ~8-12 hours, the spatiotemporal localization and stability of CRY and PER proteins are controlled through the opposing activity of kinases, phosphatases, and E3 ubiquitin ligases (8–12). A series of specific and coordinated phosphorylation events on PER proteins must occur before they can partner with CRYs to enter the nucleus to inhibit CLOCK:BMAL1 activity (13). The phosphorylation of PER proteins is critical for period determination of the clock, as inhibition of PER-targeting kinases ε (CK1 ϵ/δ) and phosphatases can have a large effect on period ranging from ~20 to 44 hours (14, 15). Furthermore, mutations in PER phosphorylation sites have been linked to human circadian disorders, such as familial advanced sleep phase syndrome (FASPS) (16, 17). While phosphorylation of PER is critical for introducing a delay in nuclear entry of PER:CRY complexes, it is not the only mechanism contributing to this slow timekeeping (18). Cytoplasmic events contribute largely to the delay in repression required for circadian oscillation, however, little is known about how CLOCK:BMAL1 are maintained in a repressed state for ~12 hours before PER and CRY proteins are turned over and the cycle begins again. Perhaps there are nuclear events that also play a critical role in establishing timing. I propose here that persistence of the repressive period within the nucleus is imparted by competitive and synergistic protein-protein interactions between the core clock components, CRY, PER, CLOCK and BMAL1. The kinetics of protein-protein

interactions have the potential to influence the assembly of the distinct 'early' and 'late' repressive complexes that are important for circadian timing.

6.1.2 Investigating the assembly of circadian repressive complexes

Forming part of the circadian timekeeping mechanism, there are distinct repressive complexes that regulate CLOCK:BMAL1 throughout the evening in the nucleus (19). One is a 'early' repressive complex that consists of CRY and PER proteins, where we hypothesize PER acts as a scaffolding protein to assist CRY proteins in binding directly to CLOCK:BMAL1 and sequester the BMAL1 TAD from coactivators (20). Through mechanisms yet to be determined, the 'late' repressive complex consists of CRY1 only at CLOCK:BMAL1 sites (Figure 6-1) (19). In efforts to determine the molecular underpinnings of these complexes, we have used purified recombinant protein constructs of PER, CRY, CLOCK and BMAL1 to examine the molecular assembly of these core clock proteins and subjected stable complexes to structure determination efforts by x-ray crystallography and cryo-electron microscopy (cryo-EM). While efforts to produce a high-resolution structure of a circadian repressive complex have not yet been fruitful, we have learned about important molecular determinants of these complexes using well defined proteins. Additionally, studying the molecular basis for assembly of pairwise combinations of recombinant proteins *in vitro* has revealed potential kinetic regulatory mechanisms of protein-protein interactions that will be described in detail below.

6.2 Results

6.2.1 CRY1 associates slowly with CLOCK PAS-B

In an attempt to assemble circadian repressive complexes of CRY1 and CLOCK:BMAL1 for structural studies, we found that the CRY1 photolyase homology region (PHR) has a slow association with CLOCK PAS-B, on the order of many hours. Brief incubation (~30 min. at 4ºC) of CLOCK PAS-B with CRY1 PHR shows an initial quick association of CLOCK PAS-B, but the interaction is always sub-stoichiometric, suggesting a relatively weak affinity (Figure 6-2). Preliminary surface plasmon resonance (SPR) studies (data not shown) and size exclusion experiments indicate that there is an initial fast association of CLOCK PAS-B with CRY1, however it is only a small population of total CRY1 protein (Figure 6-2A). By contrast, incubation of these proteins overnight at 4 ºC provides a fully bound, stoichiometric complex that can be isolated by size exclusion (Figure 6-2B). These data suggest that the association of CRY1 with CLOCK is a biochemically slow process that could contribute to the delay and maintenance of the repression phase throughout the night.

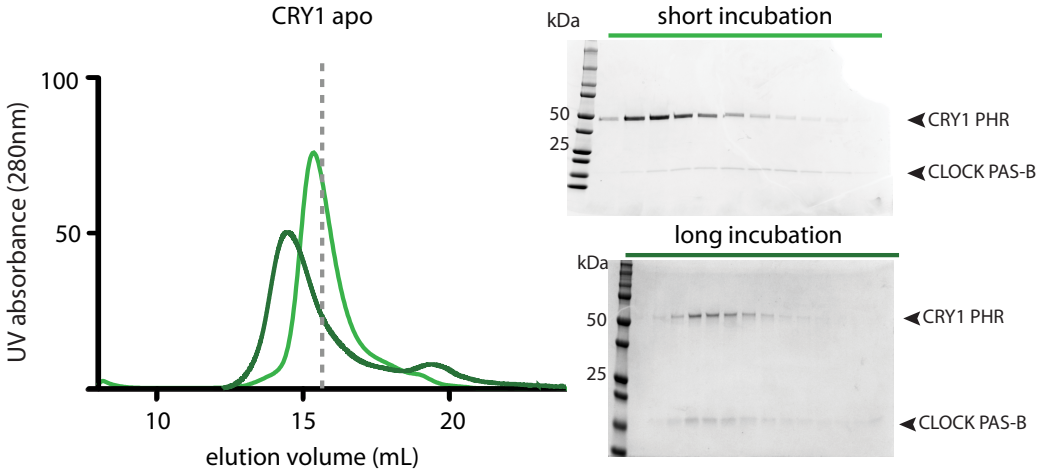

Figure 6-2. CLOCK PAS-B requires long incubation to form stoichiometric complex with CRY1 PHR.

Brief incubation of CRY1 PHR with CLOCK PAS-B (~30 min.) shows a modest gel shift (0.3 mL) on a Superdex 200 10/300 GL (light green) from the migration of CRY1 PHR alone (apo), with only a portion of CLOCK PAS-B co-migrating with CRY1 PHR as shown by SDS-PAGE analysis of gel filtration fractions (top). Overnight incubation of CRY1 PHR and CLOCK PAS-B provides a significant shift in elution volume (1 mL) from the CRY1 PHR apo peak (dark green trace) and co-migration with CLOCK PAS-B as shown by SDS-PAGE.

These findings provoked the question: what processes could give rise to a slow association? Conventionally, slow associations between two proteins are regulated by metamorphic proteins (e.g. KaiB in the cyanobacterial clock) (21), conformational changes in disordered regions (coupled folding and binding)(22) and proline isomerization (23). Interestingly, there is a disordered loop of 5 amino acids, containing a proline, in CRY1 near the secondary pocket where CLOCK PAS-B binds. Previously, we solved a high-resolution structure

of the CRY1 PHR to 1.8 Å resolution (See Chapter 2). Even at this high resolution, we did not detect electron density for this loop that allowed us to build a model of the loop in here (Figure 6-3A). Furthermore, this loop is also disordered in CRY1 when bound to the PER2 CBD, which we determined by solving a CRY1:PER2 structure in a different space group (Figure 6-3). The previously published structure of CRY1:PER2 contains a vector artifact which caused two non-native beta strands to pack against the loop, possibly artificially inducing a non-native conformation (Figure 6-3B)(24). Based on our previous findings that CLOCK PAS-B docks into the adjacent pocket, this flexible loop is therefore poised to regulate association with CLOCK PAS-B and 'gate' association of CLOCK to provide a slow k_{on}, or rate of association. Indeed, mutation of the rigid proline residue, P39, to an alanine within that loop eliminates the association with CLOCK PAS-B altogether (25) (See Chapter 2), suggesting it might change the k_{on} and k_{off} rates together to result in a higher K_d. It will be interesting to see how other mutations in this loop affect CRY1 regulation of CLOCK:BMAL1. The homologous loop in CRY2, while nearly identical in composition (4 out of 5 amino acids), shows resolvable electron density in both in the apo and PER2-bound structure (26, 27). Could this loop contribute to the differential association of CRY1/2 with CLOCK PAS-B?

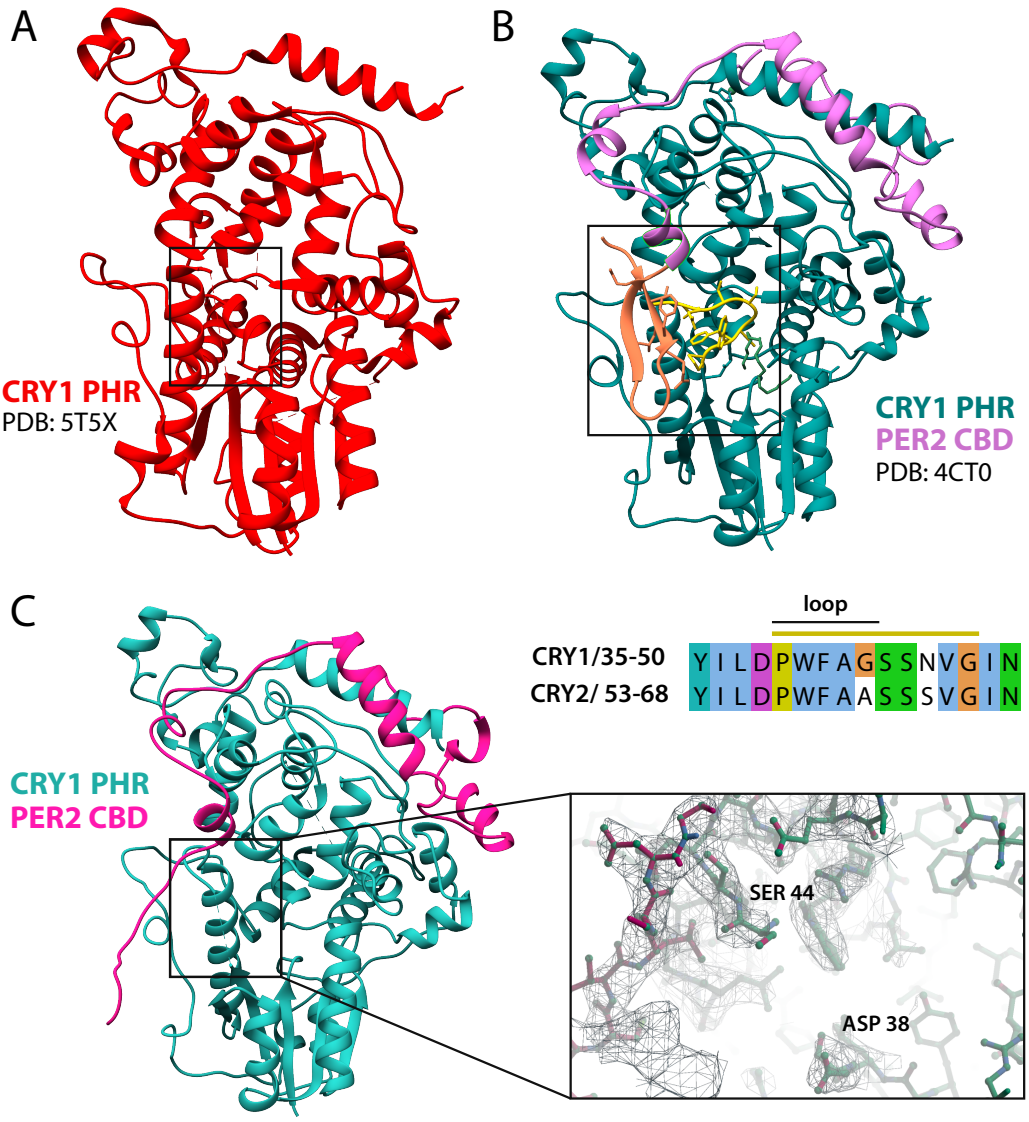

Figure 6-3. CRY1 contains a disordered loop near the CLOCK PAS-B binding pocket.

(A) CRY1 PHR (red) at 1.8Å resolution. (PDB:5T5X). Box highlights the disordered loop region. (B) Previously published CRY1:PER2 CBD structure. CRY1 PHR (sea green) in complex with PER2 CBD (violet) (PDB: 4CT0). Box highlights the ordered CRY1 loop region shown in sticks (gold) and the additional beta strands in PER2 CBD (coral). (C) CRY1 PHR in cyan, PER2 CBD in pink. Box indicates the region containing the disordered loop. Inset shows electron density for the structure, highlighting the missing electron

density for CRY1 residues 39-43. Yellow line above sequence indicates ordered region in the other CRY1:PER2 CBD structure shown in panel B.

Table 6-1 Data collection and refinement statistics for CRY1-PER2 at 3.1Å

Wavelength	
Resolution range	58.38 - 3.11 (3.28 - 3.11)
Space group	P 21 21 21
Unit cell	72.6399 81.2302 98.0997 90 90 90
Total reflections	62925(9485)
Unique reflections	10939 (1564)
Multiplicity	5.8(6.1)
Completeness (%)	100(100)
Mean I/sigma(I)	7.5(3.5)
Wilson B-factor	64.62
R-merge	17.1(65.2)
R-meas	
R-pim	7.8(29.2)
CC1/2	0.99(0.76)
Reflections used in	10897 (1068)
Reflections used for R-free	555 (49)
R-work	0.2062 (0.2925)
R-free	0.2611 (0.4271)
Number of non-hydrogen	4422
Protein residues	555
RMS(bonds)	0.002
RMS(angles)	0.50
Ramachandran favored (%)	93.24
Ramachandran allowed (%)	6.03

Ramachandran outliers (%)	0.73
Rotamer outliers (%)	0.00
Average B-factor	61.03
macromolecules	61.03

6.2.2 The PER2 CBD impedes the fast CLOCK PAS-B association with CRY1 PHR

To investigate the joint and independent roles of CRY and PER proteins in the repression of CLOCK:BMAL1, studies from the Sancar lab used purified proteins to test the binding of CRY1:PER2 complexes to CLOCK:BMAL1:E-box complexes using gel shift assays (28). Under their conditions, they suggest that PER2 interferes with the binding of CRY1 to a CLOCK:BMAL1:E-box ternary complex. To explore these findings, we set out to test the effect of the PER2 CBD on the association of CRY1 PHR with CLOCK PAS-B, hypothesizing that if PER2 is bound near the secondary pocket of CRY1, it could regulate the rate of association with CLOCK PAS-B or block interaction at that site.

To examine the effect of the PER2 CBD on association of CLOCK with CRY1, we incubated the stable preformed CRY1:PER2 CBD complex with CLOCK PAS-B briefly (~30 min.) and assessed the association of CLOCK PAS-B by size exclusion chromatography. Without PER2 CBD present in the mixture, there is a sub-stoichiometric amount of CLOCK PAS-B that initially associates with CRY1 PHR (See Figure 6-2A). However, under the same conditions, we do not detect any association of CLOCK PAS-B in the presence of PER2 CBD; these data suggest that PER2 CBD prevents the initial association of CLOCK PAS-B with CRY1 (Figure 6-4A).

To explore these findings further, we subdivided the CBD into two distinct regions based on their association with CRY1 as described in Chapter 5 (Figure 5-3). The C-terminal construct of PER2 CBD does not contain the region of PER2 CBD that wraps near the secondary pocket of CRY1 PHR, near the CLOCK PAS-B binding site. Under identical experimental conditions, the same sub-stoichiometric population of CLOCK PAS-B still associates with CRY1 PHR in the presence of only the C-terminus of PER2 CBD (Figure 6-4). These results suggest that the entire PER2 CBD is needed to impede the initial association of CLOCK PAS-B with CRY1 PHR. Regulation and slowing of the CRY1-CLOCK association by PER2 shows promise to provide another mechanism to prolong the repressive state in the nucleus.

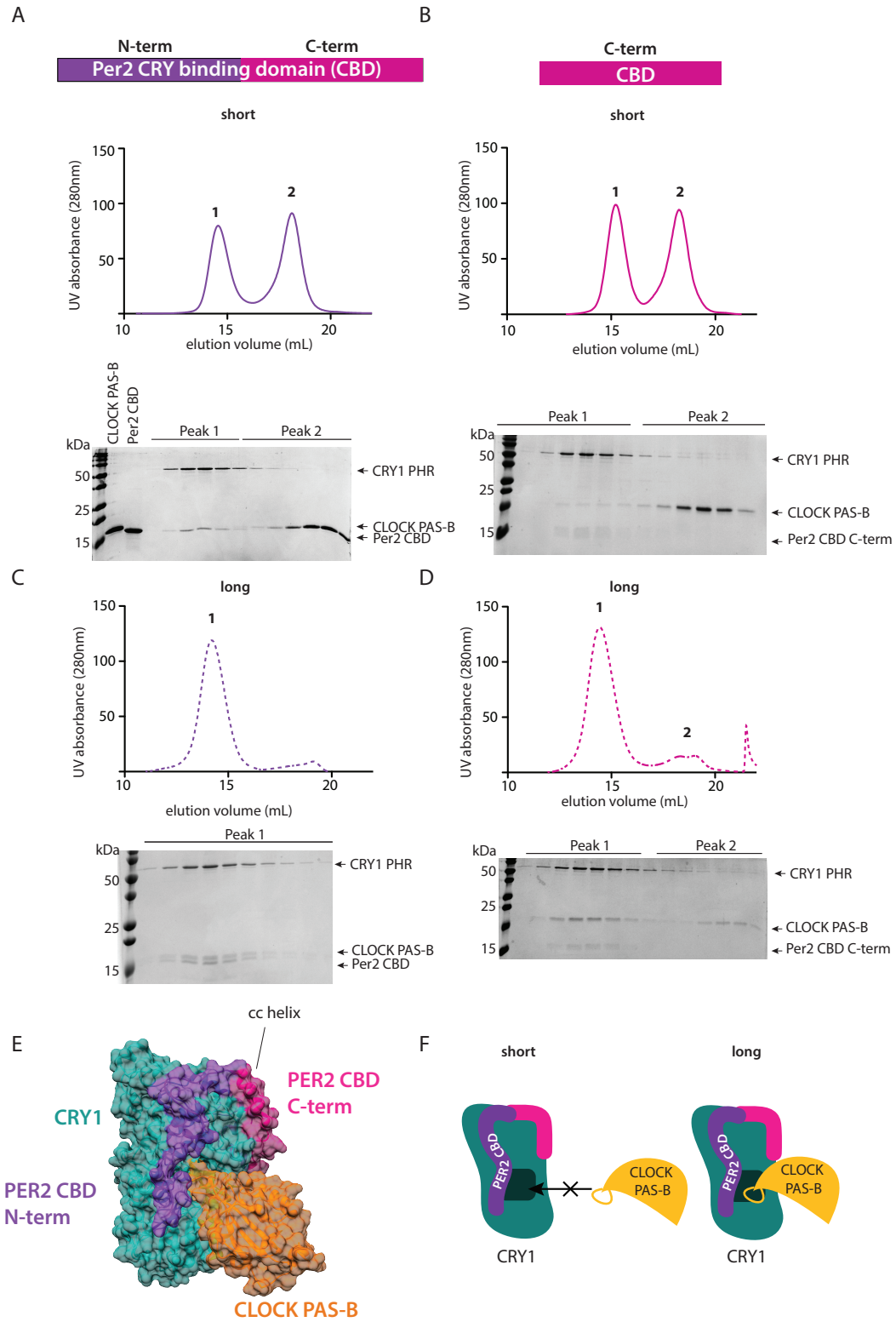
A
N-term
C-term
Per2 CRY binding domain (CBD)
short
UV absorbance (280nm)
elution volume (mL)
1
2
CLOCK PAS-B
Per2 CBD
Peak 1
Peak 2
kDa
CRY1 PHR
CLOCK PAS-B
Per2 CBD
B
C-term
CBD
short
Peak 1
Peak 2
CRY1 PHR
CLOCK PAS-B
Per2 CBD C-term
C
long
D
long
E
cc helix
PER2 CBD
C-term
CRY1
PER2 CBD
N-term
CLOCK PAS-B
F
short
long
PER2 CBD
CLOCK
PAS-B
CRY1

Figure 6-4. The N-terminus of the PER2 CBD impedes initial association of CLOCK PAS-B with CRY1 PHR.

(A) Domain schematic of the PER2 CBD indicating the N-terminus (purple) and C-terminus (magenta) referenced in these studies. Short incubation (~30 min.) of CRY1 PHR:PER2 CBD with 1.5X molar excess CLOCK PAS-B shows only a CRY1:PER2 complex, while CLOCK PAS-B elutes later on an Superdex 200 10/300 GL column. Peak fractions were analyzed by SDS-PAGE and stained by Coomassie dye. Purified CLOCK PAS-B and PER2 CBD are included on the SDS-PAGE gel for reference as they are very similar in size. (B) Domain schematic of the C-terminus of PER2 CBD used in these studies. CRY1:PER2 C-term were mixed with 1.5X molar excess CLOCK PAS-B for ~30 min. and run on an Superdex 200 10/300 GL column. Peak fractions were analyzed by SDS-PAGE and stained by Coomassie dye. A small fraction of CLOCK PAS-B (as seen in Figure 6-2) co-migrates with the CRY1:PER2 C-term complex (C and D) Incubation of CRY1:PER2 CBD or CRY1:PER2 CBD C-term with CLOCK PAS-B overnight provides a fully bound complex as shown by SDS-PAGE analysis of peak fractions. (E) Overlay of CRY1:PER2 structure with the top HADDOCK model of CRY1:CLOCK PAS-B complex (Chapter 2), highlighting the proximity of the N-terminus of PER2 CBD to the CLOCK binding pocket. (F) Cartoon model of PER2 regulation of CLOCK PAS-B association with CRY1. Dark green/black square on CRY1 indicates the secondary pocket.

While the PER2 CBD appears to gate the initial association of CRY1 with CLOCK PAS-B, incubation of these proteins overnight provides a fully bound ternary complex of all three proteins (Figure 6-4D and E). Taken together, these data suggest the N-terminus of PER2 CBD interferes with the initial association of CLOCK PAS-B and might make the apparent slow process of CRY1-CLOCK association even slower; however, given enough time, a PER2:CRY1:CLOCK complex forms. This kinetic regulation by PER2 could be important for introducing a delay in the association of CRY-PER complexes with CLOCK:BMAL1 in the early phase of repression. Further experiments could test mutations that probe these interactions *in vitro* and in cells to correlate kinetics of association with clock phenotypes.

Returning to the initial interpretation of the effect of PER2 on CRY1:CLOCK:BMAL1:E-box complex, given our data, it appears that brief incubation (~10 min.) of these complexes in previous experiments was not enough time for these proteins to form a stable quaternary complex at equilibrium (28). Our data suggest that while the N-terminus of the PER2 CBD may initially slow the association of CRY1 with CLOCK:BMAL1, a long incubation leads to a stable PER2:CRY1:CLOCK:BMAL1 complex (Figure 6-4D and E). It will be interesting to see if the PER2 CBD changes the kinetics of CRY1 with CLOCK (k_{on} and k_{off} values) using SPR studies that can measure these rates experimentally. Taken together, our data show that a PER2:CRY1:CLOCK:BMAL1:E-box complex forms under equilibrium

conditions if allowed enough time to associate. Using a biochemical reductionist approach, this work has also elucidated the core domains necessary for the PER2:CRY1:CLOCK:BMAL1 interaction. By eliminating inessential domains for this interaction we aimed to simplify the experiment; however, future studies will be needed to confirm these results in a native system with full-length recombinant proteins or cell-based assays.

6.2.3 PER2:CRY1:CLOCK:BMAL1 complexes are compatible with DNA binding

One debate in the biochemical model of the circadian clock is if and how CRY and PER affect CLOCK:BMAL1 binding to DNA. Previous *in vitro* studies demonstrate that CRY is able to bind a ternary CLOCK:BMAL1:E-box complex, yet PER alone does not bind CLOCK:BMAL1 on DNA (28). Indeed, subsequent *in vivo* studies aimed to analyze the effects of CRY1 and CRY1 plus PER on the binding of CLOCK:BMAL1 to chromatin (29). They used a mouse fibroblast cell line lacking CRYs and PERs and engineered derivative lines that express a non-native PER that can be selectively targeted to the nucleus using the estrogen receptor (ER)-mediated tamoxifen inducible nuclear localization. Using this system, they performed chromatin immunoprecipitation (ChIP) experiments to analyze CLOCK:BMAL1 genomic targeting in the presence or absence of nuclear CRY and PER proteins. Their data suggest that when PER proteins are co-expressed with CRYs, CLOCK:BMAL1 is removed from DNA (29). However, these studies were done using a non-native mechanism to

regulate nuclear entry; therefore, PER proteins are possibly inherently lacking essential post-translational modifications or association with other key proteins that could play a role in its normal function (7, 30). Conversely, numerous other studies have identified endogenous PER:CRY:CLOCK:BMAL1 complexes bound to chromatin (19, 7). While the aforementioned tamoxifen system represents a unique tool to dissect the independent roles of PER and CRY in regulation of CLOCK:BMAL1, the data were perhaps not reflective of the endogenous mechanism. More studies are needed on endogenous proteins, containing native post-translational modifications, to probe this mechanism in better detail.

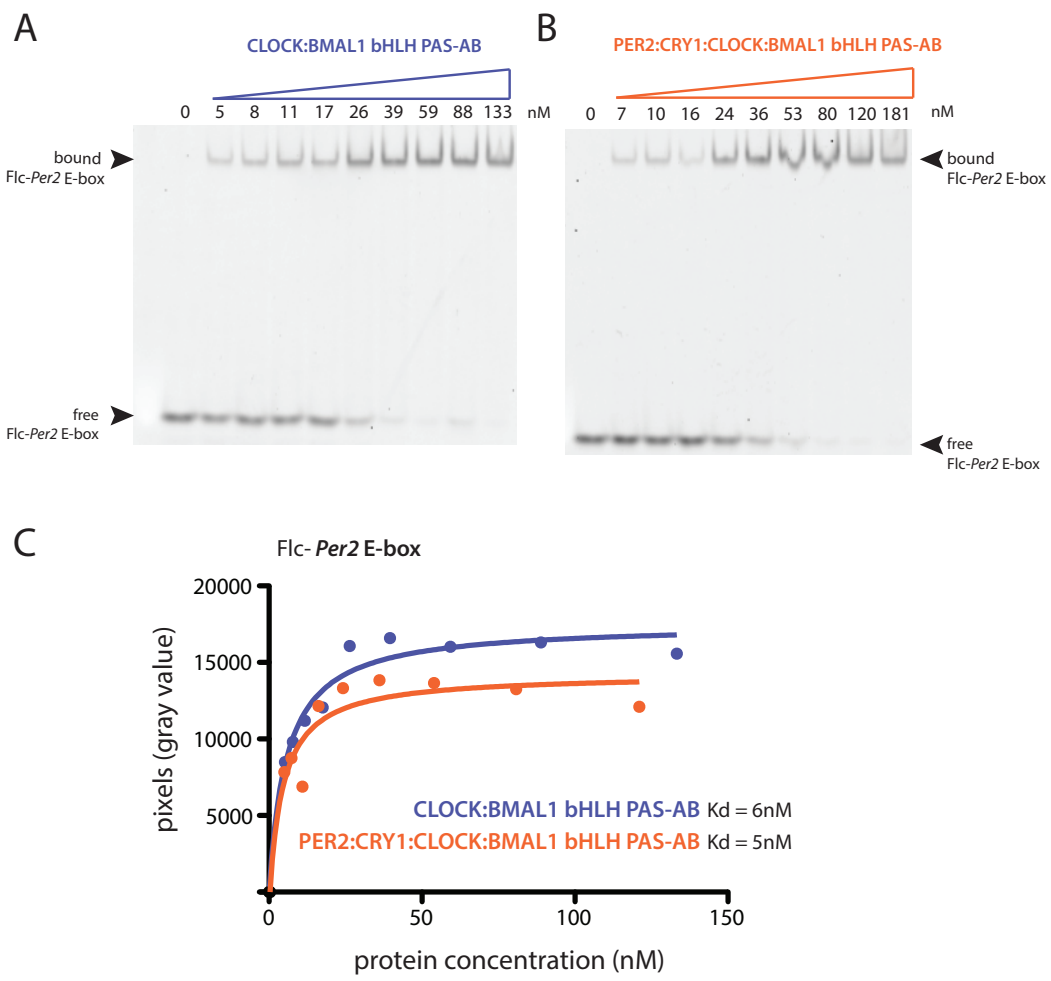

Figure 6-5. PER2 CBD:CRY1 PHR complex does not interfere with CLOCK:BMAL1 DNA binding.

(A) CLOCK:BMAL1 bHLH PAS-AB dimer was titrated into 1 nM fluorescein-labeled *Per2* E-box and reactions were run on a native PAGE gel. (B) PER2 CBD:CRY1 PHR complexes were added in stoichiometric amounts to a CLOCK:BMAL1 bHLH PAS-AB dimer with 1 nM fluorescein labeled probe and incubated overnight. Reactions were run on a native PAGE gel. (C) Quantification of gel shift assays in panels A and B. Pixels were quantified using ImageJ and plots were fit using a one-site specific binding curve.

With the individual purified protein components in hand, we aimed to test whether we could assemble a minimal PER2:CRY1:CLOCK:BMAL1 complex on DNA *in vitro*. Using an electrophoretic mobility shift assay (EMSA), we find the CLOCK bHLH PAS-AB:BMAL1 bHLH PAS-AB heterodimer (CLOCK:BMAL1 bHLH PAS-AB) is capable of binding DNA alone with a K_d of 6 nM, calculated from the amount of fluorescently tagged DNA shifted to a slower migrating, bound complex (Figure 6-5A). This value is comparable to previous values reported for CLOCK:BMAL1 bHLH PAS-AB and bHLH domains alone binding to E-box probes (31, 32). To test the effect of a CRY1:PER2 complex on CLOCK:BMAL1 DNA binding, we then added a preformed CRY1:PER2 complex to CLOCK:BMAL1:E-box complexes and let the reactions reach equilibrium overnight. With the addition of CRY1:PER2 complexes, we see approximately the same dissociation constant (5 nM), indicating that CRY1:PER2 complexes do not interfere with CLOCK:BMAL1 DNA binding *in vitro* (Figure 6-5B and C). Furthermore, PER2:CRY1:CLOCK:BMAL1 complexes appear to stay together even at dilute concentrations on cryo-EM grids as shown by negative stain (data not shown), so the assumption can be made that the slower migrating species are indeed PER2:CRY1:CLOCK:BMAL1 complexes bound to DNA. The addition of specific antibodies to individual components to supershift the complex would further strengthen this result. While it is yet to be determined if native PER and CRY affect CLOCK:BMAL1 DNA-binding *in vivo*, the assembly of this complex

on DNA *in vitro* supports the 'blocking type' mechanism of repression where CRY and PER proteins prevent CLOCK:BMAL1 from interacting with coactivators on DNA.

6.3 Conclusion

Here we propose a model where during the active phase (CT4– CT10, where CT0 indicates the onset of activity for diurnal organisms) CLOCK:BMAL1 interacts with CBP/p300 to activate transcription. During this active phase, CRY and PER proteins are first transcribed in the nucleus and translated in the cytoplasm. The role of PER appears to be most critical during this active phase where specific posttranslational modifications, including phosphorylation, of PER are critical for period determination and subsequent nuclear entry with CRY proteins. In this way, PER acts as a phosphorylation 'timer' while in the cytoplasm to provide the delay in repression required for oscillation (5, 6, 33). Once CRY and PER proteins are in the nucleus, our data now suggest that CRY proteins take the spotlight and are the primary transcriptional repressors of CLOCK:BMAL1 activity (3, 4, 28, 29). The differential roles of CRYs in the assembly of the early and late repressive complexes appear to be in part biochemical and regulated by PERs. We have yet to understand the contribution of transcriptional regulation of *Cry* to the assembly of these complexes. Our data suggest that CRY2 might rely on PERs to inhibit CLOCK:BMAL1 activity in the early complex, while CRY1 binds CLOCK:BMAL1 independently of PER (19, 25, 34). Additionally, we show here

that PER2 regulates the association of CRY1 with CLOCK and appears to 'slow' or impede the initial association, possibly contributing to the sustained repressive phase. Consistent with previous studies genome-wide studies, we find that the PER2 CBD does not prevent CRY1 from associating with CLOCK:BMAL1 on DNA, nor does it remove CLOCK:BMAL1 from DNA. Instead, we see a quaternary PER2:CRY1:CLOCK:BMAL1 complex on DNA *in vitro* using purified proteins. Future studies using endogenous purified proteins would help to clarify these findings and identify the possible experimental differences between these studies.

In summary, PER2 phosphorylation appears to be a timer in the cytoplasm that controls a delay in the initiation of the repression phase; however, once in the nucleus, CRYs directly repress CLOCK:BMAL1 activity. The CBD of PER1/2 may also directly contribute to biochemical differences in the early vs. late repressive complex assembly by modulating the kinetics of association of CRY1 with CLOCK in the early repressive complex to sustain the repressive phase until the cycle begins again. It will be interesting to see if the regulatory enzymes for PER and CRY (E3 ubiquitin ligases and kinases/phosphatases) further contribute to this timely control of the repressive phase in the nucleus and relieve repression to begin the next day-cycle.

6.4 Materials and Methods

6.4.1 Recombinant protein expression and purification.

Using the baculovirus expression system (Invitrogen) His_6-tagged mouse CLOCK bHLH PAS-AB domains (residues 26 - 395) and native mouse BMAL1 bHLH PAS-AB (residues 68 - 453) were cloned into pFastBac HTb vectors. Sf9 insect cells (Expression systems) co-expressing 6xHis tagged mouse CLOCK and BMAL1 bHLH PASAB for 72 hours were lysed by sonication in lysis buffer containing 50 mM Na_2HPO_4 pH 8.0, 300 mM NaCl, 10% v/v glycerol, 15 mM imidazole, 2.5 mM CHAPS, 5mM β-mercaptoethanol and EDTA-free protease inhibitors (Thermo). The clarified cell lysate was applied onto a NiNTA Agarose column (Qiagen) and bound protein was eluted with 250 mM imidazole. His tag was removed by treatment with TEV Protease overnight at 4°C. The CLOCK:BMAL1 bHLH PASAB complex was further purified using a heparin column followed by a size exclusion chromatography into 20 mM Hepes pH 7.5, 125 mM NaCl, 5% v/v glycerol and 2 mM TCEP.

For expression and purification of CRY1 PHR and CLOCK PAS-B, see Chapter 2. For details on expression and purification of PER2 CBD, see Chapter 5.

6.4.2 Analytical size-exclusion chromatography.

For analysis of complex formation by size-exclusion chromatography (SEC), purified proteins were injected on a Superdex 200 10/300 GL analytical column at 10-50 μM (~250μL) in 20 mM HEPES pH 7.5, 125 mM NaCl, 5%

glycerol and 2 mM TCEP. Proteins were incubated for ~30 min. or overnight and analyzed by SEC. All size-exclusion columns were calibrated with a low-molecular-weight gel filtration standards kit (GE Healthcare Life Sciences). The content of each peak was evaluated by SDS-PAGE and Coomassie staining.

6.4.3 X-ray crystallography.

CRY1:PER2 CBD complex was isolated by purifying each protein separately in a 1:1 molar ratio. Size exclusion was performed to isolate pure complex. The protein was concentrated to 5 mg/mL and crystallized by hanging-drop vapor diffusion at 22°C. Crystals formed in a 1:1 ratio of protein to precipitant in 0.2 M Magnesium chloride, 0.1 M Bis-Tris pH 5.5 and 25% PEG 3350. Data were collected at the Advanced Light Source, Lawrence Berkeley National Laboratory at Beamline (BL5.0.1). Diffraction spots were integrated using MOSFLM (45), and data were merged and scaled using Scala (46). Phases were first solved for by molecular replacement with a previous CRY2:PER2 structure (PDB: 4CT0) using Phaser (47). The structure was built with Coot and refined with PHENIX (48, 49). Coordinates and structure factors have not yet been deposited.

6.4.4 Electromobility gel shift assay.

CLOCK:BMAL1 bHLH PAS-AB complex was purified as described above. CLOCK:BMAL1 dimer was mixed in increasing concentrations with 1 nM of the N-terminally fluorescently labeled PER2 E-box [Flc]GCGCGGTCACGTTTTCCACT. CLOCK:BMAL1 bHLH PAS-AB reactions

were incubated for 15 min. and then run on an 8% native polyacrylamide gel at room temperature (10 V/cm) for 2 hours. Gel was imaged using a Typhoon Scanner (Amersham Biosciences) 9410 and excitation at 475 nm (blue). Image was processed using ImageQuant TL1 software and bands were quantified using ImageJ.

6.5 References

1. Reppert SM, Weaver DR (2002) Coordination of circadian timing in mammals. Nature 418(6901):935–41.
2. Partch CL, Green CB, Takahashi JS (2013) Molecular architecture of the mammalian circadian clock. Trends Cell Biol:1–10.
3. Vitaterna MH, et al. (1999) Differential regulation of mammalian Period genes and circadian rhythmicity by cryptochromes 1 and 2. Proc Natl Acad Sci 96(21):12114–12119.
4. Horst GTJ van der, et al. (1999) Mammalian Cry1 and Cry2 are essential for maintenance of circadian rhythms. Nature 398(6728):627–630.
5. Zheng B, et al. (2001) Nonredundant roles of the mPer1 and mPer2 genes in the mammalian circadian clock. Cell 105(5):683–694.
6. Zheng B, et al. (1999) The mPer2 gene encodes a functional component of the mammalian circadian clock. Nature 400(6740):169–173.
7. Duong HA, Weitz CJ (2014) Temporal orchestration of repressive chromatin modifiers by circadian clock Period complexes. Nat Struct Mol Biol 21(2):126–132.
8. Shirogane T, Jin J, Ang XL, Harper JW (2005) SCF??-TRCP controls Clock-dependent transcription via casein kinase 1-dependent degradation of the mammalian period-1 (Per1) protein. J Biol Chem 280(29):26863–26872.
9. Lamia KA, et al. (2009) AMPK regulates the circadian clock by cryptochrome phosphorylation and degradation. Science 326(5951):437–40.

10. Hirano A, et al. (2013) FBXL21 regulates oscillation of the circadian clock through ubiquitination and stabilization of cryptochromes. Cell 152(5):1106–1118.
11. Yoo SH, et al. (2013) Competing E3 ubiquitin ligases govern circadian periodicity by degradation of CRY in nucleus and cytoplasm. Cell 152(5):1091–1105.
12. Partch CL, Shields KF, Thompson CL, Selby CP, Sancar A (2006) Posttranslational regulation of the mammalian circadian clock by cryptochrome and protein phosphatase 5. Proc Natl Acad Sci U S A 103(27):10467–72.
13. Lee C, Etchegaray JP, Cagampang FR, Loudon AS, Reppert SM (2001) Posttranslational mechanisms regulate the mammalian circadian clock. Cell 107:855–867.
14. Hirota T, et al. (2010) High-Throughput Chemical Screen Identifies a Novel Potent Modulator of Cellular Circadian Rhythms and Reveals CKIα as a Clock Regulatory Kinase. PLOS Biol 8(12):e1000559.
15. Chen Z, et al. (2012) Identification of diverse modulators of central and peripheral circadian clocks by high-throughput chemical screening. Proc Natl Acad Sci U S A 109(1):101–6.
16. Toh KL, et al. (2001) An hPer2 phosphorylation site mutation in familial advanced sleep phase syndrome. Science 291(5506):1040–1043.
17. Xu Y, et al. (2005) Functional consequences of a CKIδ mutation causing familial advanced sleep phase syndrome. Nature 434(MARCH):640–644.
18. St John PC, et al. (2014) Spatiotemporal separation of PER and CRY posttranslational regulation in the mammalian circadian clock. Proc Natl Acad Sci U S A 111(5):2040–5.
19. Koike N, et al. (2012) Transcriptional Architecture and Chromatin Landscape of the Core Circadian Clock in Mammals. Science (80-) 338:349–354.

20. Xu H, et al. (2015) Cryptochrome 1 regulates the circadian clock through dynamic interactions with the BMAL1 C terminus. Nat Struct Mol Biol 22(6):476–484.
21. Chang Y-G, et al. (2015) A protein fold switch joins the circadian oscillator to clock output in cyanobacteria. Science (80-) 349(6245):324–328.
22. Sugase K, Dyson HJ, Wright PE (2007) Mechanism of coupled folding and binding of an intrinsically disordered protein. Nature 447(7147):1021–1025.
23. Sarkar P, Saleh T, Tzeng S-R, Birge RB, Kalodimos CG (2011) Structural basis for regulation of the Crk signaling protein by a proline switch. Nat Chem Biol 7(1):51–57.
24. Schmalen I, et al. (2014) Interaction of circadian clock proteins CRY1 and PER2 is modulated by zinc binding and disulfide bond formation. Cell 157(5):1203–1215.
25. Michael AK, et al. (2017) Formation of a repressive complex in the mammalian circadian clock is mediated by the secondary pocket of CRY1. Proc Natl Acad Sci . doi:10.1073/pnas.1615310114.
26. Nangle SN, et al. (2014) Molecular assembly of the period-cryptochrome circadian transcriptional repressor complex. Elife 3(August2014):1–14.
27. Xing W, et al. (2013) SCF(FBXL3) ubiquitin ligase targets cryptochromes at their cofactor pocket. Nature 496(7443):64–8.
28. Ye R, Selby CP, Ozturk N, Annayev Y, Sancar A (2011) Biochemical analysis of the canonical model for the mammalian circadian clock. J Biol Chem 286(29):25891–25902.
29. Ye R, et al. (2014) Dual modes of CLOCK:BMAL1 inhibition mediated by Cryptochrome and period proteins in the mammalian circadian clock. Genes Dev 28(18):1989–1998.

30. Brown SA, et al. (2005) PERIOD1-associated proteins modulate the negative limb of the mammalian circadian oscillator. Science 308(5722):693–6.

31. Huang N, et al. (2012) Crystal Structure of the Heterodimeric CLOCK:BMAL1 Transcriptional Activator Complex. Science (80-) 337:189–194.

32. Wang Z, Wu Y, Li L, Su X-D (2013) Intermolecular recognition revealed by the complex structure of human CLOCK-BMAL1 basic helix-loop-helix domains with E-box DNA. Cell Res 23(2):213–224.

33. Lee C, Etchegaray J-P, Cagampang FRA, Loudon ASI, Reppert SM (2001) Posttranslational Mechanisms Regulate the Mammalian Circadian Clock. Cell 107:855–867.

34. Xu H, et al. (2015) Cryptochrome 1 regulates the circadian clock through dynamic interactions with the BMAL1 C terminus. Nat Struct Mol Biol 22(6):476–84.

7 CHAPTER 7 — FUTURE DIRECTIONS

7.1.1 Structural studies of a PER2:CRY1:CLOCK:BMAL1 complex

To date, there is no high-resolution structure of a circadian repressive complex that contains CLOCK:BMAL1. As mentioned above, the PER2 CBD forms a stable complex with CRY1:CLOCK:BMAL1 PAS-AB given enough time (Figure 7-1A) This complex is stable and can be isolated by size exclusion. In attempts to elucidate the structure of this complex, we set up many crystallization trials and have reproduced the generation of small ~10-15 μm crystals (Figure 7-1B). Observing diffraction from such small crystals often requires a highly focused microbeam x-ray source. We are currently working to collect diffraction data at the SSRL light source at Stanford using the BL12-2 beam with these crystals.

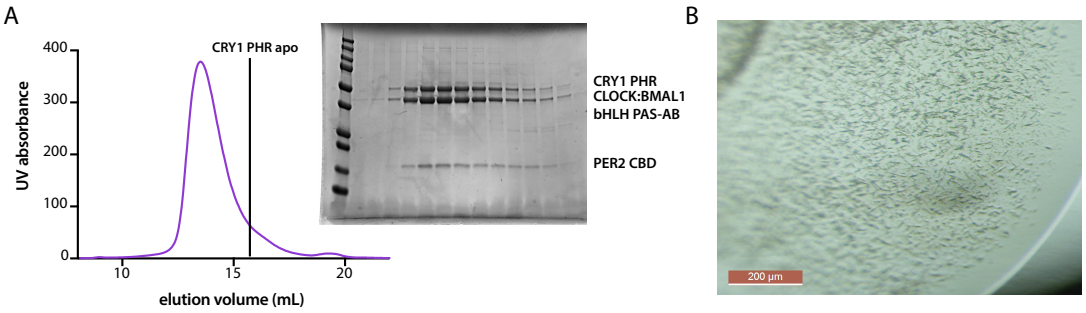

Figure 7-1. Structural studies of a PER2:CRY1:CLOCK:BMAL1 complex.

(A) Size exclusion analysis of a PER2:CRY1:CLOCK:BMAL bHLH PAS-AB complex that was used in cryo-EM trials. (B) Crystals of a PER2:CRY1:CLOCK:BMAL1 complex in 0.1 M Sodium chloride, 0.1 M CAPS pH 10.5, 20% PEG-8000. Drops were set at 6.7 mg/mL total protein concentration. The crystal hit pictured appeared in 2-3 days at 22°C.

7.1.2 Cryo-electron microscopy (EM) of PER2:CRY1:CLOCK:BMAL1 complexes

To bypass some of the hurdles of crystallography, we turned to cryo electron microscopy (EM). Cryo-EM does not require a crystal lattice and therefore has been revolutionizing structural biology with recent advances in detector sensitivity and processing techniques, allowing for structural determination of protein complexes at a much higher resolution than was previously attainable (1). Of course, even this technique has caveats. Cryo-EM requires the protein complex to be stable (i.e. not break apart into smaller particles) on negative stain grids. Furthermore, protein complexes must also be resilient to harsh cryo-freezing conditions and small protein complexes (<150 kDa) can benefit from more sophisticated techniques such as using a phase plate. First, we started with the PER2:CRY1:CLOCK:BMAL1 PAS-AB complex that gave rise to small crystals, as this suggested that the complex was highly uniform and stable. We were able to get 2D class averages by negative stain EM; however, the Relion processing software could only align smaller particles corresponding to a predicted molecular weight of ~60 kDa, suggesting that protein complexes were falling apart into CRY:PER and CLOCK:BMAL1 particles. Furthermore, this complex was near the lower limit of size constraints for structure determination using standard techniques by cryo-EM single particle reconstruction with a mass of 144 kDa.

In order to increase the particle size and hopefully improve the 3D alignment, we re-cloned our recombinant proteins to add the bHLH DNA-binding domains onto CLOCK:BMAL1. After optimization of the protein purification and validation of this new complex, we were able to isolate a PER2:CRY1:CLOCK:BMAL1 bHLH PAS-AB complex (Figure 7-1). In addition to increasing the overall particle size, the bHLH domain is a very rigid body that protrudes from the PAS domain core, which will likely help with particle alignment. This strategy also primes us to add DNA to cryo-conditions and see how this complex assembles on DNA. This work is ongoing and further optimizations of cryo-conditions and complex preparations aim to provide a pseudo-atomic model of a PER2:CRY1:CLOCK:BMAL1 repressive complex.

7.2 References

1. Bai X chen, McMullan G, Scheres SHW (2015) How cryo-EM is revolutionizing structural biology. *Trends Biochem Sci* 40(1):49–57.